Stony Brook University

Synoptic Flow Patterns that Influence Wind-Induced Mixing and the Temporal Evolution of Hypoxia over Western Long Island Sound

A Thesis Presented

By

Sean Dennis Bratton

to

The Graduate School

in Partial Fulfillment of the

Requirements

for the Degree of

Master of Science

in

Marine and Atmospheric Science

Stony Brook University

December 2011

Stony Brook University

The Graduate School

Sean Dennis Bratton

We, the thesis committee for the above candidate for the

Master of Science degree, hereby recommend

acceptance of this thesis.

Dr. Brian Colle (Thesis Advisor)
Professor
Institute for Terrestrial and Planetary Atmospheres
School of Marine and Atmospheric Sciences

Dr. Robert Wilson (Reader)
Associate Professor
School of Marine and Atmospheric Sciences

Dr. Sultan Hameed (Reader)
Professor
Institute for Terrestrial and Planetary Atmospheres
School of Marine and Atmospheric Sciences

This thesis is accepted by the Graduate School

Lawrence Martin
Dean of the Graduate School

Abstract of the Thesis

Synoptic Flow Patterns that Influence Wind-Induced Mixing and the Temporal Evolution of Hypoxia over Western Long Island Sound

by

Sean Dennis Bratton

Master of Science

in

Marine and Atmospheric Science

Stony Brook University

2011

Bottom dissolved oxygen (DOb) concentrations in wLIS have exhibited both a long-term decline as well as marked inter-annual variability over the last several decades (1950-2009). This behavior continues despite New York City having reduced the quantity of nitrogen in upper East River Water pollution Control Plants (WPCPs) over the last two decades (Wilson t al. 2008). Processes controlling the inter-annual variability, intensity, spatial extend, and duration of hypoxia is still not fully understood. A number of studies have focused on anthropogenic factors, but air-sea interactions have also been documented to be important. The objective of this study is to identify physical factors including wind direction and speed in the form of 'mixing events', to help explain inter-annual and inter-decadal DOb variability.

NYC DEP and EXRX LISCOS buoy DOb and temperature data were used in conjunction with La Guardia (LGA) and NBDC buoy 44022 meteorological data to identify wind speed and directional criteria preferred for water column mixing. It was found that for winds 30°-110° with magnitudes >= 4 m s^{-1} are the most efficient for mixing. Using these wind criteria resulted in a 1.5 mg L^{-1} increase in DOb on average within the water column. A synoptic climatology was created, using NCEP/NCAR Reanalysis data, based on the above wind criteria. These events were then categorized based on relevant location and type of the synoptic system into one of three groups; high pressure patterns, low pressure patterns, or hybrid patterns. Synoptic average and anomaly patterns, including 500-hPa geopotential heights and mea sea-level pressure (mSLP), were used for daily lag periods -4 to 0 days prior to the start of a mixing event to determine the synoptic evolution of low and high pressure patterns that produced mixing events. It was determined that high pressure patterns, including Pre-High and Extended High patterns, result in the highest percentage of total mixing events (76.3%) and display a significant increasing trend suggesting the frequency of anticyclones is a significant indicator for the frequency and trend of mixing events. Lastly, a connection between seasonal DOb/hypoxia data and mixing event metrics including; frequency, spacing, and duration are used to determine the extent of the relationship and if mixing events are able to help explain the recent (20-30 year) trends in seasonal DOb. It was found that mixing events are a strong indicator of the inter-annual fluctuations in DOb and the duration of hypoxia, however are not able to explain the 20-30 year DOb and hypoxia trends represented in these datasets.

Dedication Page

This thesis is dedicated to my parents, David and Debbie Bratton

Table of Contents

List of Tables **Page**

Chapter 2

Chapter 3

Chapter 5

List of Figures

Chapter 1 **Page**

Chapter 2

Chapter 3

Chapter 4

Chapter 5

Acknowledgments

Financial support for this research project was given by New York State Sea Grant.

I would like to thank my advisor, Dr. Brian Colle, for his continued support and guidance throughout this project. His encouragement during my years at SoMAS was greatly appreciated.

A Special thanks to New York State Sea Grant who were always enthusiastic about my research and helped support me financially and academically for the last two and a half years, including a thesis completion award for my last semester at SoMAS. They also helped provide funds for my trip to the 2010 MABPOM conference in Hoboken, NJ.

I also should thank my committee members, Dr. Robert Wilson and Dr. Sultan Hameed, for their assistance and help. They were more than willing to listen to my endless questions about physical oceanography and statistics.

I would like to acknowledge staff members Cliff Jones, Carol Dovi and Gina Gartin for all their help and assistance. They were always willing to lend a helping hand.

Particular thanks go to my colleagues and friends at SoMAS for always offering a helping hand and kept my spirits up over the last three years.

Lastly, and most importantly, I want to thank my parents, David and Debbie Bratton for their advice and endless support. Their words of wisdom and perspective never went unnoticed and helped me tremendously to complete my thesis.
.

Chapter I: Introduction

The objective of this thesis is to investigate the relationship between synoptic-scale weather systems and the summer season evolution of hypoxia over western Long Island Sound (wLIS) (Fig. 1.1). This is motivated by the fact that seasonal bottom dissolved oxygen (DOb) concentrations have been decreasing at an alarming rate over the past several decades (O'Donnell et al. 2006, Wilson et al. 2008), resulting in an anomalous number of hypoxic events. In particular, when the seasonal minimum DOb has reached severe hypoxic levels (< 2mg L^{-1}) more frequently over the recent decades (Fig. 1.2). Because hypoxia has detrimental effects on aerobic organisms and the Long Island Sound (LIS) ecosystem, it is critical to determine what controls these hypoxic seasons. The overall goal of this thesis is to determine relevant synoptic patterns conducive to mixing over wLIS, which may help limit the development of hypoxia.

1.1. Seasonal evolution of hypoxia over wLIS

Hypoxia is defined as a concentration of DOb that is low enough to adversely influence aquatic life, typically below 3.5 mg L^{-1} as defined by the Long Island Sound Study (CT DEP 2010). Seasonal hypoxia typically develops when the need for biological oxygen exceeds rates of dissolved oxygen resupply to bottom waters by physically mixing the water column and/or advective processes (Anderson and Taylor 2001). These hypoxic conditions normally occur

during the summer and are mainly confined to the Narrows and western part of LIS where 90-100% of the summer seasons result in hypoxia (CT DEP 2010) (Fig. 1.3).

LIS is 160km long and 30 km wide (From west to east) with an average depth of 21m (Gay et al. 2004). It is connected to the Atlantic Ocean through the Race over extreme eastern LIS. The western end is connected to the lower Hudson River through the East River (Vieira 2000). LIS can be segmented into four major basins, separated by various sills and shoals which influence the circulation of bottom waters (Lee and Lwiza 2007) (Fig. 1.4). Because wLIS has a broad, deep central axis with limited shoal area the volume of bottom water below the pycnocline is substantial, especially at deeper stations (Welsh and Eller 1991). The unique topography over wLIS favors more frequent seasonal hypoxic episodes. For regions west of the Hampstead Sill (Fig. 1.3) basin morphology induces a series of physical conditions that slows the circulation of bottom water, and results in seasonally permanent stratification. This increases the residence time of the deep water, which restricts horizontal transport and mixing processes and increases the biological removal of oxygen, making the region susceptible to becoming hypoxic (Welsh 1994). Tidal mixing is also relevant, but to a limited extent over wLIS. In general, wLIS has little tidal mixing since it is at a nodal point to the tidal standing wave in this estuary (Hao 2008), with strong flow (>10cm s^{-1}) to the east of the Race, and weak flow (~ 1-3cm s^{-1}) over wLIS. Due to the lack of near bottom turbidity from tidal flow, wLIS is more susceptible to stratification compared to points to the east (Crowley 2005).

Nutrient discharge from various waste treatment plants on the Hudson River can flow through the East River to the extreme western end of LIS (Anderson and Taylor 2001, Wilson et al. 2008). Secondary treatment of this material converts organic nitrogen to inorganic nitrogen, which is more biologically available (Wilson et al. 2008). During summer these nutrients,

especially nitrogen, assist in the production of phytoplankton in LIS. When these phytoplankton die they settle to the bottom, where bacteria breaks down the organic material for fuel while consuming oxygen (Anderson and Taylor 2001). Nutrient enrichment has been shown to be proportional to the abundance of algae and therefore high levels of oxygen consumption (CT DEP 2010). Since there are inter-annual variations of oxygen deletion, the contribution of benthic metabolism is difficult to predict (Welsh et al. 1995). However, it does appear that metabolic dominance shifts to the water column as the stratified warm season progresses. A consequence is that the entire lower water column can become uniformly depleted of oxygen (Walsh et al. 1978). These processes combined with persistent density stratification with a strong, horizontally oriented pycnocline, and lack of vertical mixing associated with hot, calm weather, prevents re-ventilation of oxygen and other nutrients to bottom waters (Levinson et al. 1995). Eventually, DOb levels return to normal in late August or early September, when the water column is more efficiently mixed and oxygen is replenished to bottom waters (Welsh 1994).

1.2. Environmental effects of hypoxia

Hypoxia has long been a problem for parts of the mid-Atlantic and Northeast U.S coastal regions. In 1976 a hypoxic episode in the New York Bight caused widespread shellfish mortality and economic damages of 60 million dollars (Falkowski et al. 1980). wLIS experienced mass mortalities of the American lobster (*Homarus americanus)*, the single largest commercial fishery remaining in LIS, during the summer of 1999 due to low bottom temperatures and DOb concentrations, inducing stress to the lobster population (Wilson and Swanson 2005). Many of

the benthic organisms affected cannot escape the low-oxygen water, especially lobster, clam and other shellfish species, affecting commercial harvests and the health of impacted ecosystems (Lowery 1998).

1.3. Physical relationship between DOb and wind

One of the more important mechanisms to consider for water column de-stratification is the residual circulation that sets up within LIS. Horizontal density gradients are of primary importance in establishing and maintaining this non-tidal residual circulation in LIS. Throughout most of the Sound there is a region near mid-depth at which the baroclinic pressure gradient is reduced to near zero. This corresponds closely to the existence of a well developed two-layer non-tidal transport system within the sound, which is due to the gravitational circulation. Within the upper layers the pressure surfaces slope downward toward the sea and sustain a residual flow toward the sea. At depths, pressure surfaces slope downward toward the head of the estuary and sustain a residual flow in that direction (Wilson 1975). Figure 1.5 taken from Vieira (2000) shows eastward currents in the upper layers and westward flows in the deeper layers, which is consistent with the gravitationally determined circulation described above. This two-layer residual circulation creates sheared flow enhanced by the strength of the along-channel density gradients (O'Donnell et al. 2008).

The physical terrain of the sound and its associated transport processes establishes the rate of resupply of oxygen and in return determines how much biological activity the system can accommodate (Welsh 1994). Recently, attention has been given to the importance of wind-induced circulations and their influence on mixing (Goodrich et al. 1987). Walsh et al. (1978)

found a link between the upwelling and downwelling experienced within the water column during wind events and the nutrients needed for productivity in wLIS estuarine system. Understanding the wind induced physical processes is an important step to determine the extent these physical mechanisms play in the evolution of hypoxia over these estuarine waters.

During periods of enhanced density stratification, the vertical shear can become augmented, resulting in the development of a strong thermocline, in which there is little exchange between the surface and bottom waters. This is why physical processes play an important role in modulating the vertical water column structure throughout the summer season (Goodrich et al. 1987; Scully et al. 2005; O'Donnell et al. 2008; Wilson et al. 2008; Chen and Sanford 2009; Whitney and Codiga 2011). The two main mechanisms in which winds alter the physics of the water column to assist in ventilating bottom waters is through direct wind mixing (stirring) and wind-induced straining (Scully et al. 2005).

Traditional views of ventilating estuarine bottom waters is that direct vertical mixing across the pycnocline controls the exchange of oxygen to sub-pycnocline waters (Scully 2010a). For this direct mixing case, wind drives mixing through a combination of vertical shear and turbulence near the surface that is proportional to the wind speed cubed. Alternatively, Scully et al. (2005) determined that the rate of vertical mixing is a consequence of the wind's influence on the vertical stratification through its modification of the baroclinically forced residual circulation; a process labeled wind induced straining of the estuarine density field (O'Donnell 2006).

Wind-driven modulation of the along-channel residual flow has been documented to play an important role in altering the extent of hypoxia through wind-induced straining (O'Donnell et

al. 2008,Wilson et al. 2008,Chen and Stanford 2009, Scully 2010a). During westward (up-estuary) winds (Fig. 1.6b), a reduction or even reversal in the vertical shear associated with the residual circulation results in a decrease in stratification over wLIS. This is accomplished by the wind decelerating the transfer of fresh water over the denser deepwater. Simulations by Whitney and Codiga (2011) indicate that stratification decreases over wLIS for both westerly and easterly wind directions but this decrease is twice as large for easterly flow. The lower stratification during easterly winds allows the flow to infiltrate deeper into the water column. Isopycnal straining acts with westward advection and vertical mixing to decrease stratification in this region. This results in larger eddy viscosities during periods of up-estuary directed wind (Scully et al. 2005; Chen and Sanford 2009). When water relaxes back into the channel post up-estuary wind event, it results in enhanced surface fluxes allowing a net influx of oxygen into the hypoxic layer (Scully 2010a).

In contrast, eastward (down-estuary) winds for wLIS (Fig. 1.6a) increases the sub-tidal two layer exchange flow, and accelerates the transport of fresher water, which in turn strains the along channel density gradient to increase stratification (Scully 2010a). As a result vertical mixing is reduced and dissolved oxygen in the bottom water declines at a rate consistent with Welsh and Eller (1991) due to benthic consumption (O'Donnell 2006). In addition, while strong winds associated with down-estuary storm events have the potential to destratify and mix the water column for partially mixed estuaries, weak to moderate wind events can further stratify the water column through wind-induced straining (Goodrich et al. 1987; Chen and Stanford 2009).

1.4. Previous research investigating link between DOb changes on synoptic timescales

There have been limited studies investigating wind-induced modifications to surface currents and DOb oscillations on synoptic timescales. Chen and Stanford (2009) and O'Donnell (2008) determined that wind can modify estuarine stratification at a frequency of 2–7 days. There have been numerous studies investigating the relationship between wind and the physical impacts to the water column and DOb (Geyer 1996, Scully et al. 2005, Wilson and Swanson 2005, Codiga et al. 2008, O'Donnell et al. 2008, Wilson et al. 2008, Chen and Stanford 2009, Scully 2010a). Kaputa and Olsen (2000) found a relationship between the timing of tidally and meteorologically forced DOb variability and areas of the LIS most impacted by hypoxia for summer. It was found that DOb fluctuations are inherently periodic and occur intermittently throughout the summer. In the extreme case, in which there is no exchange of DO to bottom wLIS waters, rates of DO would decline to anoxic conditions within 13-50 days, however the observed rate is on the order of 150 days (McCardell and O'Donnell 2006). Welsh (1995) found anomalously warm weather with calm wind conditions near the end of the summer have the tendency to lengthen the stratified period and in turn enhance DO depletion while stormy conditions, specifically in August, reduce depletion. Wilson et al. (2008) identified specific years including, 1988 and 1992, which isolated the importance of wind-induced current shear on the control of stratification and vertical mixing. It was found that inter-annual variations in both the direction and directional constancy of summertime winds over wLIS can help control the ventilation of bottom waters and thereby the seasonal development of hypoxia. However, the above study only took into consideration a few select anomalous years instead of comparing a series of years to determine if this relationship was significant.

Some studies have briefly investigated physical atmospheric phenomena attached to de-stratification of the water column, including Austin and Lentz (1999) who inspected late summer cyclone variability over the inner shelf east of North Carolina. A key finding was the mixing response to the surface heat flux and wind stress to cold frontal passage. Scully (2010b) demonstrated the importance of wind direction in controlling the extent and severity of summertime hypoxia In Chesapeake Bay. Scully (2010b) found significant positive correlations between daily hypoxia and the duration of westerly winds. In the same sense, a negative correlation was found between hypoxia and duration of southeasterly winds. For an extreme example, Li et al. (2007) studied the influences of hurricane Isabel on mixing in the Chesapeake and found that the hurricane force winds resulted in a steady deepening of the surface mixed layer, which resulted in accelerated de-stratification over the water column. For cases over wLIS, O'Donnell et al. (2008) showed that there are oscillations of DOb for components of wind stress from 52°(northeast), related to either vertical mixing or horizontal advection, the same time frame of synoptic systems. Wilson and Swanson (2005) speculated that extratropical cyclones just east of the New England coast are the predominant synoptic systems producing northwesterly to northeasterly winds associated with wLIS mixing. In addition, Wilson and Swanson (2005) found wind stirring and surface cooling associated with a frontal passage made a very significant contribution to vertical mixing, producing a rapid increase in bottom temperature and dissolved oxygen from approximately 3 mg L^{-1} to 6.5 mg L^{-1}.

On a decadal scale, there has been evidence to support inter-decadal variations in the frequency of summer winds, can be linked directly to DOb variability (O'Donnell et al. 2006, Scully 2010b). Since decreases in DOb are a result of both the water column respiration rate and wind-induced ventilation, O'Donnell et al. (2006) concluded that the above phenomenon can be

applied to trends in the decadal variations of duration and severity of hypoxia in wLIS. Since 1997 summer time winds from the northeast have become more frequent on average for the last 50 years, suggesting ventilation has become more frequent than before (O'Donnell et al. 2006).These studies are limited to speculation however; based on the assumption that because wind forced ventilation has the potential to significantly alter the rate of seasonal decline of the DO concentration, then a similar trend would be observed on longer decadal timescales. A Similar approach is taken over Chesapeake Bay, in which Scully (2010b) found a decadal signal between DOb and winds using the Bermuda high index (BHI), which is defined as the normalized pressure difference between Bermuda and New Orleans, Louisiana. This index was used to categorize summer wind forcing trends over Chesapeake Bay. A positive index is indicative of a higher percentage of southerly winds that help de-stratify the water column.

1.5. Motivation

Bottom dissolved oxygen concentrations in wLIS have exhibited long-term decline, extending from the mid-1940's to present, with inter-annual variability (Wilson et al. 2008 , NYC DEP 1993) (Fig. 1.7). Originally, it was thought that the primary cause of the intensification of hypoxic conditions was due to eutrophication resulting from the increase in nutrient loading from waste treatment plants (Wilson et al. 2008). However, since strict restrictions were implemented for the total maximum daily load of nitrogen, DOb level continue to show a downward trend over wLIS (Welsh 1994; Levinson et al. 1995; Anderson and Taylor 2001; Lee and Lwiza 2007; O'Donnell et al. 2008; Wilson et al. 2008). Dividing the seasonally averaged DOb time series (1968-1992) into three segments shows that the majority of the summertime hypoxia events occurred in the 1980s followed by a subsequent increase in the

1990s (not shown), with more recent observations showing an accelerated decline of DOb occurring since 2000 (Wilson et al. 2008).

Due to the detrimental impact hypoxic conditions have on marine life, and the unexplainable rate in which DOb over wLIS is declining; it is important to understand all possible influencing factors contributing to the seasonal evolution of DOb over wLIS. More recently many studies have provided strong evidence for the potential impact wind, associated with synoptic scale patterns, has on DOb. McCardell (2006), O'Donnell et al. (2008), Wilson et al. (2008), and Whitney and Codiga (2011) have examined short term, synoptic oscillations within the DO field. O'Donnell (2006) observed that approximately 80% of the water column ventilation intervals were associated with increased vertical mixing. When seasonal comparisons were made between the covariation of DO and wind stress, measurements suggested that along-sound components of the wind controls the occurrence of these ventilation episodes. In addition, Whitney and Codiga (2011) used ferry-based current observations to make connections to wind orientation and the physical mechanisms that modify stratification parameters over LIS.

Given the discussion above, a lucid relationship can be made between wind forcing for winds and changes to the wLIS water column profile, specifically DOb, on synoptic time scales. For this study, understanding the synoptic behavior of high and low pressure systems during summer is important to successfully identify atmospheric patterns that stimulate these wind-induced ventilation periods. Due to the relationship between summer wind variability and DOb it is important to understand summer synoptic pattern variability and connections to climatology studies over the northeast U.S region.

Several studies (Zishka and Smith 1980; Harman 1987; Agee 1990; Rogers 1990; Sinclair 1997; Zhang et al. 1999; McCabe et al. 2000; Mesquita et al. 2007) have focused on the northward extension of weather system tracks over the U.S. due to a northward shift and reduction of baroclinicity during summer. This can have implications on the surface environment due to the possible changes in wind regimes over wLIS. Leibensperger et al. (2008) found inner-annual variability in the frequency of mid-latitude cyclones as a major predictor of pollution episodes over the eastern U.S. Leibensperger et al. (2008) also found a significant long-term (1980-2006) decline in the number of summertime mid-latitude cyclones tracks extending from 40°-50°N. Additional studies (Agee 1990; McCabe et al. 2000; Mesquita 2007) have more recently found a general decrease in the frequency of cyclones and anticyclones during the summer months accompanied by warming temperature trends.

Although the issues of wind regimes and oscillations in DO on synoptic time scales have been established, studies lack the specific relationship for different directions, speeds and durations of winds and the inherent effects on DOb. To this point many studies use arbitrary directional fields such as ‘up and down estuary’, ‘cross channel’, ‘along sound’, ‘east’ ,etc… to describe favorable winds for mixing (Levinson et al. 1995, Scully et al. 2005, O’Donnell et al. 2008, Chen and Sanford 2009,Whitney and Codiga 2011) . This lingo however is not specific, and can be open to interpretation by the reader. In addition, only suggestive comparisons have been made to link seasonal and decadal DOb variability to wind frequencies from a climatological perspective (O’Donnell 2006). Most importantly, there is little indication of what atmospheric environments foster these wind induced mixing events, so it is difficult to determine what generates favorable wind conditions. This study highlights wind direction and speed criteria necessary for a mixing event over wLIS, and how efficient different wind criteria are at altering

DO and stratification. Additionally, this study will look at specific spatial synoptic patterns that result in mixing events.

Because the involvement of wind processes controlling the inner-annual variability, intensity, spatial extent, and duration of the hypoxic episodes are not fully understood the following questions/objectives will be addressed:

1. Evaluate the relationship between wind forcing and DOb within wLIS on daily, seasonal, and decadal temporal scales.
2. Determine the most efficient wind directions and speeds to induce vertical water column de-stratification.
3. Evaluate the water column response within LIS to the passage of synoptic high and low pressure systems including effects of de-stratification on the intensity of DOb ventilation, using 'mixing event' criteria.
4. Categorize the most relevant synoptic spatial patterns (high/low pressure) that are most consistent at influencing mixing. What longer term trends exist in the climatology?
5. What is the large scale synoptic evolution, at the surface and upper levels, that exist up to and including times of mixing?
6. Are winds and mixing events able to help explain the inter-annual variability and recent downward trend in seasonal DOb?

Figures

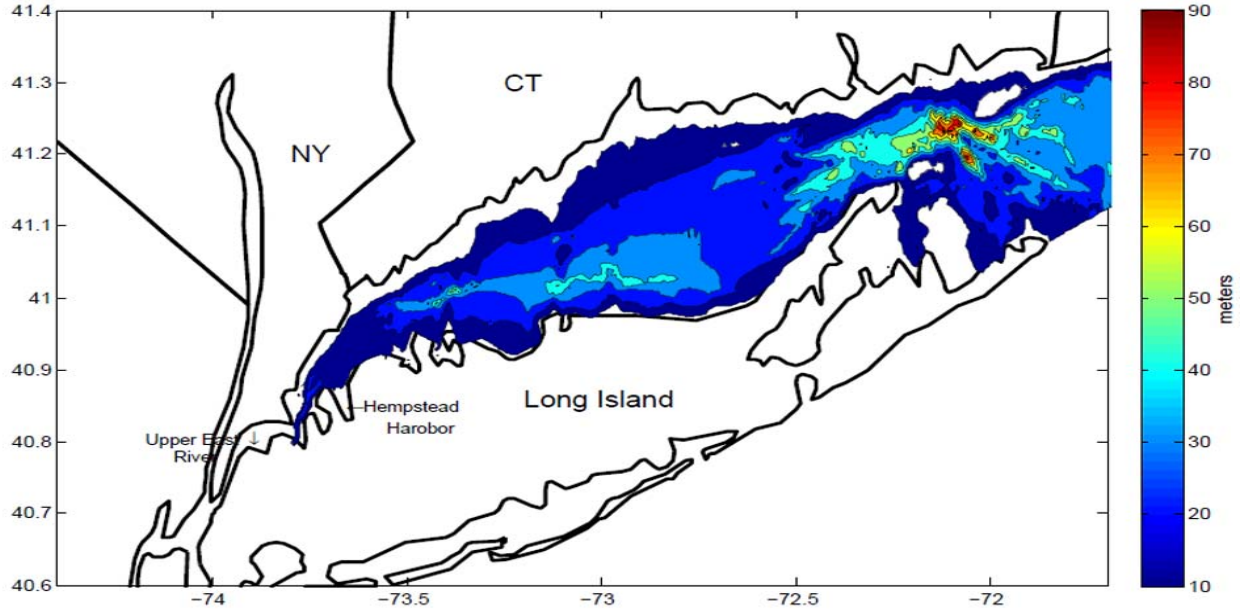

Figure 1.1 Map of LIS and the surrounding region including bathymetry (m) with specified locations of Hempstead Harbor and upper East River.

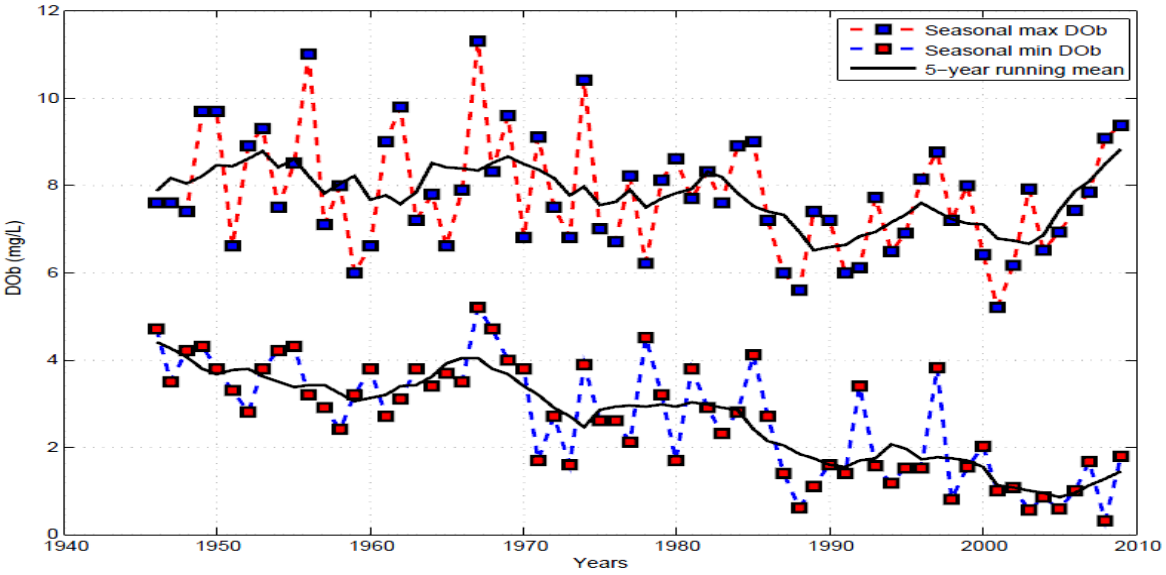

Figure 1.2 Seasonal (June-September) time series (1946-2009) of maximum (red dashed) and minimum (blue dashed) DOb values with a 5 year running mean. DOb data taken from NYC DEP Hart Island mooring station (E10).

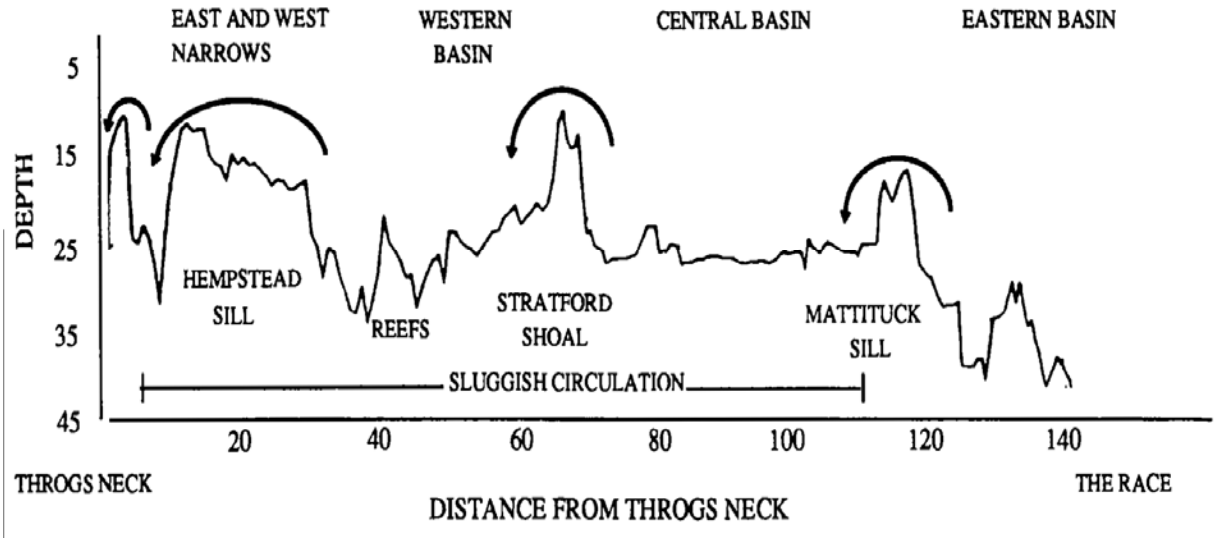

Figure 1.3 Plot of axial topography including basins, reefs and sills. Y-axis represents depth of the sound. X-axis represents the distance from Throgs Neck Bridge stretching east toward The Race. Figure taken from Welsh (1993).

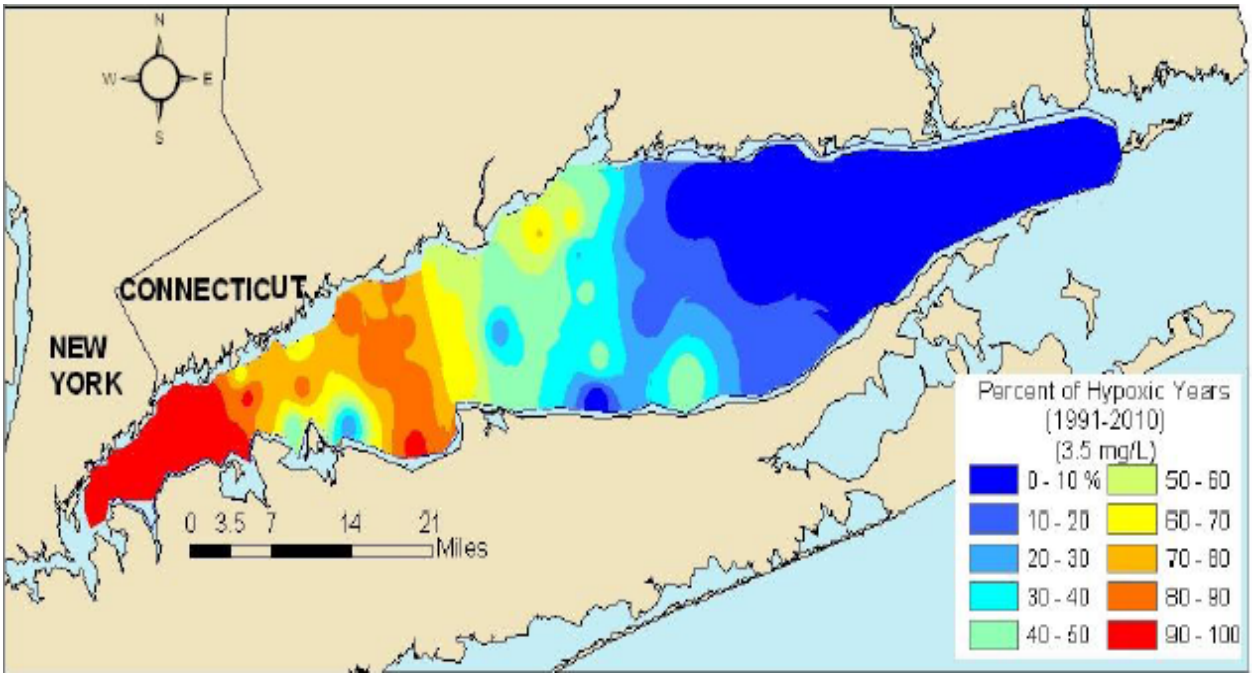

Figure 1.4 The percent of years from 1991-2010 that were associated with hypoxic conditions of 3.5 mg L^{-1} or less. Plot contoured every 10%. Figure taken from CT DEP 2010 Long Island Sound Hypoxia Season Review (2010).

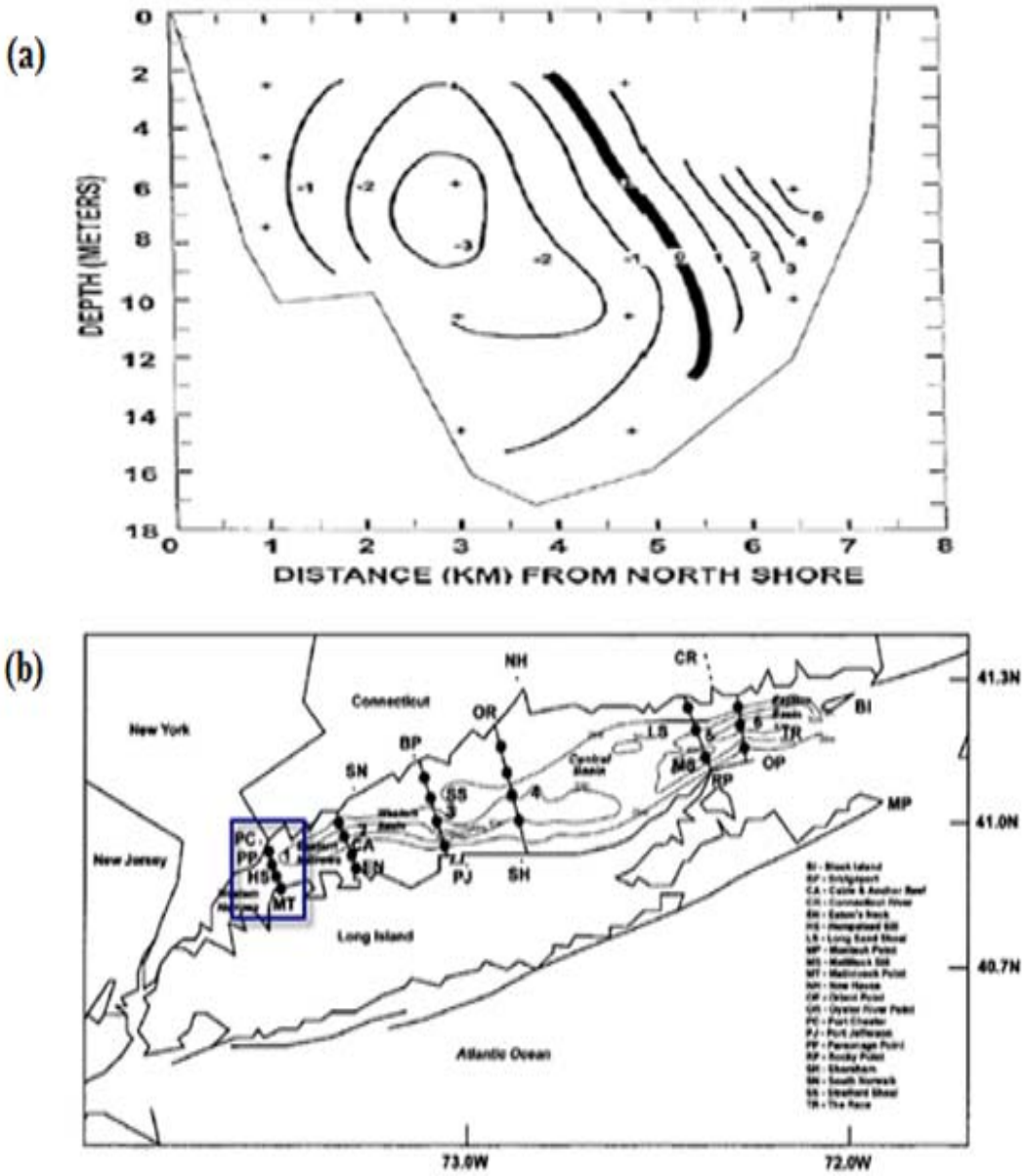

Figure 1.5 (a) Cross-Section at (b) transect 1, indicated by the blue square, showing long-term residual longitudinal current isotachs in cm s^{-1}. Positive values represent eastward flow; negative values represent westward flow. Current meter positions denoted by +. Figure taken from Vieria (2000).

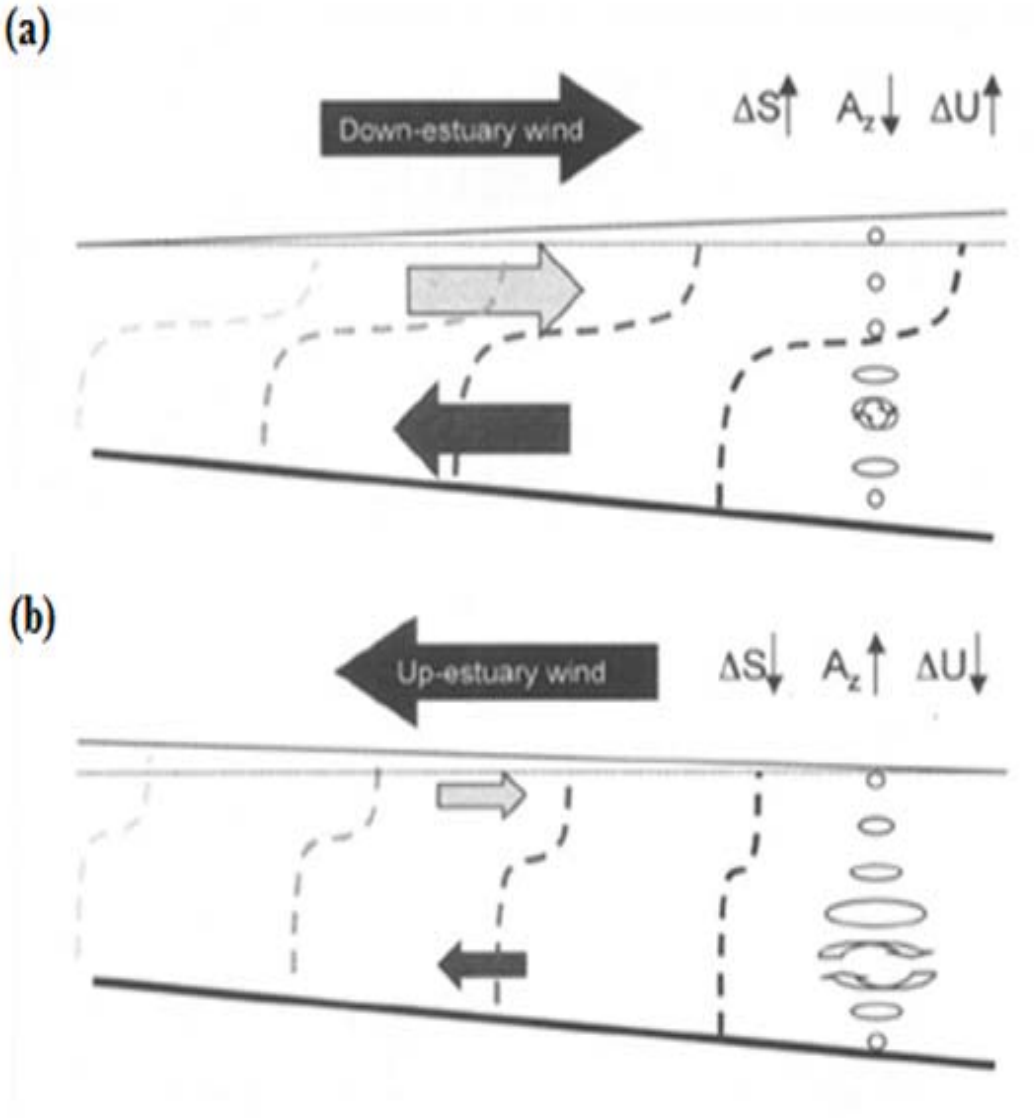

Figure 1.6 Idealized model of wind-induced straining over the estuarine density field with corresponding exchange flows for (a) down-estuary and (b) up-estuary wind schemes. Figure taken from Scully et al. (2005).

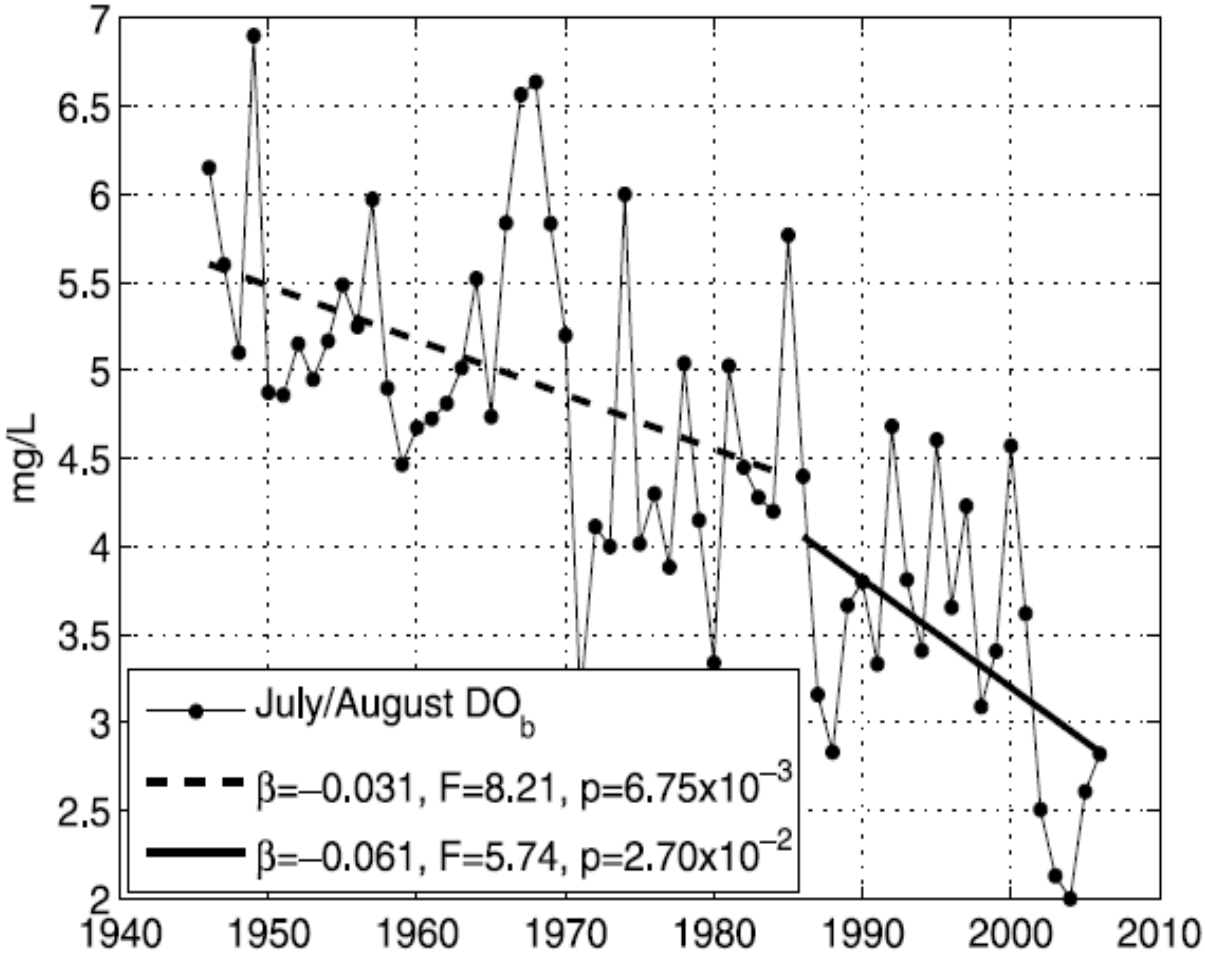

Figure 1.7 Time series for DOb at NYC DEP mooring station E10 averaged over July and August. Figure taken from Wilson et al. (2008).

Chapter II: Data and Methods

2.1. Observational datasets

2.1.1. DOb observations

The primary data source for long term DOb records over wLIS was obtained from the New York City Department of Environmental Protection (NYC DEP) database of water quality data. The NYC DEP routinely conducts water quality surveys throughout the upper East River and wLIS, including dissolved oxygen, temperature and salinity. Station E10 (Hart Island on Fig. 2.1), was used to examine trends in DOb. Since 1946, the sampling period has been weekly or biweekly from June through September (Wilson et al. 2008). From 1946 to 1984, the azide modification of the Winkler methods was used to measure dissolved oxygen. From 1985 through 1987, YSI meters were additionally used. These were calibrated each sampling day using the azide modification of the Winkler method (American Public Health Association 1985). In addition, starting in 1987 a longer cable was used, to extend deeper into the water column, over this station to record DOb. This provided a more accurate measure of the dissolved oxygen content over the bottom waters.

The Long Island Sound Integrated Coastal Observing System (LISICOS) was established in 2003 as a part of a regional/national ocean observing system (O'Donnell et al. 2008). To observe the variability of DO in wLIS at higher temporal resolutions, an instrumented buoy was used to observe vertical changes within the water column near Execution Rock at a mean water

depth of ~ 22.6 m. This buoy is equipped with salinity, temperature and DO sensors (YSI 6920 Sondes) at (1) 0.3m, (2) 7.5m, and (3) 15.5m depths that measured every hour (http://lisicos.uconn.edu/) during 2006, 2008 and 2009 summer seasons. For the 2006 season data was only available 15 August through 20 September. In 2008 the data system failed in early August resulting in about a three week data gap. 2009 was associated with several data gaps including 6 June through 16 June and 7 July through 17 July.

Since 1991, the Connecticut Department of Environmental Protection (CT DEP) has conducted an intensive year-round water quality monitoring program on Long Island Sound. Water quality is monitored at up to forty-eight sites. This data is used to quantify and identify annual trends and differences in water quality parameters relevant to hypoxia, especially nutrients, temperature, and chlorophyll. During the summer (June- September) CT DEP conducts additional summer hypoxia surveys at bi-weekly intervals to better define the areal extent and duration of hypoxia (CT DEP 2010).

Specifically, the variables of duration days and maximum area (table 2.1) are used from the dataset described above, as a proxy for determining the severity of seasonal hypoxia for the seasons of 1991 through 2009 based on the CT 3.5 mg L^{-1} water quality standard. Duration days are defined as the number of consecutive days within the summer season in which DOb values of 3.5 mg L^{-1} or less were observed. In addition, maximum area is used and defined as the maximum areal extent over LIS in which DOb values of 3.5 mg L^{-1} or less were observed.

2.1.2. Atmospheric surface observations

Wind data from La Guardia Airport (LGA) located in northern Queens, New York (Fig. 2.1) was used to estimate the wind conditions over wLIS. This station was chosen given its close

proximity to wLIS and its long-term data availability back to 1935. Wind directions and speeds (m s^{-1}) were obtained from the National Oceanic and Atmospheric Administration (NOAA) National Climate Data Center (NCDC) historical data archives (http://www7.ncdc .noaa.gov/CDO/dataproduct) for the years of 1948 through 2009. For the period extending from 1965 to 1972, wind observations were taken every three hours. From 1948 to 1964 and 1973 to 2009 wind observations were routinely taken every hour.

Bridgeport, CT Airport (BDR) on the north side of LIS was used to determine whether the same trends at LGA extend over a broader region (Fig. 2.1). Using the available BDR data from 1973-2009, the trend in wind speed from June to September is similar between both airports (0.62 correlation). Both datasets show a declining trend in seasonally averaged wind speeds, with the most significant drop occurring from the early 1980's onward. To verify the consistency in wind direction, hourly directional differences are summed every 10° (Fig. 2.3a). The average difference in wind direction difference is 41°, with the most frequent wind direction difference from 1° to 10°.

Since LGA wind data is not over water, the Execution Rock (EXRX; buoy number 44022 at 40.88°N, -73.73°W in Fig. 2.1) buoy wind data over wLIS was used to compare with LGA winds from 2005-2009. The EXRX data was extracted from the National Buoy Data Center (NBDC) website (http://www.ndbc. noaa.gov/station_history.php?station=44022). Since the buoy anemometer height is 3.5m above the surface and the height of the LGA wind data is 10m above the surface; the logarithmic wind profile is used to determine LGA winds at a reduced height of 3.5m (U_1 in equation 2.1), so winds are at the same level to be fair.

$$U_1 = U_2 * \left[\frac{\ln \frac{Z_1}{Zo_1}}{\ln \frac{Z_2}{Zo_2}} \right]$$

(2.1)

in which U_1 is the desired LGA wind speed (m s^{-1}) at 3.5m, U_2 is the LGA wind speed (m s^{-1}) at 10m, Z_1 is the desired wind instrument height (3.5m), Z_2 is the original wind instrument height (10m), and Zo_1 and Zo_2 are the aerodynamic roughness lengths over land (.03m). Since the high resolution LISICOS DOb buoy data and EXRX buoy wind measurements essentially cover the same time period, both sites will be used together to help determine the relationship between winds and DOb over wLIS. Figure 2.4 displays a scatter plot directly relating the winds over LGA (x-axis) reduced to 3.5m, and buoy 44022 (y-axis). A high correlation of 0.86 was found between both of these datasets.

The EXRX buoy 44022 and LGA wind data were directly compared at their original heights of 3.5m and 10m respectively to determine how similar the LGA wind directions and speeds were to those experienced over the wLIS at the buoy location. The relationship between the EXRX buoy wind speeds and LGA has a 0.86 correlation coefficient and an average wind speed difference of 0.75m s^{-1} (Table 2.2). The unfiltered wind speeds were also correlated with a lower correlation coefficient of 0.67 and an average speed difference of 1.26 m s^{-1} (Table 2.2). Figure 2.3b shows the histogram in the wind differences (every 10 degrees) between the EXRX buoy and LGA wind directions (in degrees). The average difference between the wind directions is 38° and most common difference is 10°. Overall, these results suggest that LGA compare favorably with EXRX, thus providing realistic wind forcing conditions over wLIS.

2.1.3. Reanalysis data

Mean sea-level pressure (mSLP) data was extracted using the once daily 2.5° National Centers for Environmental Prediction (NCEP) and National Center for Atmospheric Research (NCAR) reanalysis datasets (Kalnay et al. 1996). This data was utilized to analyze synoptic patterns associated with the wLIS mixing events. Data was downloaded from the Earth Systems Research Laboratory Physical Sciences Division website (http://www.esrl.noaa.gov/psd/data/ gridded/data .ncep.reanalysis.html) from 1948 through 2009. The 500-hPa geopotential heights were also used to evaluate the synoptic scale environment associated with mixing events. The spatial domain extracted from this dataset extends from 25°N to 70°N and 160°W to 50°W.

2.1.4. Daily weather maps

In order to more accurately identify the synoptic weather pattern for each mixing event, NOAA daily surface maps were utilized (http://docs.lib.noaa.gov/rescue/dwm/data_rescue_ daily_ weather_maps.html). These maps were compiled at 00 UTC (19 EST), over the continental U.S. which shows air temperature, barometric pressure, wind velocity and direction, and a general indication of the weather for various cities around the country on the map.

2.2. Methods

2.2.1. DOb and wind analysis

The relationship between DOb and wind was determined over extreme wLIS, where LGA and many of the available DO instruments are located. This includes areas west of Hempstead Harbor and east of the upper East River (Fig. 2.1), where seasonal hypoxia is most

severe and vertical stratification is maximized (Wilson et al. 2008). The temporal scale for this study includes the summer months from June through September during the years1948 to 2009. The years (1948-2009) were selected based on the available NCEP/NCAR reanalysis data for meteorological synoptic analysis, which extends from 1948 to present. The summer months of June and September were selected because the lowest monthly DO typically values occur during these months. The correlations between the seasonally (June-September) averaged DOb and monthly average DOb for each month break down as follows; June (0.53), July (0.73), August(0.82),and September(0.38). Because the high correlations of minimum DOb that occur during July and August, these months are isolated for selected analyses to obtain the most robust responses.

The spatial domain for the synoptic analysis for the DOb mixing events ranges from an area extending within the quadrilateral perimeter seen in figure 2.5. This area size was chosen to identify as many relevant synoptic systems as possible, while at the same time focusing in around northeast U.S. and southeast Canada. All synoptic events for the months of June through September are included for years 1950-2009.

2.2.2. Filtering techniques

All data analyses including; *u* and *v* wind components, DO, and temperature variables were filtered using a low-pass digital Butterworth filter (http://www.mathworks.com/help/toolbox/signal/ref/butter.html). It returns the filter coefficients in length $n+1$, with coefficients in descending powers of z. The low-pass filter for H(z) can be expressed using equation 2.2 below.

$$H(z) = \frac{b(1) + b(2)z^{-1} + \cdots + b(n+1)z^{-n}}{1 + a(2)z^{-1} + \cdots + a(n+1)z^{-n}}$$

(2.2)

in which b and a are the numerator and denominator filter coefficients respectively of the infinite impulse response filter (IIR) designated in the 'butterworth' function. A 5th order low-pass filter with a cut off frequency of 34 hours, consistent with studies conducted by O'Donnell (2008) and Wilson et al. (2008), was used to filter out the diurnal wind variations, and tidal influences that can contaminate DO and temperature measurements. This filter is used in an attempt to isolate regimes on the temporal scale of synoptic periods over LIS.

2.2.3. Criteria for mixing events

The following methods were utilized to determine the most relevant and efficient wind speeds and directions in calculating seasonal mixing event frequencies. For the below analyses all potential mixing event criteria will be referred to 'wind events' to reduce confusion.

The duration (in days) of summer hypoxia from the CT DEP hypoxia was utilized to acquire a relationship between LGA, buoy winds and hypoxia on a seasonal scale. Seasonal wind percentages were extracted for 18, equally spaced wind bins (every 20°) and three wind speed thresholds (2, 4, and 6 m s^{-1}). These wind criteria were then correlated to how many consecutive hypoxic (less than 3.5 mg L^{-1}) days were observed.

Lagged correlations were performed between directional wind stress over EXRX buoy 44022, and DOb as well as thermal stratification data using the LISICOS (EXRX) monitoring buoy station data. The thermal stratification parameter was calculated by subtracting surface water temperatures from bottom water temperatures. These correlations were then displayed

as lagged values to better understand the temporal response due to wind. A cross correlation analysis was also performed to determine the relationship between bottom temperature and DOb and the associated temporal lag.

Understanding the temporal influence specific wind events have on the water column is essential in verifying and understanding the physical nature of synoptic wind events and vertical mixing/ventilation of bottom DO. EXRX buoy 44022 meteorological data and LISICOS (EXRX) monitoring buoy station data was used in a set of analyses to evaluate the effectiveness of wind events in ventilating bottom waters and increasing DOb. Different criteria were then compared using these various analyses to determine what directional and speed thresholds were most efficient and consistent at inducing periods of 'ventilation' or mixing. For many of the analyses speed thresholds of 2, 4, and 6 m s^{-1} were used to determine the sensitivity of the physical response to wind velocity. In addition, directional bin intervals of 20° for bins of either 20° (i.e. 20°-40°) or 80° (i.e. 0°-80°) were used to obtain the most precise wind relationship possible.

The vertical cross sections of average DO and temperature for 24 hours prior and 60 hours after wind events were evaluated to assess average trends in the vertical water column structure pre and post wind events. High resolution DO and temperature data were used for the years 2006, 2008, and 2009 over the LISICOS (EXRX) monitoring buoy station. Each time step, spanning a total of 84 hours, was averaged over each calculated wind event. DO values were then averaged for time steps +12hrs through +60hrs for three levels: surface (0.3m depth), mid-level (7.5m depth), and bottom (~15.5m depth). This provided a way to visualize the average response of the water column after the passage of a synoptic wind event. Contour plots were then created for each averaged time step. Differences between surface and bottom, as well as surface and mid-level DO values were calculated to determine periods of uniformity between the bottom

and surface DO fields. Additionally, to determine the rate at which DO fluctuated, the hourly percentage change of DO was calculated for time steps +24hrs through +60hrs using a first time derivative of DO ($\frac{\partial DO}{\partial t}$) and temperature ($\frac{\partial T}{\partial t}$).

For the decadal analysis, correlations were preformed between seasonal percentages of winds between 30°-110° and equal to or greater than 4 m s^{-1}, and seasonally averaged DOb using NYC DEP data, for three 20 year periods (1950-1969, 1970-1989, and 1990-2009).

The Wedderburn (*W* in eq. 2.3) number was also used to help accurately determine the most accurate wind stress (speed) value to use for defining mixing events. This is a non-dimensional parameter with relative importance between wind stress and baroclinic pressure gradient force (Chen and Sanford 2009). The Wedderburn number can be determined by using

$$W = \frac{12\tau}{g\nabla\rho H^2} \quad (2.3)$$

where τ is wind stress magnitude (N/m^2), g is gravity (m/s^2), $\nabla\rho$ is the horizontal density gradient (kg/m^4) within the water column and *H* is water column depth (m). When $W >> 1$; the applied wind stress is less than the buoyancy force indicating strong vertical stratification with limited horizontal variability. For $W \sim 1$; assumes the wind stress and buoyancy forcing are equivalent, signifying water column mixing is important. When $W << 1$; the temporal period for vertical mixing is reduced compared to horizontal advection (Monismith 1986).

2.2.4. Calculation of mixing events

In order to develop a daily time series of mixing events over wLIS, mixing event days were calculated for each season using specific direction, speed and duration criteria using filtered

LGA wind data. Days in which at least 50% of the daily wind observations exceeded 4m s^{-1} and were within the 30°-110° directional bin, were designated as a 'mixing event'. The reason for these criteria will be highlighted below in section 2.2.6. The start of a mixing event was defined at 00 UTC of the calculated mixing day. A 24 h period had to exist between recorded mixing events to allow the water column to return back to steady state. The monthly and seasonal frequency of mixing events were then totaled and classified depending on the type and position of relevant synoptic cells. In addition, anomalous seasons were labeled as active or inactive according to standard deviations based on the long term 1950 to 2009 averages. Important to note that the term 'mixing event' does not necessarily mean that any particular event results in a subsequent increase in DOb due to de-stratification of the water column. Instead, 'mixing event' refers to a day in which the directional, speed, and durational criteria are favored for mixing. In addition, wind direction bins of 10° on either side of the original 30°-110° directional thresholds as well as 2 m s^{-1} and 6 m s^{-1} were tested to determine how sensitive the mixing event frequency output was to changes in wind direction and speed.

2.2.5. Determining synoptic systems for mixing/stratifying event climatology

Once the mixing events were obtained, National Oceanic and Atmospheric Administration (NOAA) surface weather charts were used to manually classify the synoptic patterns associated with mixing event days. The monthly and seasonal frequency of mixing events were then totaled and classified depending on the type and position of the synoptic pressure pattern or front during the time of mixing. For a system to be defined as a "cyclone" the center of the system must enter the spatial domain explained in section 2.2.1 and have a closed mSLP pattern with a value <= 1012hPa. The "anticyclones" had to be >= 1020hPa, but they did not need to be a closed pressure system. If a system failed to meet any of the above criteria then

it was not considered for the climatology (event days in which the pattern was unidentifiable were referred to as miscellaneous events). Each event was then categorized based on the type and location of synoptic systems involved during the time of mixing. There were three classification groups with each group containing sub-category synoptic patterns: low pressure, high pressure and hybrid groups. Each synoptic pattern (Regional Low, Coastal Low, Pre-High, Extended High, Northern High west, Northern High center, Northern High east) is described below, strongly following the synoptic classification categories of Yarnal (1993).

The Regional Low (RL) pattern is associated with a cyclone passing through the northeast region typically to the north and west of LIS (Fig 2.6a). These patterns are comparably weak to the coastal low patterns, and approach from the west-northwest and bring precipitation and northerly winds. The Coastal Low (CL) pattern can be associated with extra-tropical storms and hurricanes that are along the northeast U.S coast, and then track out to sea, thus inducing strong northeast winds and precipitation over LIS (Fig 2.6b). To be classified as a CL the system was required to be over water during the time of the mixing event day.

The Pre-High (PH) patterns is defined when a high pressure system, typically over the Great Lakes region, trails the passage of a cold front usually associated with a low pressure system to the north over the Hudson Bay region (Fig 2.6c). These systems typically track in a northwest to southeast manner. The Extended High (EH) pattern is associated with an extensive blocking surface high feature that typically extends from southeastern Canada through the northeastern states, usually orientated northeast to southwest (Fig. 2.6d). This pattern often precedes a cold frontal passage and possesses relatively strong northeast winds.

The Northern High west (NHw) hybrid patterns is typically associated with a high over the Great Lakes region followed downstream by a surface low, typically off the coast (Fig. 2.7a). The Northern High center (NHc) pattern is associated with a high pressure cell to the north, typically just downstream of the Great Lakes, with corresponding low pressure cell to the south (Fig 2.7b). The low pressure system is usually weak with a frontal pattern extending into the northeast domain with winds on average from the east. The Northern High east (NHe) patterns typically results in very strong pressure gradient inducing strong northeast winds. This hybrid pattern is coupled with a high extending over the northeast and low pressure typically off the northeast coast (Fig 2.7c).

2.2.6. Surface and upper-level synoptic background environments.

Determining the large scale synoptic environment during the times of synoptic mixing events is essential to better understand relevant environments conducive to mixing. Mean and anomaly 500-hPa geopotential heights will be composited using NCEP/NCAR reanalysis data for each synoptic pattern. Composites will also be made for inactive and active seasons to aid in determining significant synoptic features. In addition, the surface and upper-level synoptic evolution for low and high pressure events, including Regional Low, Coastal Low, Pre-High and Extended High patterns, will be analyzed based on mSLP and 500-hPa geopotential height mean and anomaly composites for daily time lags of -4 to 0 days.

2.2.7. Bootstrap method

The bootstrap method was used to determine the statistical significant for many of the results (Xu 2006). Using the available data as an approximation for the population density function, data are resampled several times randomly, replacing the original observed sample to

generate uniform random numbers to draw data from the available raw data. For this case, data are resampled 2000 times and calculated to the 90% confidence interval.

Tables

Year	Estimated Start Date	Estimated End Date	Maximum Area (km ^{2})	Duration Days
1991	July 8, 1991	September 1, 1991	681.68	56
1992	July 7, 1992	September 12, 1992	503.75	68
1993	July 5, 1993	September 12, 1993	869.98	70
1994	July 1, 1994	September 16, 1994	1330.48	71
1995	July 9, 1995	August 28, 1995	1076.40	51
1996	June 26, 1996	September 13, 1996	881.63	80
1997	July 15, 1997	September 17, 1997	132.09	65
1998	July 2, 1998	September 19, 1998	741.00	80
1999	June 27, 1999	August 24, 1999	594.14	59
2000	June 29, 2000	August 8, 2000	673.91	41
2001	July 5, 2001	September 24, 2001	558.66	82
2002	June 20, 2002	September 4, 2002	502.20	76
2003	June 30, 2003	September 3, 2003	1115.25	66
2004	July 23, 2004	September 26, 2004	666.92	66
2005	July 7, 2005	September 23, 2005	777.51	79
2006	July 4, 2006	August 29, 2006	896.39	57
2007	July 12, 2007	September 21, 2007	916.86	72
2008	June 30, 2008	September 20, 2008	932.14	83
2009	July 12, 2009	September 3, 2009	957.26	54
Average	July 4	September 10	761.46	66
Deviation	+/- 7 days	+/- 14 days	+/- 274.54 km^2	+/- 13 days

Table 2.1 1991 to 2009 start and end dates for duration days including maximum area (km^2). Averages and deviations are also included for each category. Numbers are courtesy of CT DEP 2010 Long Island Sound Hypoxia Season Review (2010).

Statistic	3.5 m Buoy and 10m LGA Filtered wind magnitudes	3.5 m Buoy and 10m LGA Unfiltered wind magnitudes
correlation	0.86	0.67
Average difference	0.75 (m s^{-1})	1.26 (m s^{-1})

Table 2.2 Statistics including correlations and average wind magnitude differences between 34 hour low-pass filtered and unfiltered 3.5m buoy 44022 and 10m LGA wind magnitude data.

Figures

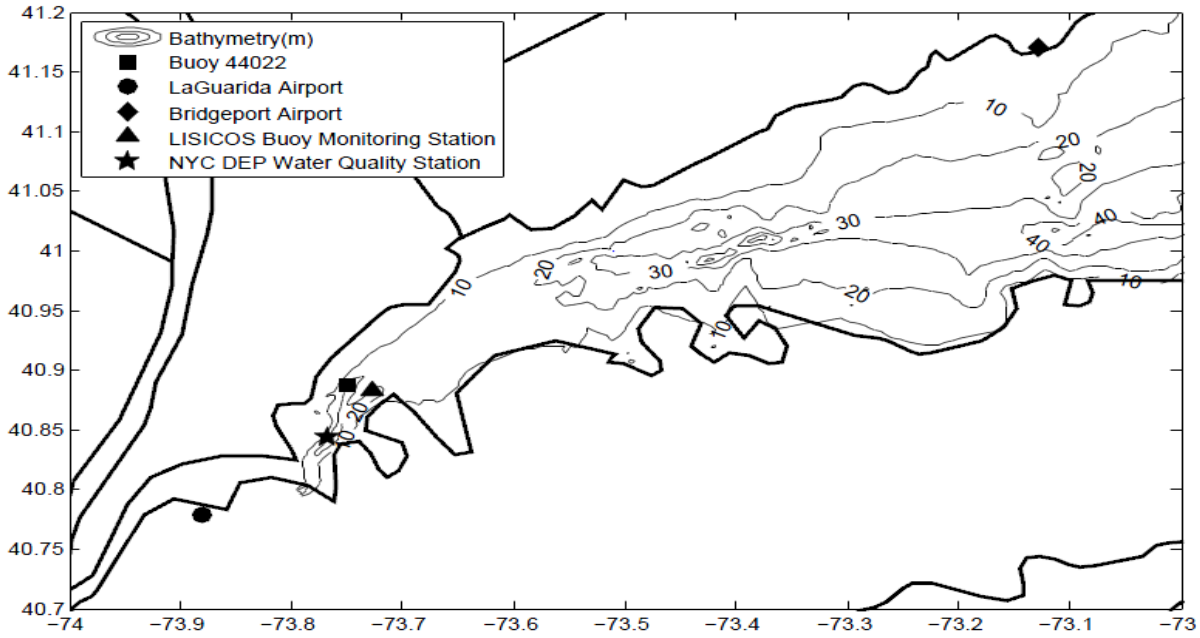

Figure 2.1 Map of wLIS including data site locations. Bathometry (m) is contoured.

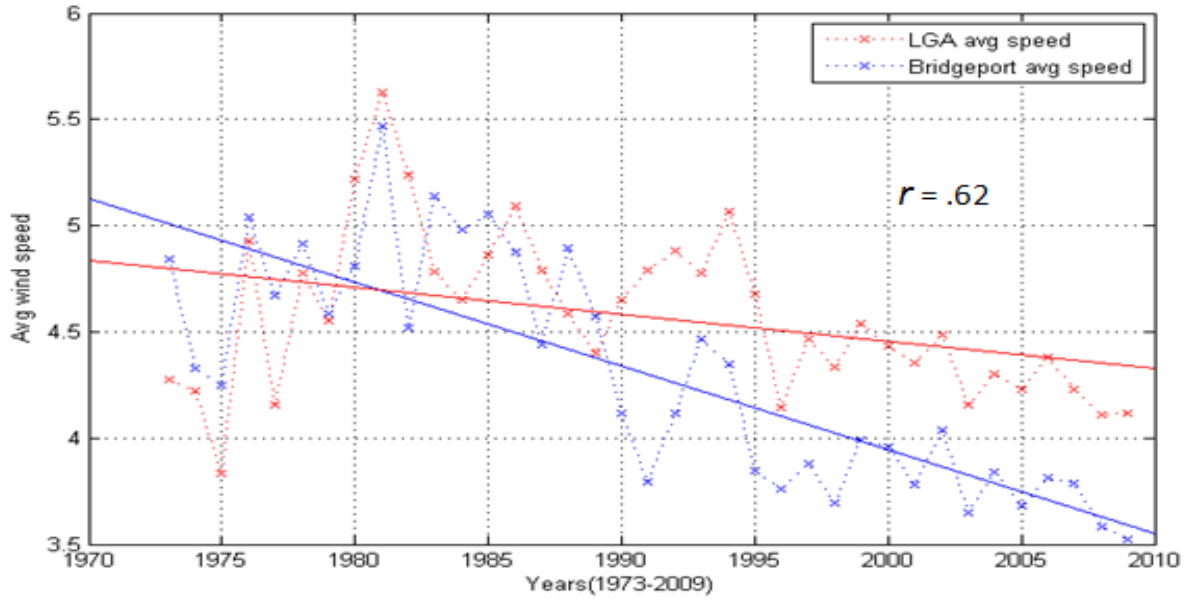

Figure 2.2 Seasonal (June-September) average wind speed (m s^{-1}) for years 1973-2009 for LGA (red) and BDR (blue). Regression lines are also included with *r* value of .62.

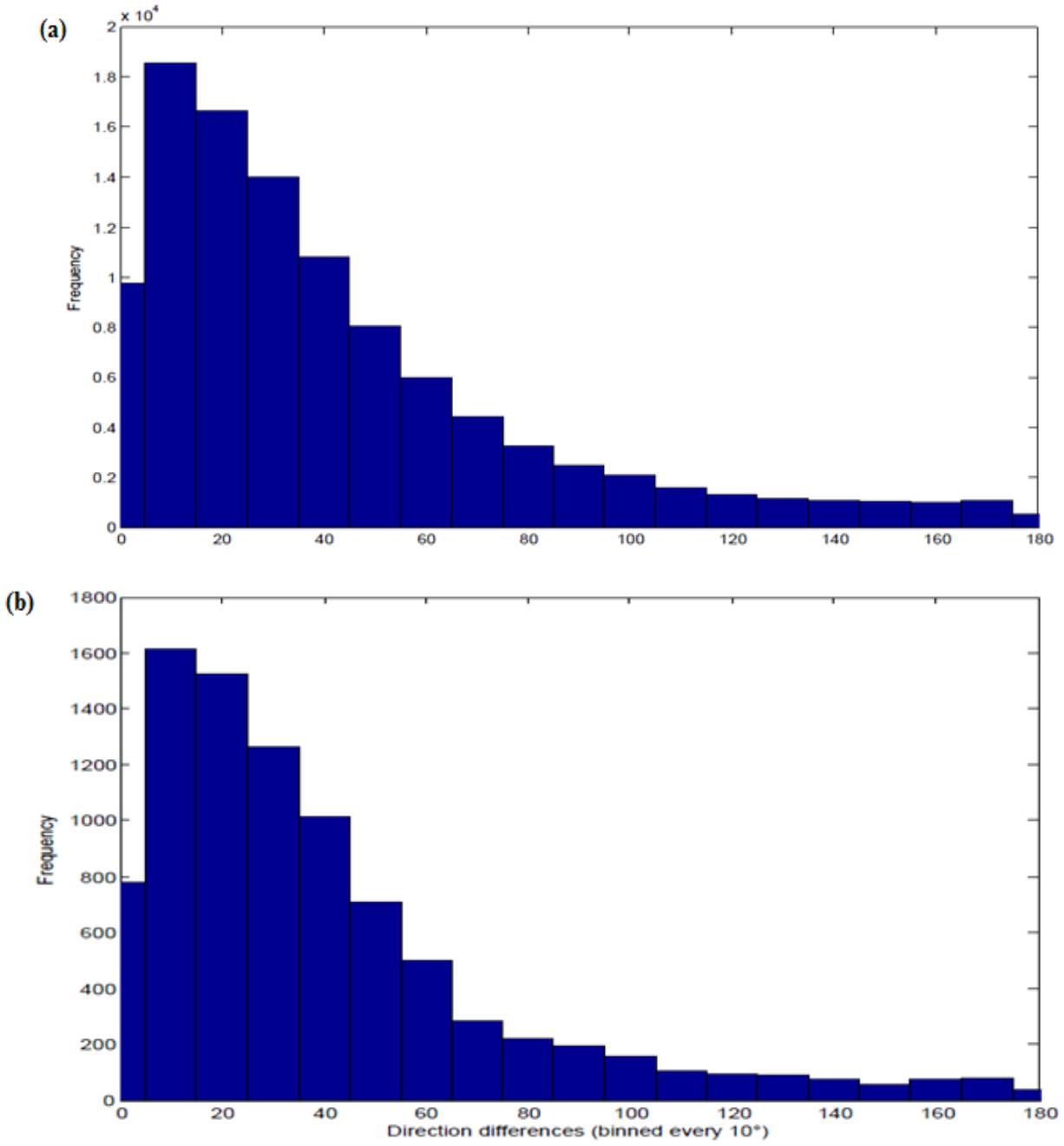

Figure 2.3 Histogram of frequency directional wind differences between (a) LGA and BDR and (b) LGA and buoy station 44025 datasets. Note y-axis in (a) is multiplied by 10^4. Directional bins incremented every 10°.

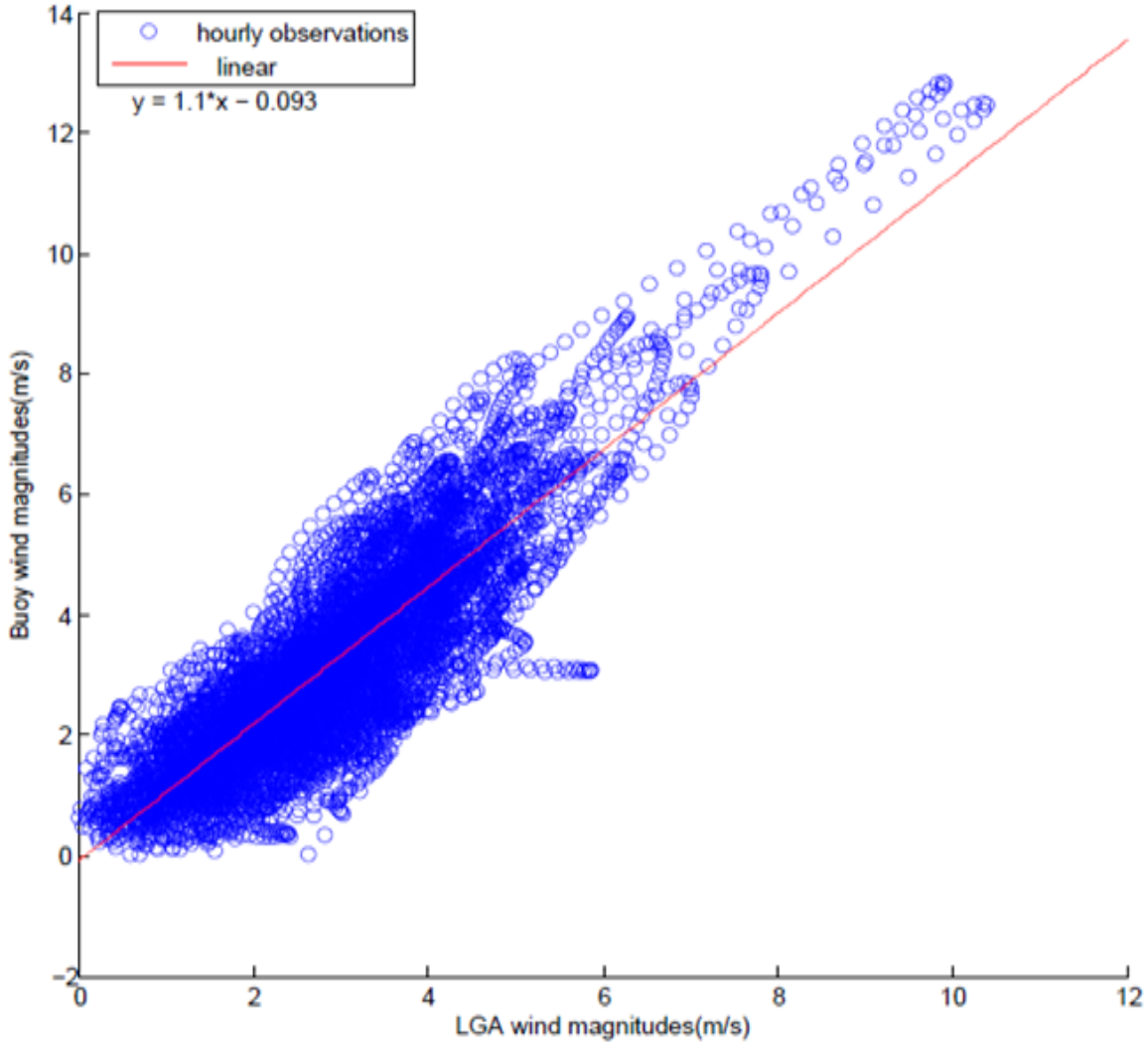

Figure 2.4 Scatter plot of filtered 3.5m EXRX buoy 44022 wind magnitudes and 3.5m LGA wind magnitudes. LGA wind magnitudes reduced from 10m to 3.5m using logarithmic wind profile equation. Linear regression line (red) also included.

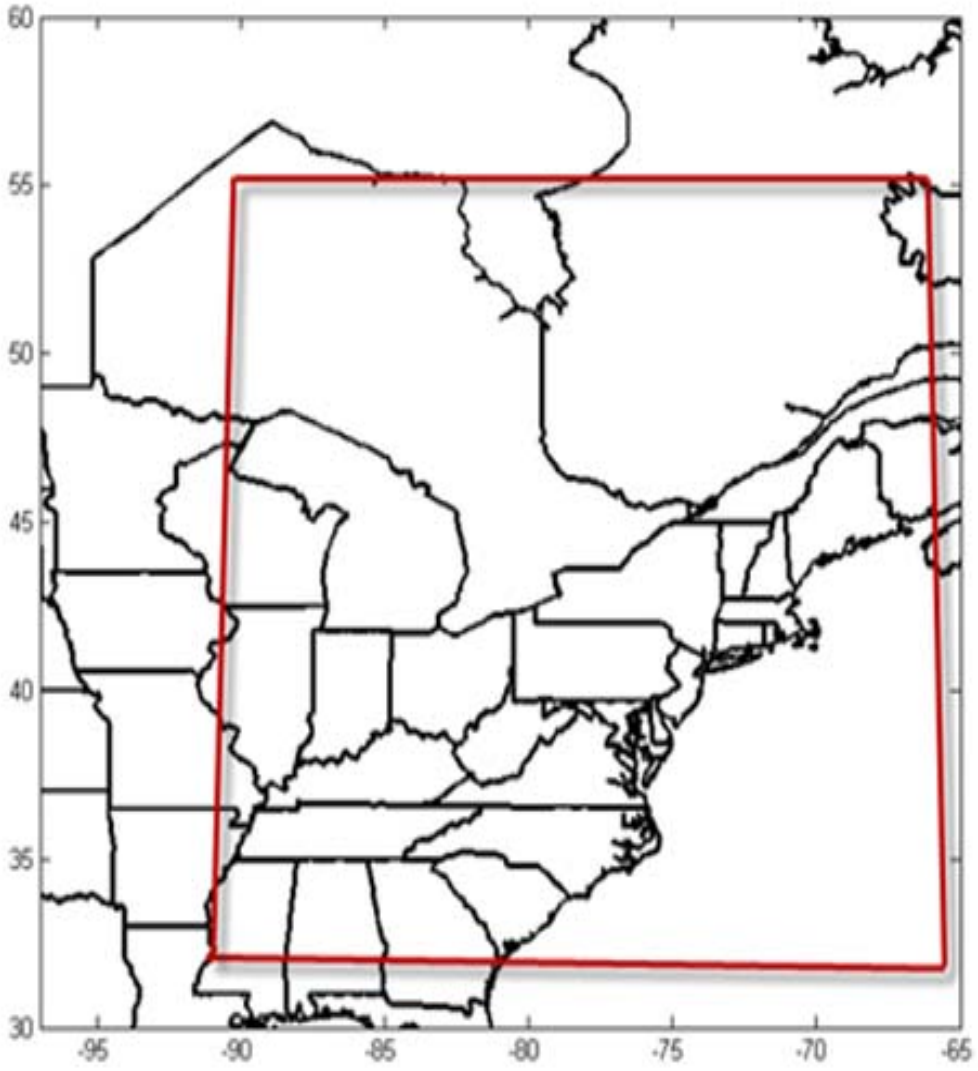

Figure 2.5 Quadrilateral domain for synoptic climatology. Center of synoptic system had to come within the perimeter to be considered for the climatology.

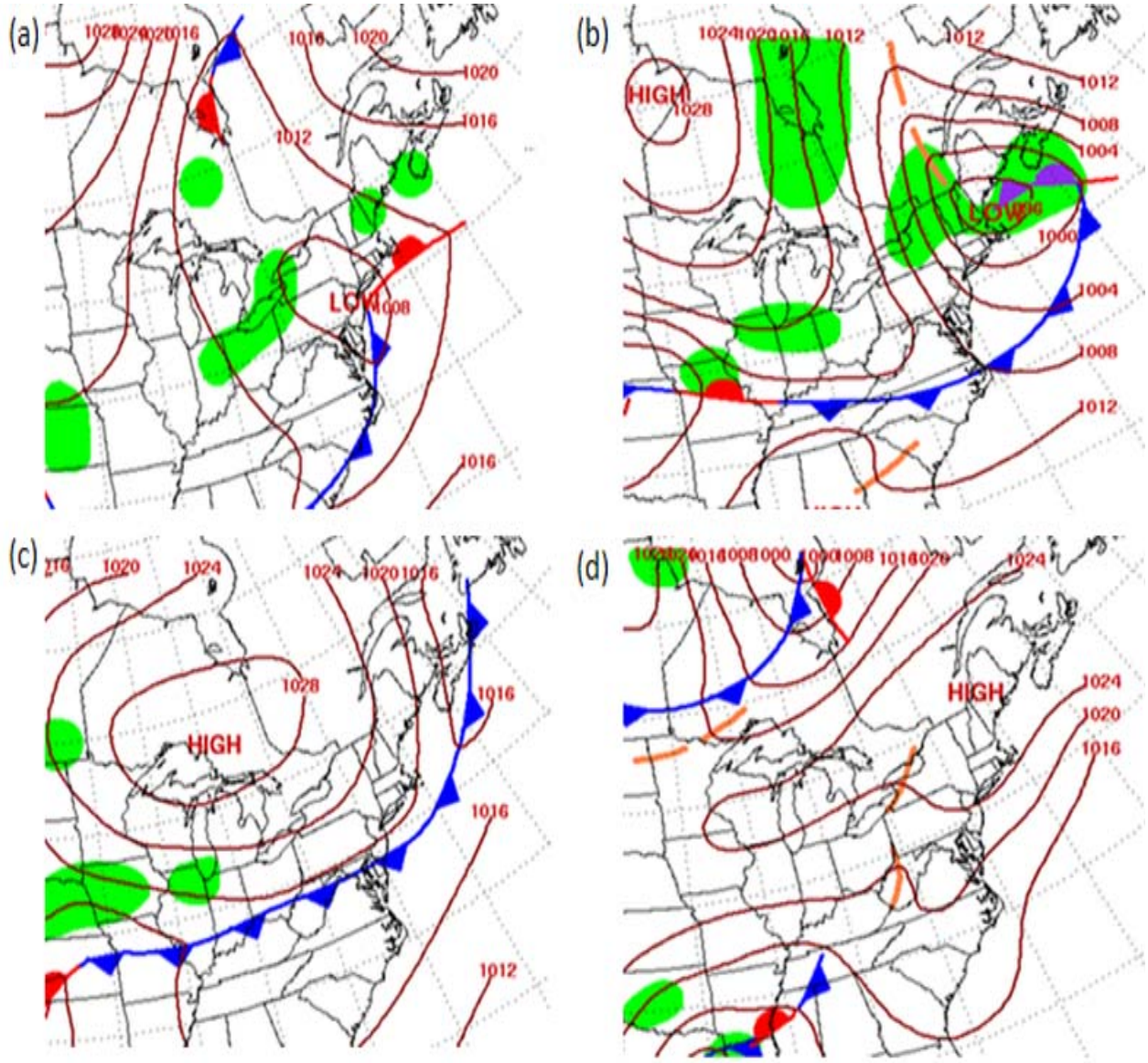

Figure 2.6 Examples of low pressure patterns: (a) Regional Low (RL) 2 July 2009 12 UTC and (b) Coastal Low (CL) 10 June 2006 12 UTC . High pressure patterns: (c) Pre-High (PH) 10 September 2006 12 UTC and (d) Extended High (EH) 17 September 2009 12 UTC using NOAA daily surface plots.

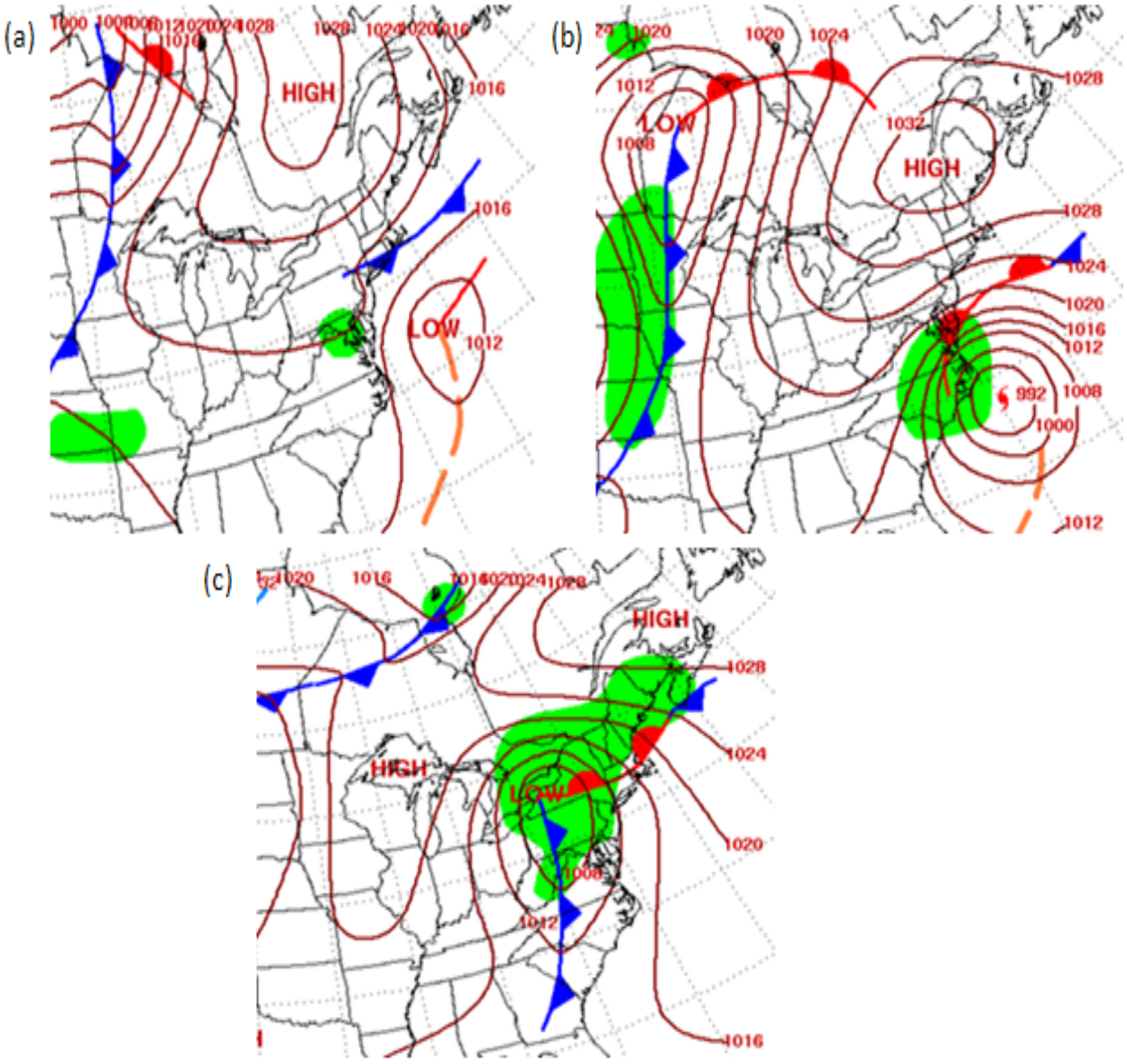

Figure 2.7 Examples of hybrid patterns : (a) Northern High west (NHw) 9 September 2009 12 UTC , (b) Northern High center (NHc) 18 September 2003 12 UTC, and (c) Northern High east (NHe) 11 July 2003 12 UTC using NOAA daily surface plots.

Chapter III: Relationship between seasonal evolution of DOb and synoptic wind regimes

This chapter investigates the relationship between surface winds and the effects on DOb for various temporal scales. This section utilizes several data sources that help explore ways wind forcing can be linked to different time evolutions of DOb.

3.1. DOb variations for different temporal scales

3.1.1. Seasonal DOb variations

Figure 3.1 highlights how DOb changes throughout the year over wLIS. DOb was averaged for each month, including years 1948 to 2009, using the NYC DEP Hart Island (E10) mooring dataset. Maximum DOb values are observed in March when the water column is thoroughly mixed. After March the DOb values for each month subsequently decrease until a minimum is observed in August. The winter season, January through March, are associated with the highest values on average while the summer season, July through September, has the lowest DOb concentrations.

3.1.2. Inter-annual DOb variations

Figure 3.2 shows the decadal variability of wLIS DOb for June and August from 1948 to 2009, as well the seasonal average (June, July, August, September) DOb. June has a slight

decreasing trend starting from roughly 7 mg L^{-1} in the 1950's through the 1960's to near 6 mg L^{-1} in the 1990's and early 2000's. In comparison, the monthly averaged DOb for August has a more significant decreasing trend, with DOb from approximately 5 mg L^{-1} on average in the early part of the 1950's to well below 3 mg L^{-1} in the early 2000's. The seasonal average DOb shows a general decline that becomes accelerated in the early 1980's into the late 2000's. This illustrates that the more frequent hypoxic episodes experienced over wLIS in recent decades are more likely the result of late season declines in DOb as opposed to the entire season being anomalous low.

3.1.3. Daily DOb variations

DOb fluctuations also exist on daily to weekly time scales due to surface wind stress forcing and mixing. For example, from 19 July 2008 to 29 July 2008, the DOb at the EXRX buoy increased from 1 mg L^{-1} on 22 July to over 3 mg L^{-1} on 25 July 2008 (Fig. 3.3b). NCEP/NCAR daily composite mSLP on 21 July at 12 UTC shows an extratropical cyclone over the Nova Scotia region (Fig. 3.4). With this storm to the northeast of the New England states, the large scale wind flow over wLIS was north-northeasterly for the period extending from 21 July through the 23 July as seen in the LGA wind data (Fig. 3.3a).The winds remained north-northeasterly for almost three consecutive days, after which the LGA winds became southerly and the DOb values subsequently decreased to between 1.5 mg L^{-1} and 2 mg L^{-1}.

A second example of short-term DOb increases is provided that involves a surface high pressure event from 24 August 2008 through 31 August 2008. The increase in DOb associated with this event was more gradual from 26 August, when the DOb value was roughly 1.25 mg L^{-1}, to 30 August when its maximum value of around 3 mg L^{-1} was reached (Fig. 3.5b).This event was associated with a Pre-High synoptic pattern, in which surface high pressure approaches from

the west after a cold frontal passage over the northeast U.S. (Fig. 3.6). As the front passes over the region and the high builds in, the surface winds shift from southerly on 25 August to north-northeasterly on 26 August (Fig. 3.5a). This pattern continues until 28 August when winds become light and variable and shift to a more southerly component. What is noteworthy about this case is the relaxation of the water column, typically resulting in a subsequent decrease in the DOb field, does not occur during this case. Instead, approximately two days after the time the winds become lighter and more variable on 28 August, DOb values drop slightly to 2.5 mg L^{-1} on 30 August, but consequently rise again after the winds shift to a northerly component on 31 August.

3.2. DOb dependence on wind speed and direction

3.2.1. Daily DOb and wind relationships

Temperature of the water column is often a good proxy for vertical mixing due to the exchange of water properties between the surface and bottom water interfaces when vertical water column ventilation occurs. To determine the extent of this relationship over wLIS a cross-correlation analysis was performed using low-pass filtered LISICOS EXRX buoy DOb/temperature data (Fig. 3.7). A maximum correlation of 0.42 at lag hour -1 is found with decreasing values on either side, indicating a similar relationship between DOb and temperature.

Figure 3.8a displays the lagged correlation values between buoy 44022 wind direction data and LISICOS EXRX buoy DOb. A robust correlation pattern is apparent with the highest positive correlations associated with winds between the north and east directions (0° - 100°). There exist moderate negative correlations for winds from the south to west directions (180° - 280°). Highest correlations, indicated by the '+' ('*') symbols, are centered at 62° (245°) for

wind directions that favor mixing (stratifying). This figure also illustrates that a lag of approximately two days exists between the time of winds and the response to DOb values. Correlations between thermal stratification and wind directions were also performed (Fig.3.8b). The thermal stratification is calculated by subtracting the surface water temperature from the bottom water temperature for a given hour. In general the correlations experienced are considerably less than those for DOb in figure 3.8a; however, the change in sign of the correlation for different wind directions is similar to the DOb and wind relationship.

Figure 3.9 represents the frequency of observations, for each of the eighteen 20° buoy 44022 wind bins, in which both LISICOS EXRX buoy temperature and DOb increased (minimum increase of .0025 mg $L^{-1}h^{-1}$) for the years 2006, 2008, 2009. The DOb and temperature increase is associated with a high frequency of northeast winds, specifically for the 60° to 100° directional bins; with the least frequent increases occurring for winds from 250° to 330°.

3.2.2. Seasonal hypoxia and wind variability

A robust seasonal wind directional relationship was found between the CT DEP hypoxia duration days for 1991 to 2009 and the percent of hourly summer winds from different directions (Fig. 3.10a). High negative correlations of at least -0.4 were found for winds out of the northeast (340° -80°), with the most significant correlations centered on 50° for both 2 m s^{-1} and 4 m s^{-1} speed thresholds (-0.70 correlation coefficient). The p-value distribution is consistent with the correlation values (Fig. 3.10b), where the highest confidence (p-values less than .05) can be attributed to the 40° to 60° directional bin. These statistics imply that seasons associated with an anomalously high percentage of winds that are out of the northeast (40°-60°) and >=4 m s^{-1} result in a reduced frequency of hypoxia duration days.

When comparing the seasonal percentage of winds to maximum areal extent of hypoxia data from CT DEP, positive correlations are modest for stratifying wind directions (140°-180°) and negative correlations are insignificant for north and east mixing wind directions (Fig 3.11a). The highest correlations and p-values (Fig. 3.11b) occur with winds centered at 170° associated with winds greater or equal to 2 m s^{-1}. This illustrates that when a high percentage of winds are weak and southerly, the areal extent of hypoxia is enhanced. However, no relationship is apparent between the relevant mixing wind directions (north to east) and the seasonal areal extent of DOb.

3.2.3. Decadal relationship between wind and DOb

Seasonal wind percentages for the summer seasons of 1950 through 2009 are provided for winds 30° - 110° using speed thresholds of 2 m s^{-1}, 4 m s^{-1} and 6 m s^{-1} ; using the NYC DEP Hart Island mooring DOb data and LGA wind data (Fig. 3.12). Additionally, seasonally averaged DOb is included for comparison in figure 3.12. Table 3.1 is provided to highlight correlations between seasonal wind percentages and seasonal DOb for decadal periods including; 1950-1969, 1970-1989 and 1990-2009.

Least square regression lines are applied to wind speeds of 2 m s^{-1} and 6 m s^{-1}, represented by black dotted lines in figure 3.12 to represent the climatological trends (1950-2009). An increasing decadal trend (1950-2009) of wind speed is visible for the 2 m s^{-1} threshold; however the 6 m s^{-1} trend shows little speed variability over this 60 year period. For the 1950-1969 period (Table 3.1), significant correlations exist (0.65) and p-values close to 0 while 0.52 correlations with p-values of .02 exist for the 2 m s^{-1} and 4 m s^{-1} thresholds respectively. In contrast, for the 1970-1989 periods, no significant correlations were reported for any of the three

speed thresholds. Correlations become more apparent during 1990-2009, for the 4 m s^{-1} and 6 m s^{-1} threshold (0.42 correlations with 0.07 p-value and 0.46 with 0.04 p-value respectively), but the correlations are less than the 1950-1969 period.

3.3. DOb wind events

Understanding the temporal influence specific wind direction and speed criteria have within the water column is essential in verifying and understanding the physical nature of synoptic wind events and vertical mixing/ventilation of bottom DO. To determine the best criteria for mixing, this section will test different "wind event" criteria to evaluate the effectiveness of wind-induced ventilation processes and increasing DOb. EXRX buoy data for the years 2006, 2008, and 2009 are used. In addition, due to the relatively small sample size and low correlations in the previous section for the 6 m s^{-1} threshold, it is disregarded; and only the 2 m s^{-1} and 4 m s^{-1} will be utilized.

3.3.1. Wind event criteria comparisons

Figure 3.13 provides hit rate percentages of wind events that resulted in an increase of DOb. This was calculated by extracting the total number of wind events for 18 different 80° wind bins incremented every 20° (i.e. 0°-80°, 20°-100°, 40°-120° etc..) using 2 m s^{-1} and 4 m s^{-1} thresholds. After the total number of wind events was identified for each wind bin, the DOb slopes for each of these events were calculated using the period of -12 h before the start of the events to +36 h after the start of the event. This provides a slope of Δ DOb (mg L^{-1}) per observation hour over a 48 h period. If the slope was greater than 0 mg L^{-1} h^{-1} then it was extracted as an increasing DOb event. The number of wind events that resulted in increasing

DOb were then divided by the total number of wind events to obtain a percentage for each speed and directional bin. It was found that winds out of the northeast, specifically wind events calculated with the center of the directional bin between 60° and 110° and winds greater than 4 m s^{-1} , have the highest probability of resulting in an increase in bottom DO. This directional range has percentages exceeding 85% (Fig. 3.13). In addition, for southerly winds, percentages decreased dramatically with the center of directional bins 180° to 280° resulting in 0% hit rate for the 4 m s^{-1} threshold and less than 30% for the 2 m s^{-1} threshold.

Figure 3.14 shows a comparison between the total number of days in which DOb increases and the number of wind events associated with rising DOb values. All days in which DOb increased were compared to wind event days, using all 18 directional bins for the 4 m s^{-1} speed threshold. All positive slope days were considered and compared to the corresponding wind event day as well as one day after the wind event, providing a 48 hour window for the water column to respond to the wind events. Matching periods were then obtained as a percentage of all positive slope days associated with wind events. Additionally, the +1 standard deviation values about the mean for the slope days were calculated. Only days that exceeded this +1 standard deviation threshold were extracted. The +1 standard deviation DOb slope days were then re-compared to the wind event days to obtain a total percentage. The largest percentage increases are attributed to directional bins centered between 60° and 120°in which percentages increased from ~20% to greater than 40% using DOb increases at or above +1 standard deviations. This is compared to wind events with directional bins centered out of the south between 180° and 240° in which these directional bins account for 0% of the daily DOb increases for days in which DOb increased +1 standard deviation.

Using the Wedderburn number is a way of expressing a balance between surface wind stress and the pressure gradient force within wLIS. For this study, it is used as a diagnostic to help determine the best wind speed to utilize in describing wind events. Average documented conditions representing the wLIS environment are used for equation 3.1:

$$\omega = \frac{12\tau}{g\nu\rho H^2}$$

(3.1)

From Crowley (2005), g = 9.8 m s^{-2}, ρ = 5.056x10^{-5} kg m^{-3} and H = 23 m were used to describe the conditions over wLIS. The wind stress (τ) values of 0.0126 N m^{-2}(2 m s^{-1}) and 0.0224 N m^{-2} (4 m s^{-1}) were used to determine which ω value is closest to 1. It was found that for the 0.0126 N m^{-2} (2 m s^{-1}) case the ω value is only 0.577, suggesting that the time scales for vertical wind are small compared to horizontal advection. In contrast, the 0.0224N m^{-2} (4 m s^{-1}) case resulted in a ω value of 1.02, which indicates that wind induced mixing is relevant over this region. This confirms the choice of using 4 m s^{-1} as a minimum threshold to use in identifying wind events for synoptic temporal scales. This is consistent with the correlation results from previous sections that document 4 m s^{-1} as the most efficient speed thresholds to use for water column mixing.

Based on the results presented in the above sections, a wind direction range of 30° to 110° and speeds greater than 4 m s^{-1} are the most appropriate criteria to use in extracting mixing events that induce significant short term increases in DOb. Important to note that these mixing events are really events that have winds that increase the likelihood of mixing, since there are other factors that control mixing other than winds. Sensitivity tests were performed to determine if a significant change in mixing event frequency would occur if the directions and speeds

changed. Correlations between directional ranges of 30°-110° and 20°-100° (correlation 0.95) and 40°-120° (correlation .82) were preformed(Table 3.2a). In addition, correlations of 0.60 and 0.51 for the 2 m s^{-1} and 6 m s^{-1} speed thresholds were found respectively (Table 3.2b). These correlations validate that mixing event frequencies and trends are not overly sensitive to slight differences in speed and directional criteria.

3.3.2. Time-depth evolution for mixing events.

A time-depth analysis allows one to visualize the ventilation process in the water column before and after the time of a mixing event. The directional thresholds used throughout this analysis to represent mixing events will be 30°-110° and speeds greater than 4 m s^{-1} using LGA wind data. All mixing events (10) for the 2006, 2008, and 2009 summer seasons are extracted, and their DOb and temperature values are averaged for periods -24 h before the start of an event to +60 h after the start of an event using LISICOS EXRX buoy data.

Figure 3.15a shows surface water DO decreasing on average from 6.5 mg L^{-1} at the start of the event (hour 0) to around 5.5 mg L^{-1} 24 h afterwards. Conversely, bottom water DO increases on average from 2.5 mg L^{-1} to over 4 mg L^{-1} about 48 h after the start of the event. Figure 3.15b displays this difference between the surface and bottom DO values that result in a steady decrease. Subsequently the line plateaus at 2 mg L^{-1} 36 h after the event, indicative of a well mixed environment. In support of this finding, figure 3.16a shows a significant gradient of changing bottom DO that exists at around 12 to 24 h after the event, with rate percentages as high as 1% per hour within the bottom layer. This indicates a rapid flux of oxygen to the bottom waters during this period. Figure 3.16b demonstrates the difference between percentage change in DO at the surface and percentage change in DO at the bottom (blue line). Values start to

decrease prior to the start of the event and continue to decrease till they reach - 2% about 15 hours after the event associated with subsequent increases. This indicates that initially there was an exchange of DO from the surface to bottom layers until the system relaxed gravitationally and the oxygen gradient between the air and surface water layer increased, inducing a flux of oxygen into the surface water layer. This is apparent by the increasing rate of DO change over the surface layer 30 to 40 h after the event.

Figures 3.17a and 3.18a indicate that temperatures are observed to decrease over the surface layer at around 12 h after the mixing event, while bottom waters continue to warm until maximum temperatures are observed about 36 h after the mixing events (Fig. 3.17a). Surface minus bottom temperatures decreased by 25% on average, starting at 2°C before the events, and then decreasing to 1.5°C after the events (Fig. 3.17b). In figures 3.18a and 3.18b, although the rate percentages of change are not significant (- .06% to +.12%), the pattern that exists from the surface to the bottom waters is noteworthy. Waters cool rapidly 8 to 12 h before the start of the event, followed by significant warming of the bottom waters 12 to 24 h after the event (Fig. 3.18a). This is a typical response one would expect to see during vertical water column mixing due to de-stratification. Initially, the surface layer responds quickly to the decreased residual shear involving the exchange of warm surface waters to the mid-level waters, which is lagged by the response of the bottom waters.

The bootstrap method is used to calculate the 90% confidence intervals for bottom DO values every 3 hours throughout the 84 hour (-24 to +60) period (Fig. 3.19). This plot examines the variability about the mean for each of these time intervals to the 90% confidence level with intervals ranging +/- .3 to +/- .7 mg L^{-1} for each time step. Important to note is that on average DO increases from about 2.7 mg L^{-1} before the start of the event (indicated by the solid vertical

red line) to ~4 mg L^{-1} after the event, an average increase of almost 50% which is significant at the 90% level.

Tables

Wind direction bin	Decadal breakdown																	
	1950-1969						1970-1989						1990-2009					
	2 m/s		4 m/s		6 m/s		2 m/s		4 m/s		6 m/s		2 m/s		4 m/s		6 m/s	
	r	*p*	*r*	*p*	*r*	*p*	*r*	*p*	*r*	*p*	*r*	*p*	*r*	*p*	*r*	*p*	*r*	*p*
30-110°	0.65	0.00	0.52	0.02	0.05	0.83	-0.07	0.78	0.11	0.63	0.15	0.52	0.33	0.16	0.40	0.08	0.44	0.05

Table 3.1 Correlations and p-values between seasonal wind percentages for 30° - 110°wind bin using 4 m s^{-1} threshold over three decadal periods (1950 -1969, 1970 -1989, and 1990 - 2009) and NYC DEP station E10 seasonally average DOb concentrations. Boxes shaded in red represent *r* values greater than 0.35 and p-values less than 0.1.

(a)

Directional comparisons (using 4ms^{-1})		Years	Correlation for: Number of mixing events
20-100°	30-110°	1948 - 2009	0.95
40-120°	30-110°	1948 - 2009	0.82

(b)

Speed comparisons (using 30-110°)		Years	Correlation for: Number of mixing events
2ms^{-1}	4ms^{-1}	1948 - 2009	.60
6ms^{-1}	4ms^{-1}	1948 - 2009	.51

Table 3.2 (a) Correlations of mixing event frequencies, for all years 1948 to 2009, between mixing events calculated using 30°-110° threshold and directional bins 10° on either side of this directional range. (b) Same as (a) but for correlations between mixing events calculated using 4m s^{-1} and 2m s^{-1} in addition to 4m s^{-1} and 6m s^{-1}.

Figures

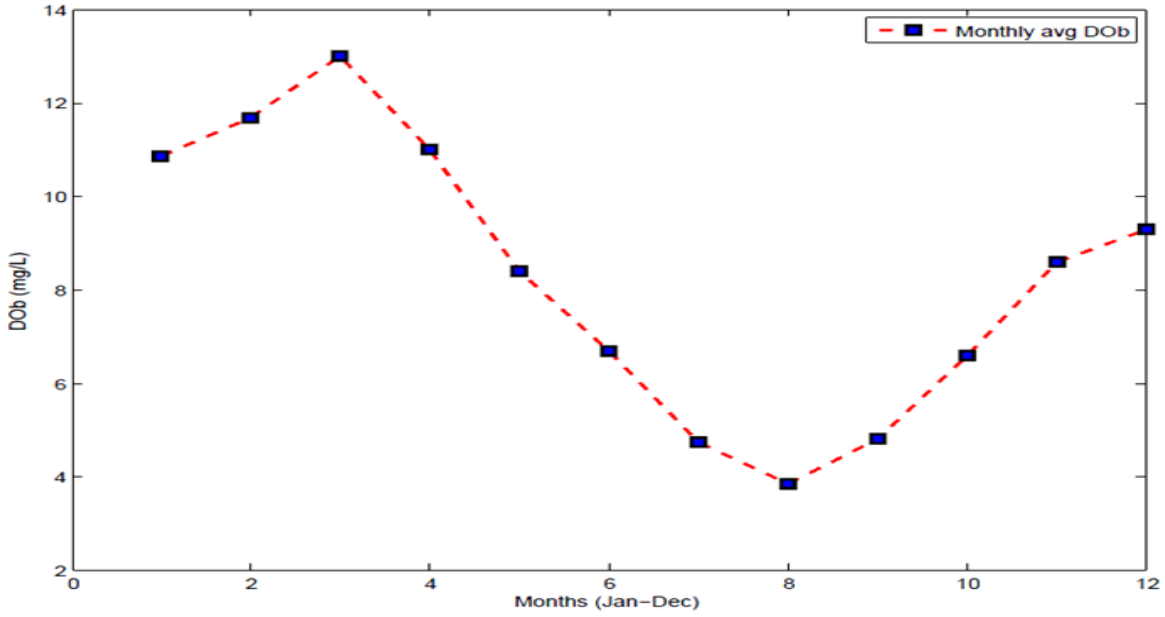

Figure 3.1 NYC DEP station E10 averaged (1946-2009) DOb for months (Jan-Dec). DOb is lowest on average during the months of July, August and September.

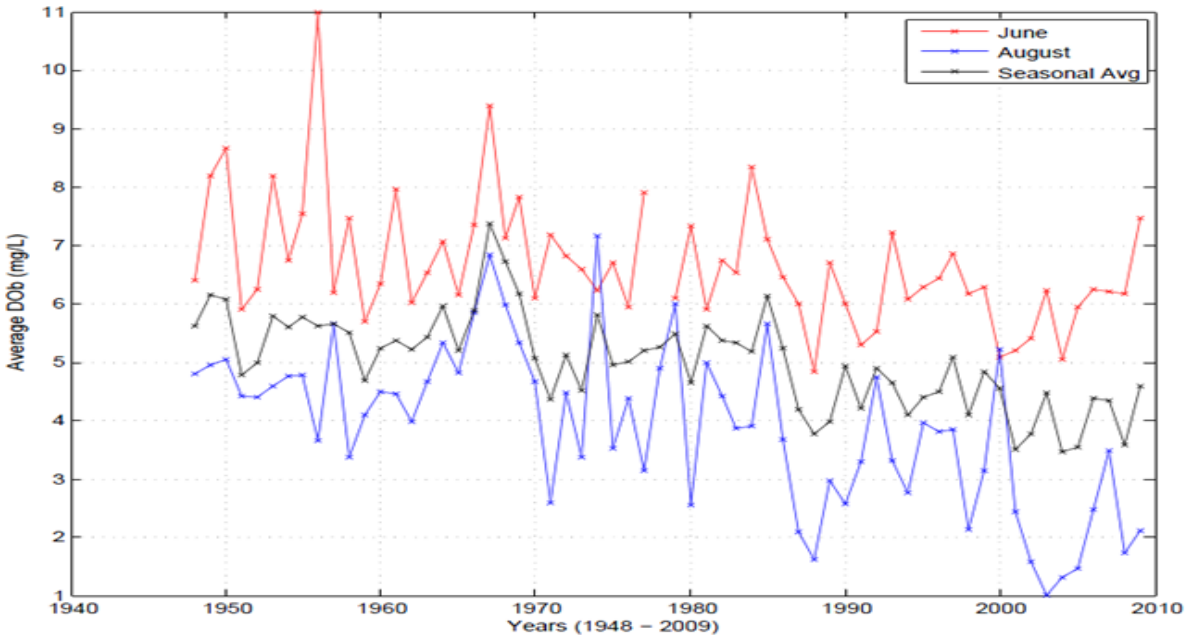

Figure 3.2 Time series of monthly averaged NYC DEP station E10 DOb for months June (red), August (blue), and seasonal average(June, July, August, September) for years 1948 to 2009.

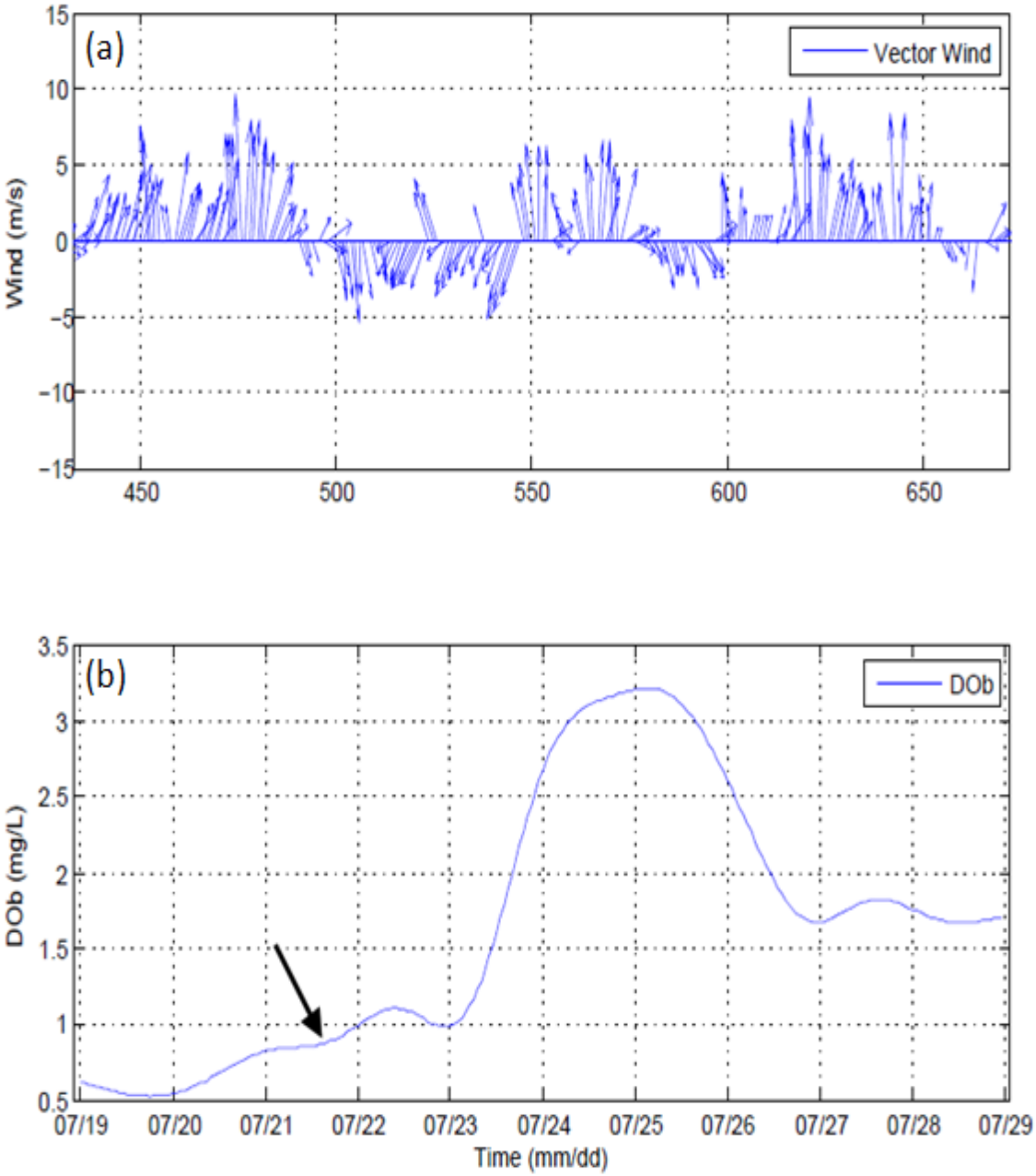

Figure 3.3 (a) Buoy 44022 Vector winds (m s^{-1}) and (b) LISCOS EXRX buoy DOb (mg L^{-1}) for the period of 19 July 2008 through 29 July 2008. Black arrow indicates time of synoptic passage over area as indicated in figure 3.4.

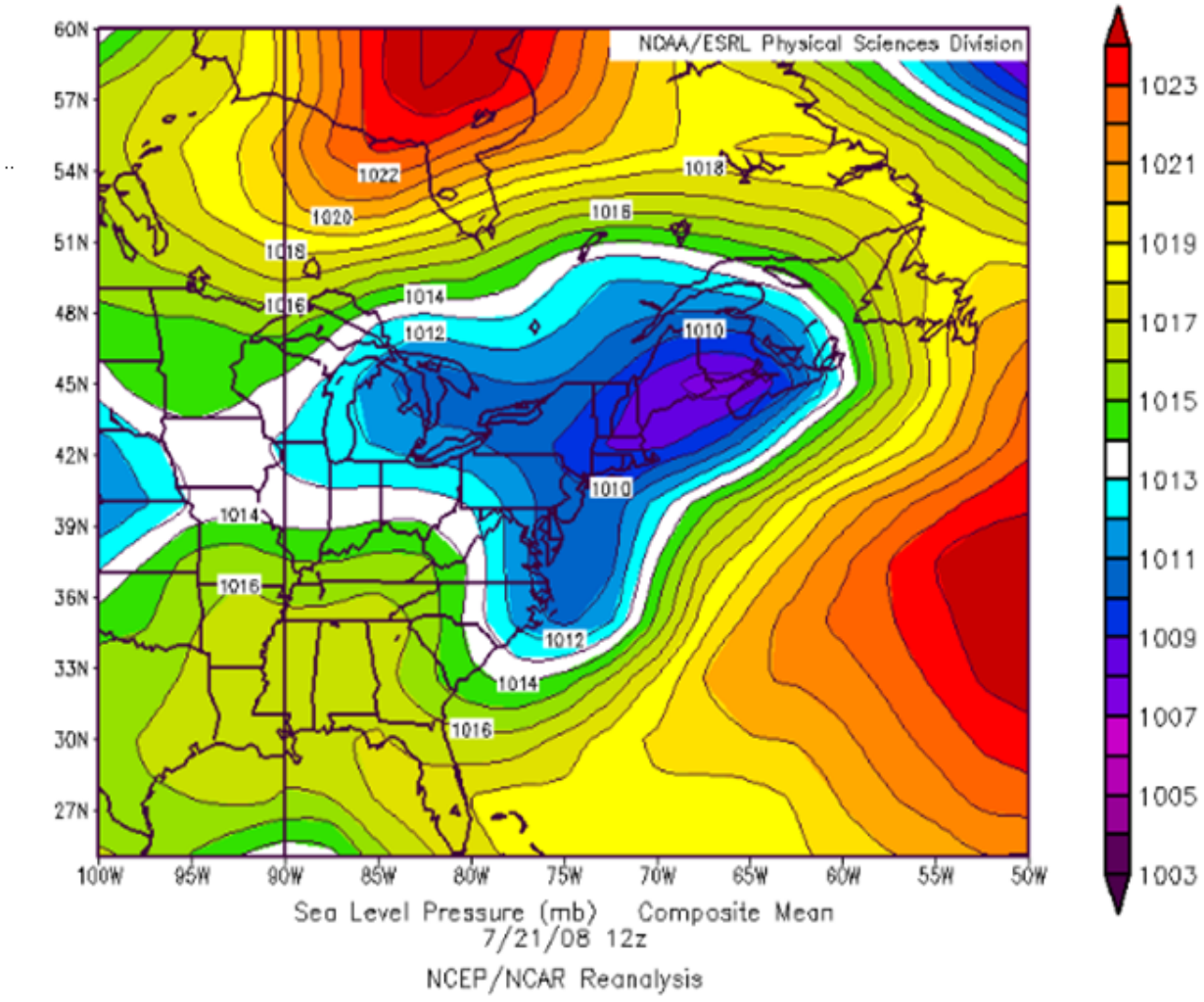

Figure 3.4 mSLP (hPa) plot taken 21 July 2008 at 12Z using NCEP/NCAR reanalysis dataset from ESRL composite webpage. Contour intervals every 1hPa.

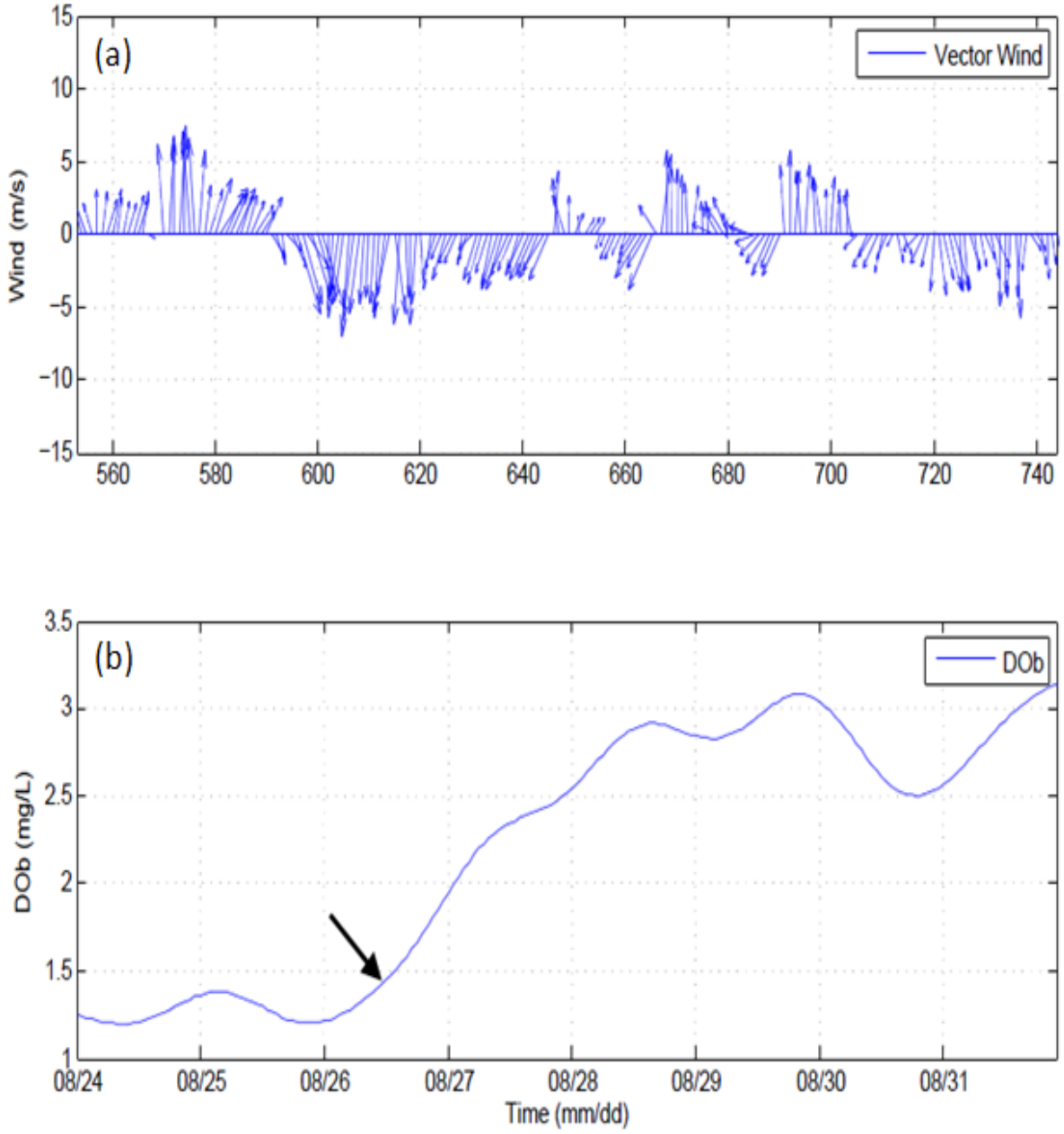

Figure 3.5 (a) EXRX buoy 44022 vector winds (m s^{-1}) and (b) LISCOS EXRX buoy DOb (mg L^{-1}) for the period of 24 August 2008 through 31 July 2008. Black arrow indicates time of synoptic passage over area as indicated in figure 3.6.

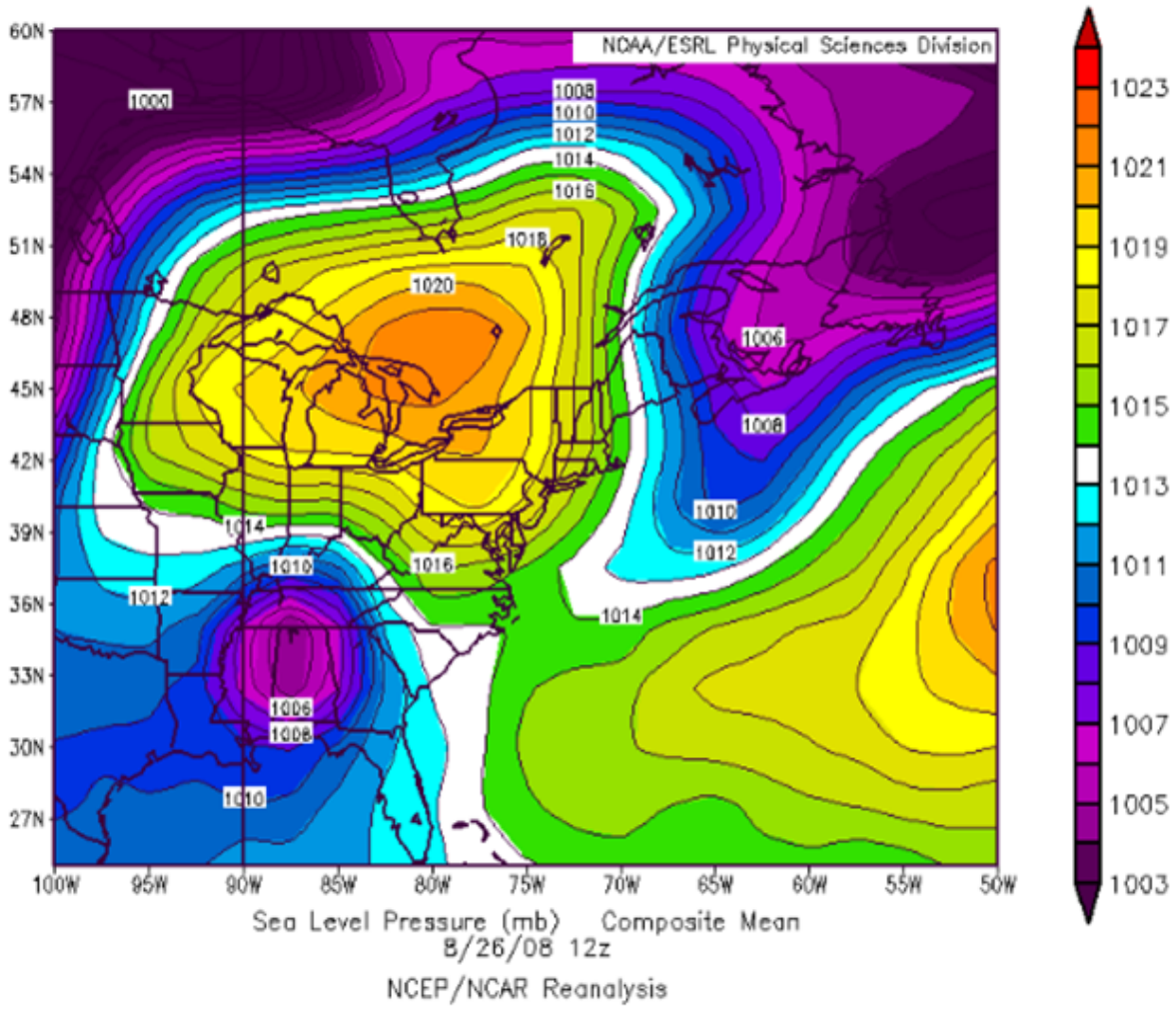

Figure 3.6 mSLP (hPa) plot taken 26 August 2008 at 12Z using NCEP/NCAR reanalysis dataset using ESRL composite webpage. Contour intervals every 1hPa.

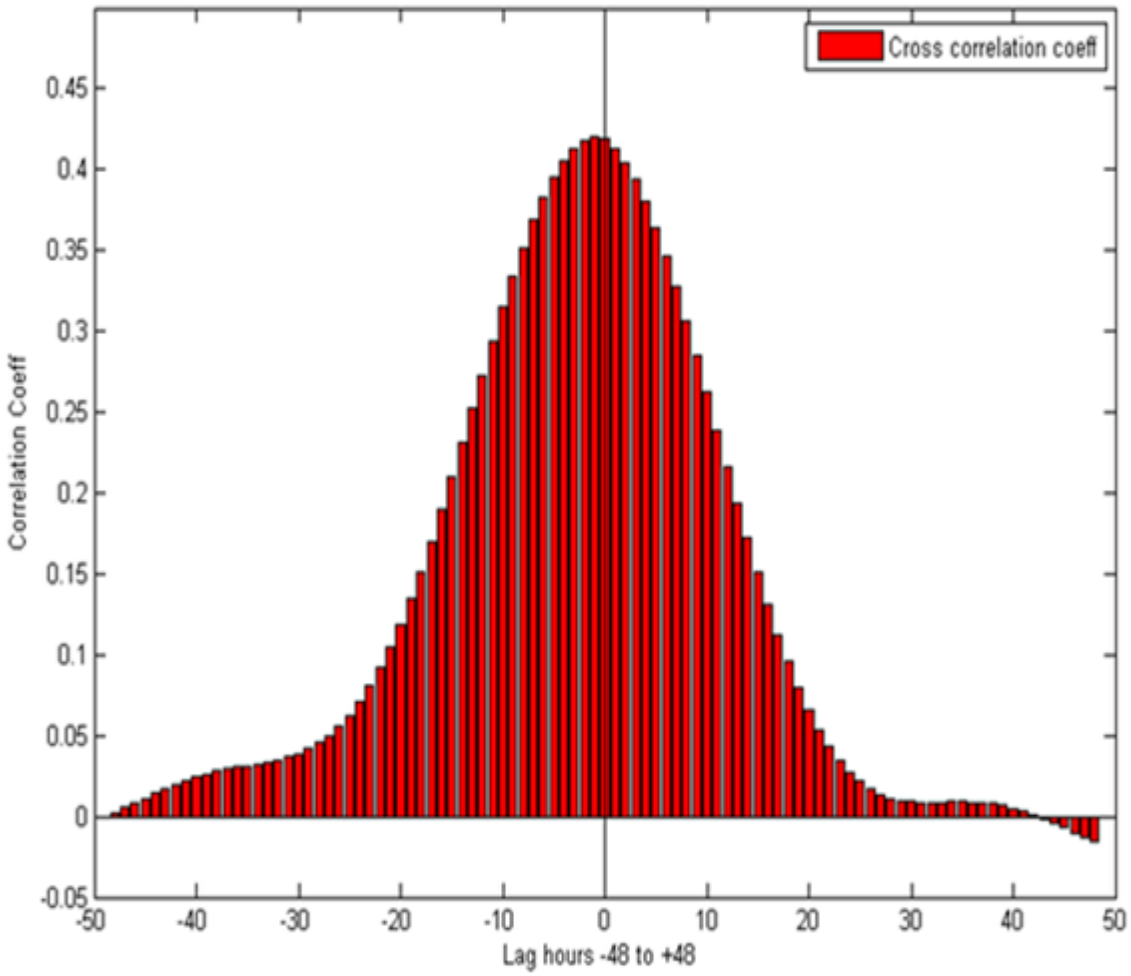

Figure 3.7 Cross- correlation between first time derivative of 34-hour low-pass filtered LISCOS EXRX buoy DOb and bottom temperature data. Correlation is maximum at lag hour -1. X-axis represents lag hours from -48 to +48 hours (+/- 2 days).

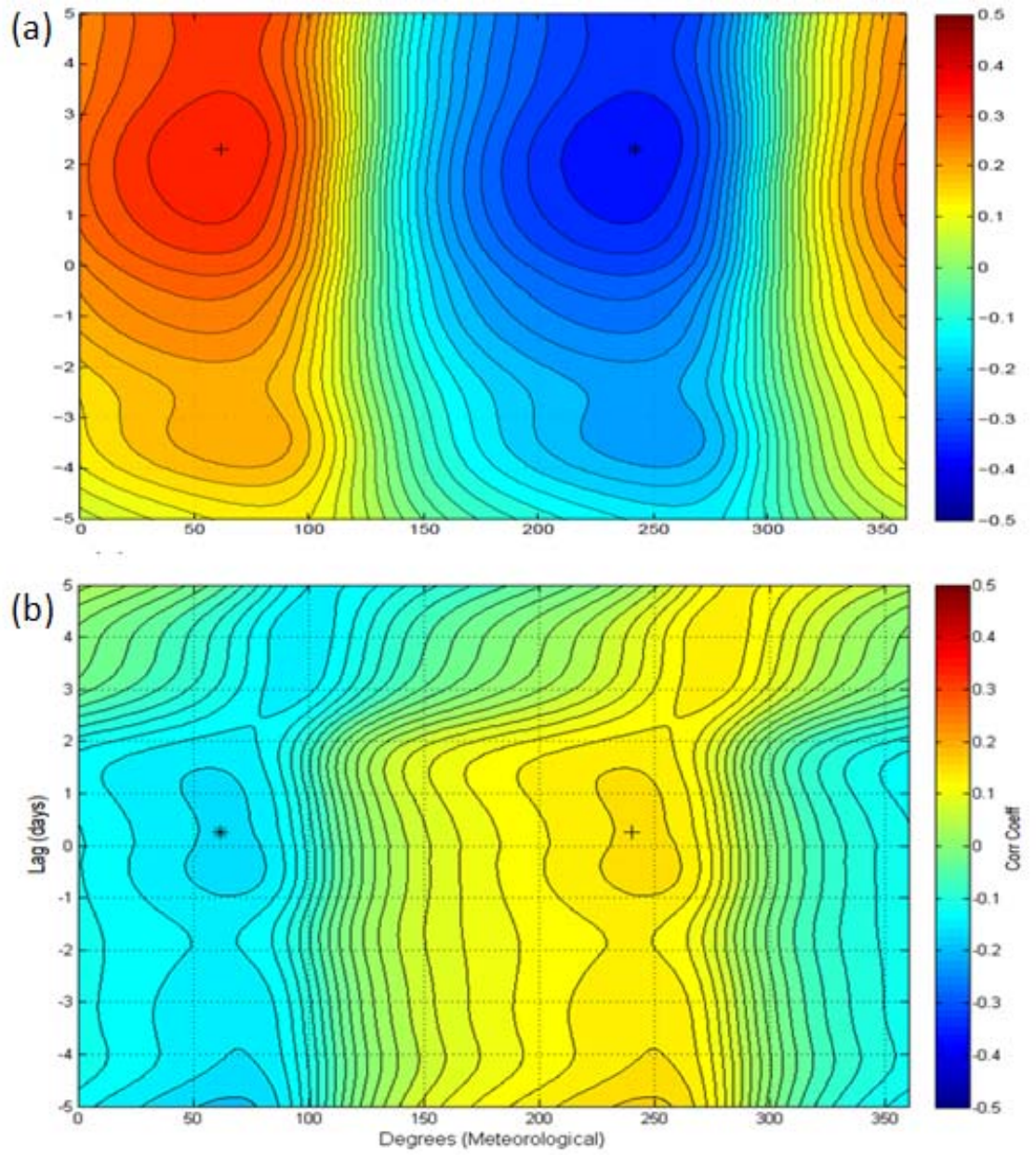

Figure 3.8 (a)Lagged correlations (days) between direction of NBDC EXRX buoy(44022) wind data and LISCOS EXRX buoy DOb and (b) thermal stratification.'+' sign represents point in which positive correlation is highest, '*' sign represents point in which negative correlation is highest.

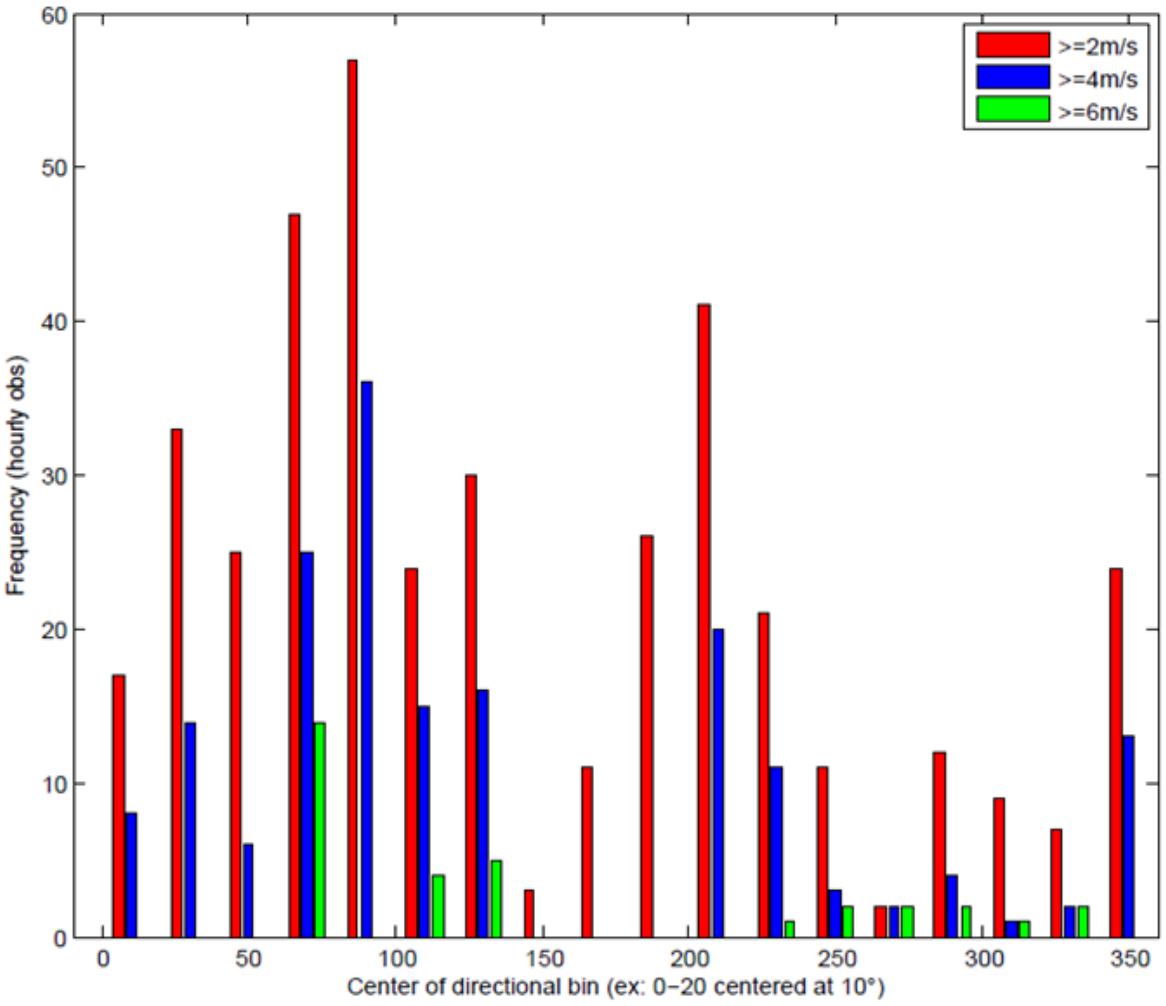

Figure 3.9 Frequency histogram of wind buoy 44022 directions that result in positive hourly rates of LISCOS EXRX buoy DOb and temperature change for eighteen equally spaced 20° wind bins.

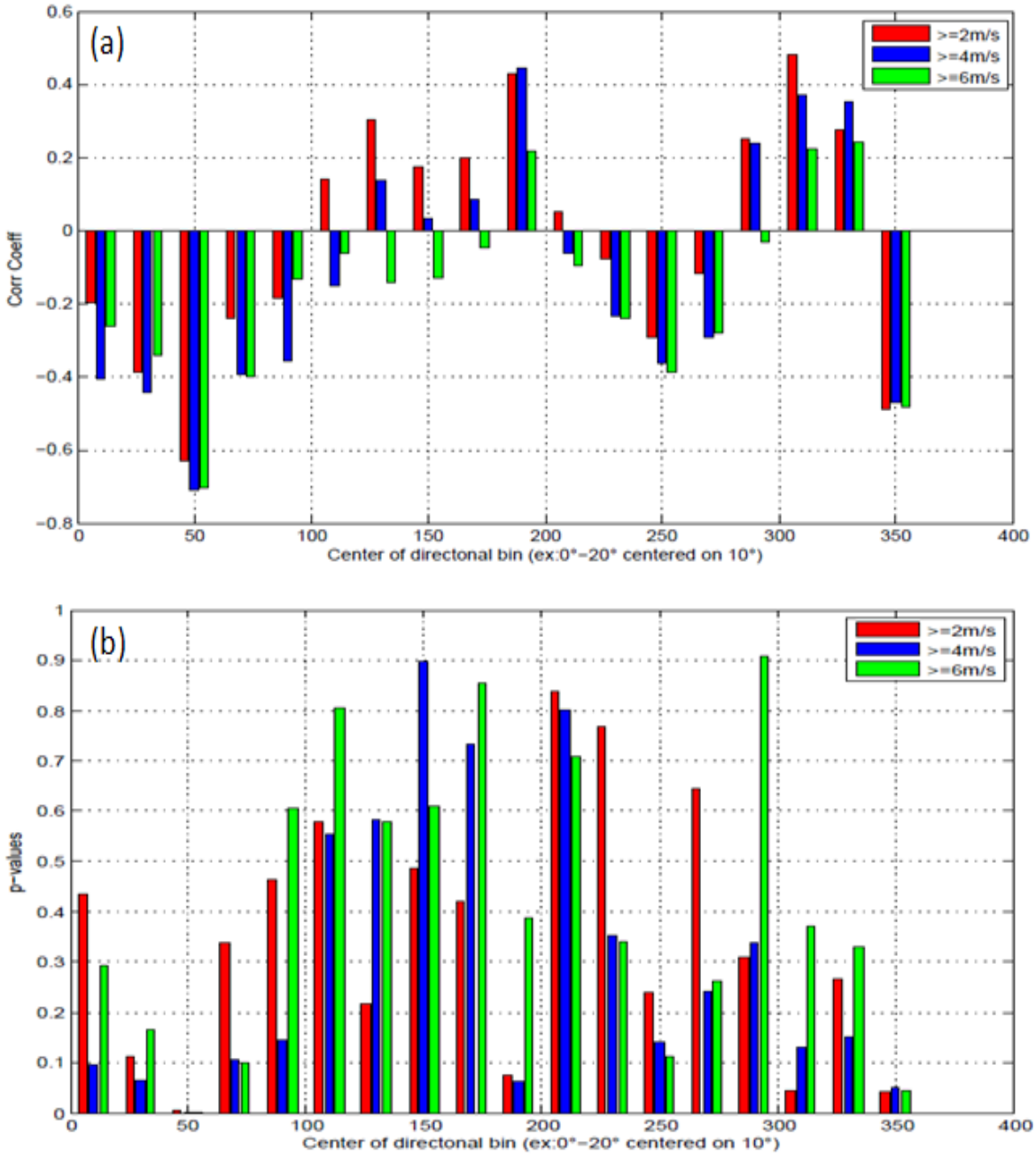

Figure 3.10 (a) Correlations between LGA seasonal wind percentages for eighteen equally spaced wind bins incremented every 20° and the number of CT DEP hypoxia duration days for seasons 1991 through 2009. (b) Associated p-values for the correlations in (a).

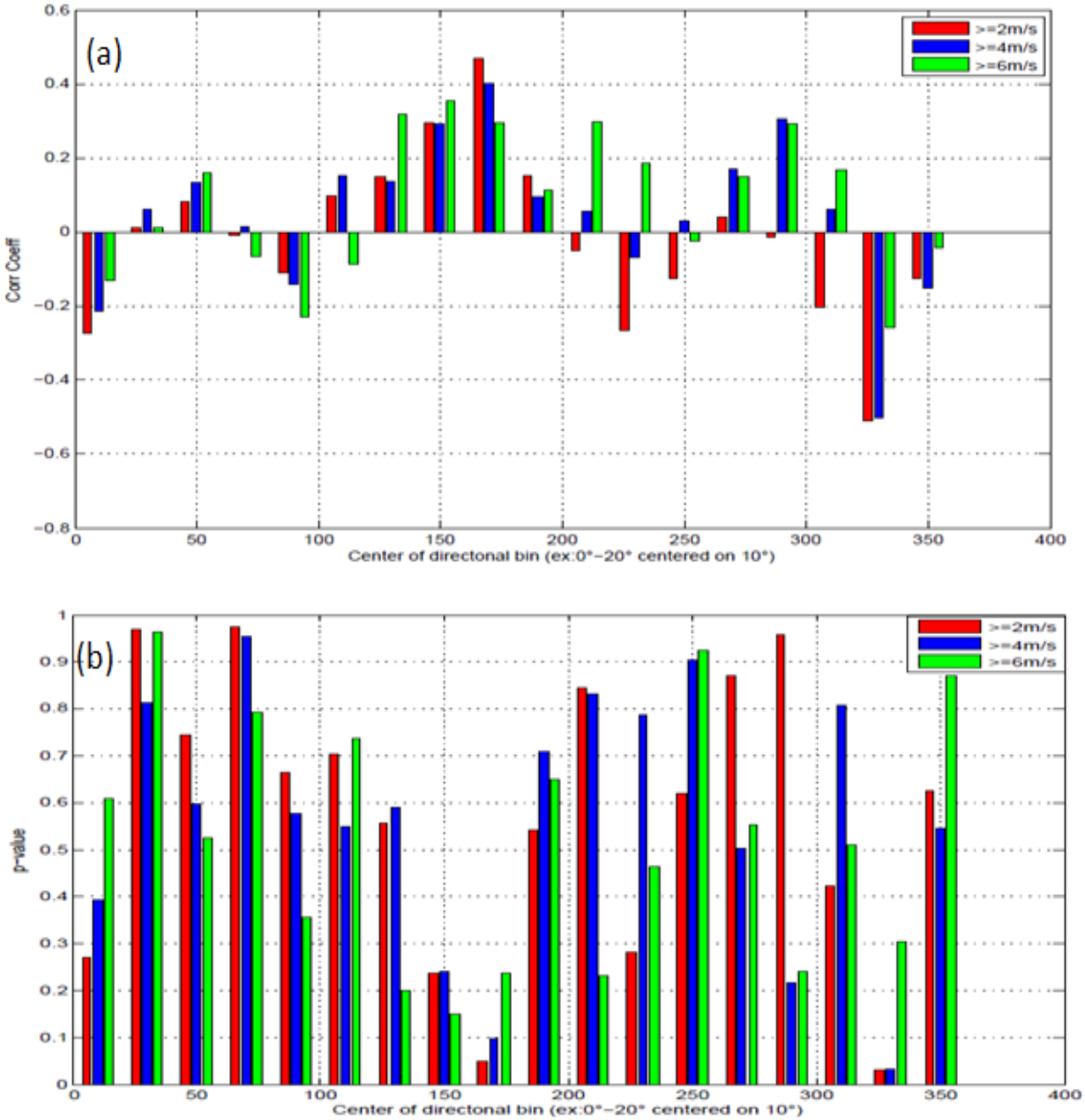

Figure 3.11 Same as figure 3.5 but for CT DEP maximum areal extent of hypoxia data.

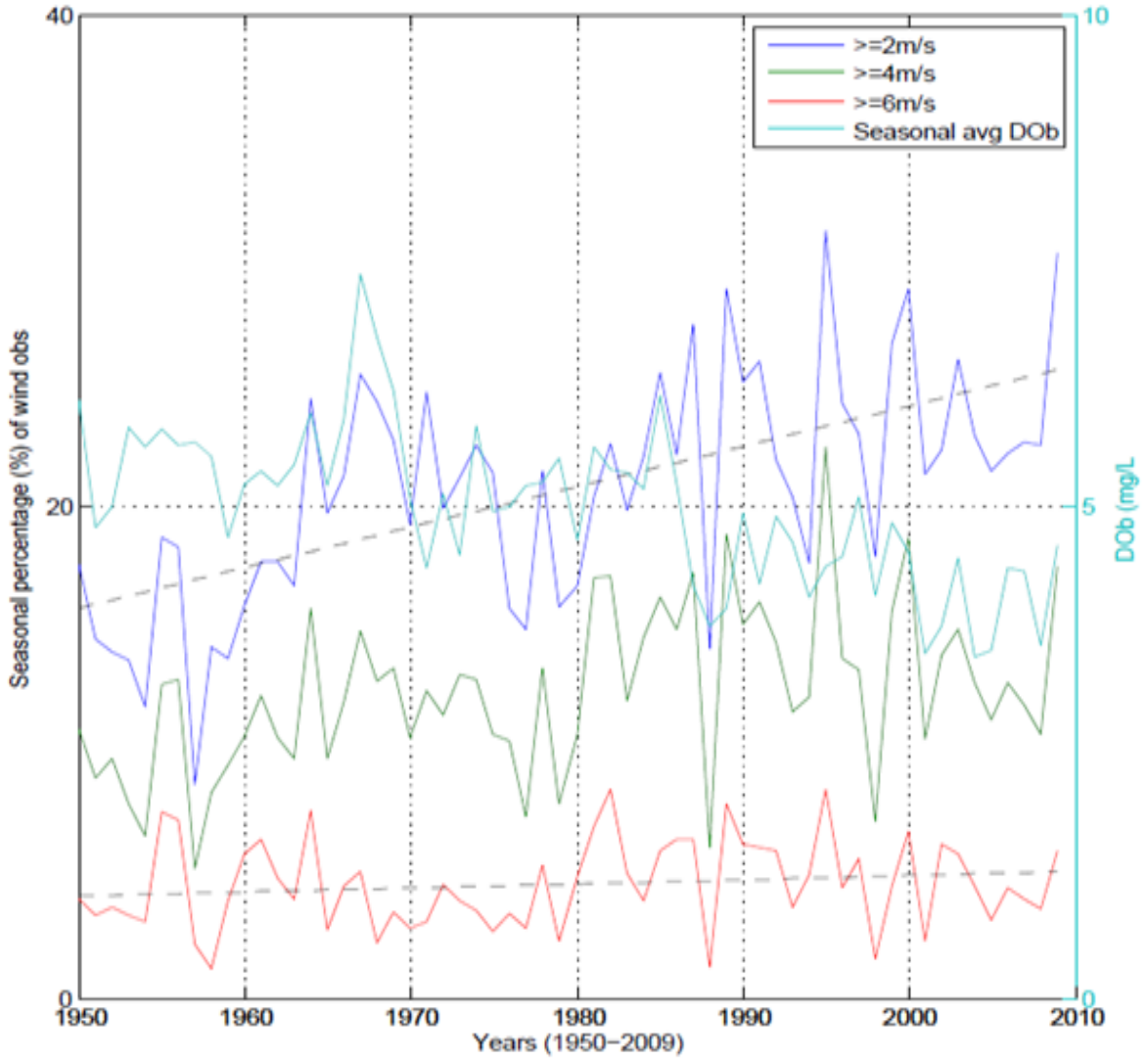

Figure 3.12 Season wind percentages (%) for the 30°-110° wind bin using three speed thresholds including 2,4, and 6 m s^{-1} over periods extending from 1950-2009 using LGA wind data. Seasonally averaged DOb data (mg L^{-1}) is also included using NYC DEP station E10 data. Black dashed lines represent least square trends from 1950-2009.

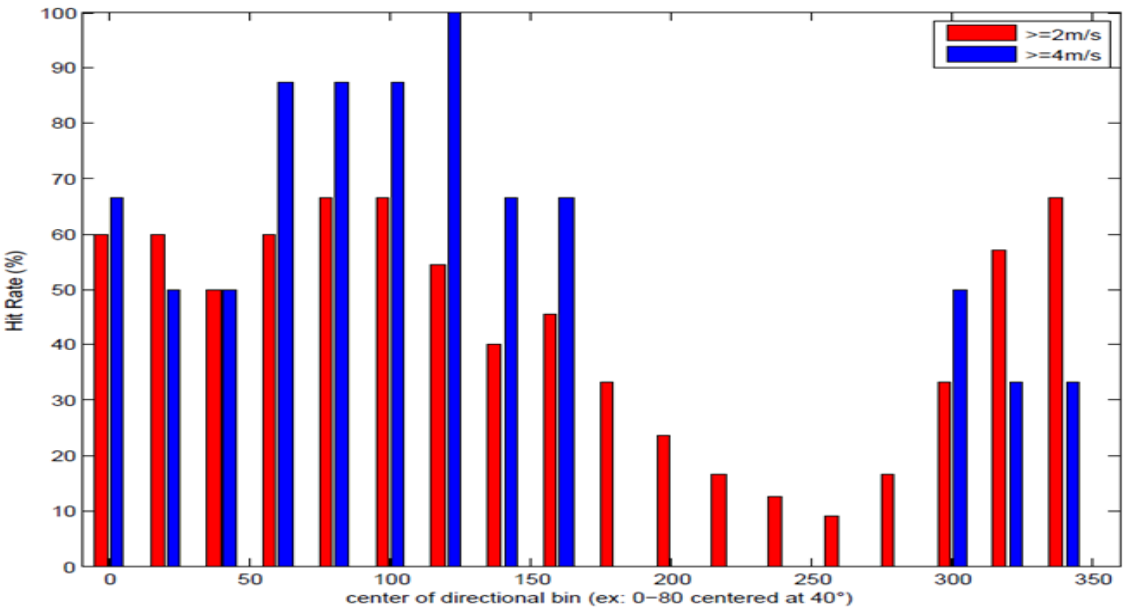

Figure 3.13 'Hit rate' percentages for wind event criteria including buoy 44022 wind directions incremented every 20° for 80° bins, that resulted in a positive sloped change in LISCOS EXRX buoy DOb from -12 hour before to +36 after the calculated events.

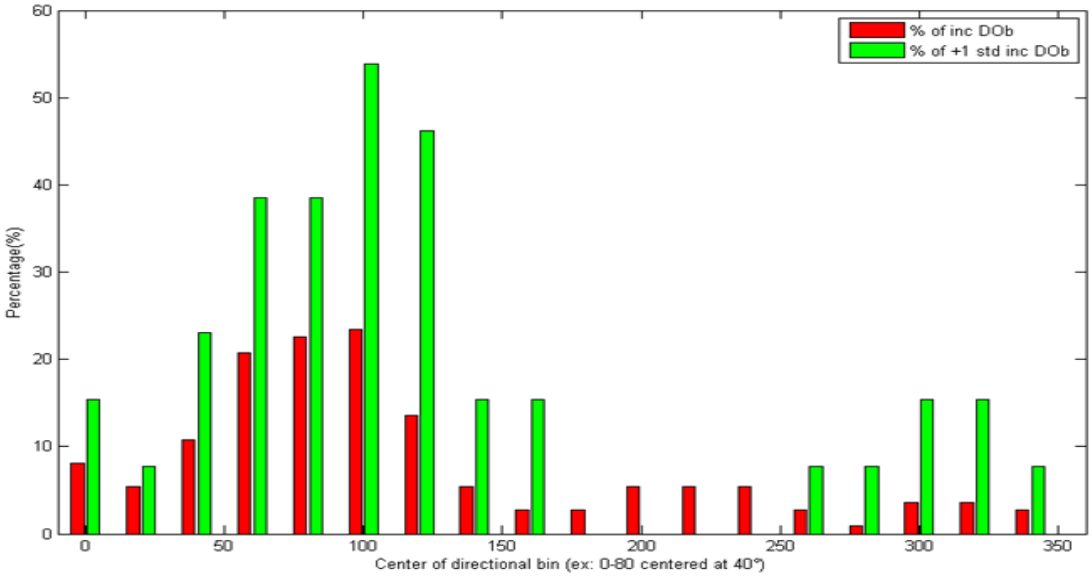

Figure 3.14 Total percentages of increasing LISCOS EXRX buoy DOb events associated with buoy 44022 wind induced events. If a mixing event was present during or one day prior to the increase in DOb then it is counted as a 'hit'. This is done for all DOb increase events (red) and also ones in which the DOb increased by at least 1 standard deviation from the mean (green).

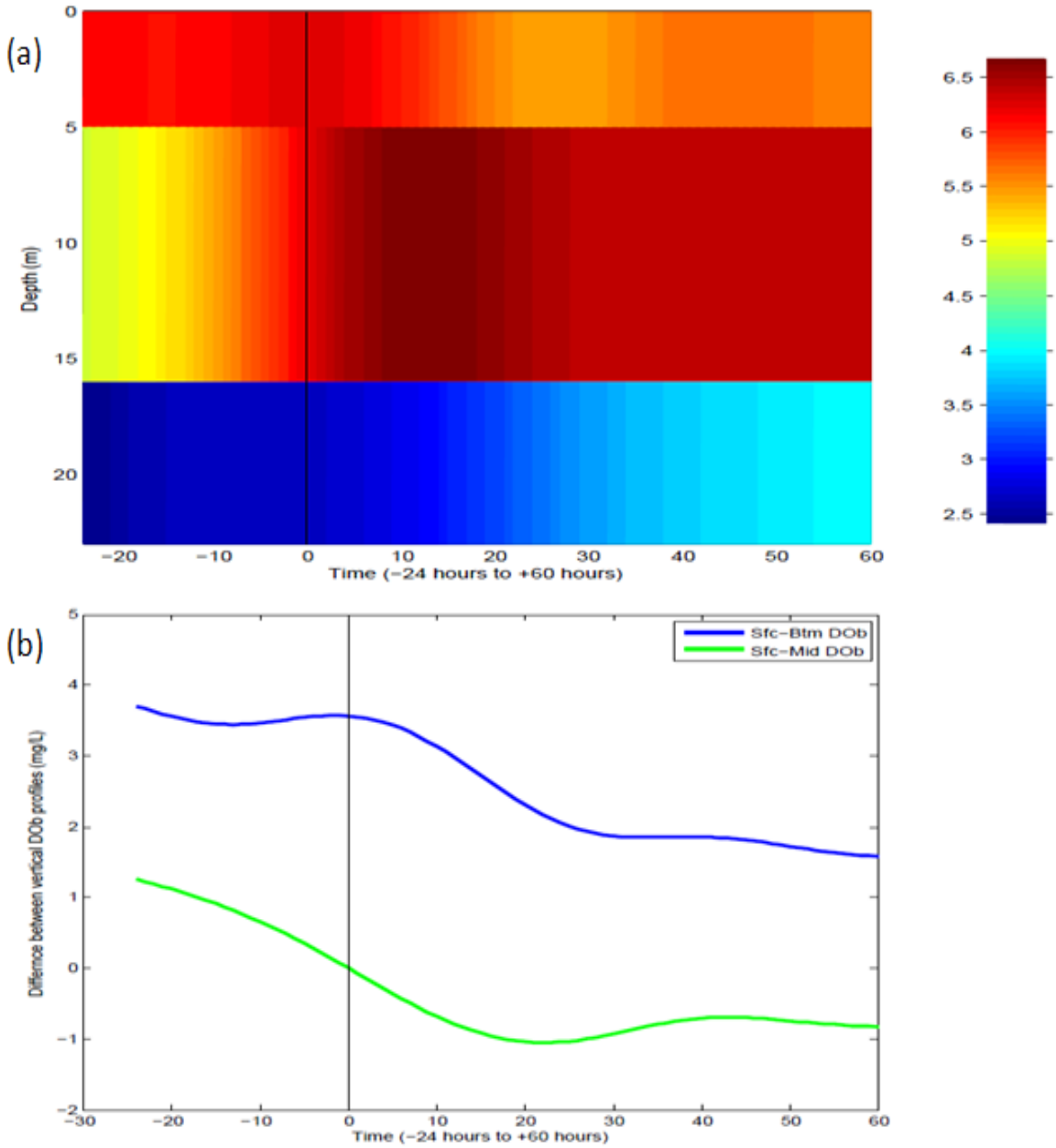

Figure 3.15 (a) Average vertical DO (mg L^{-1}) profile for values 24 hours prior to 60 hours after mixing events for three column depths, .3 m , 7.5 m, and 15.5 m.(b) Average difference between surface and bottom(blue line) and surface and mid-level (green line) DO values for each observation period.

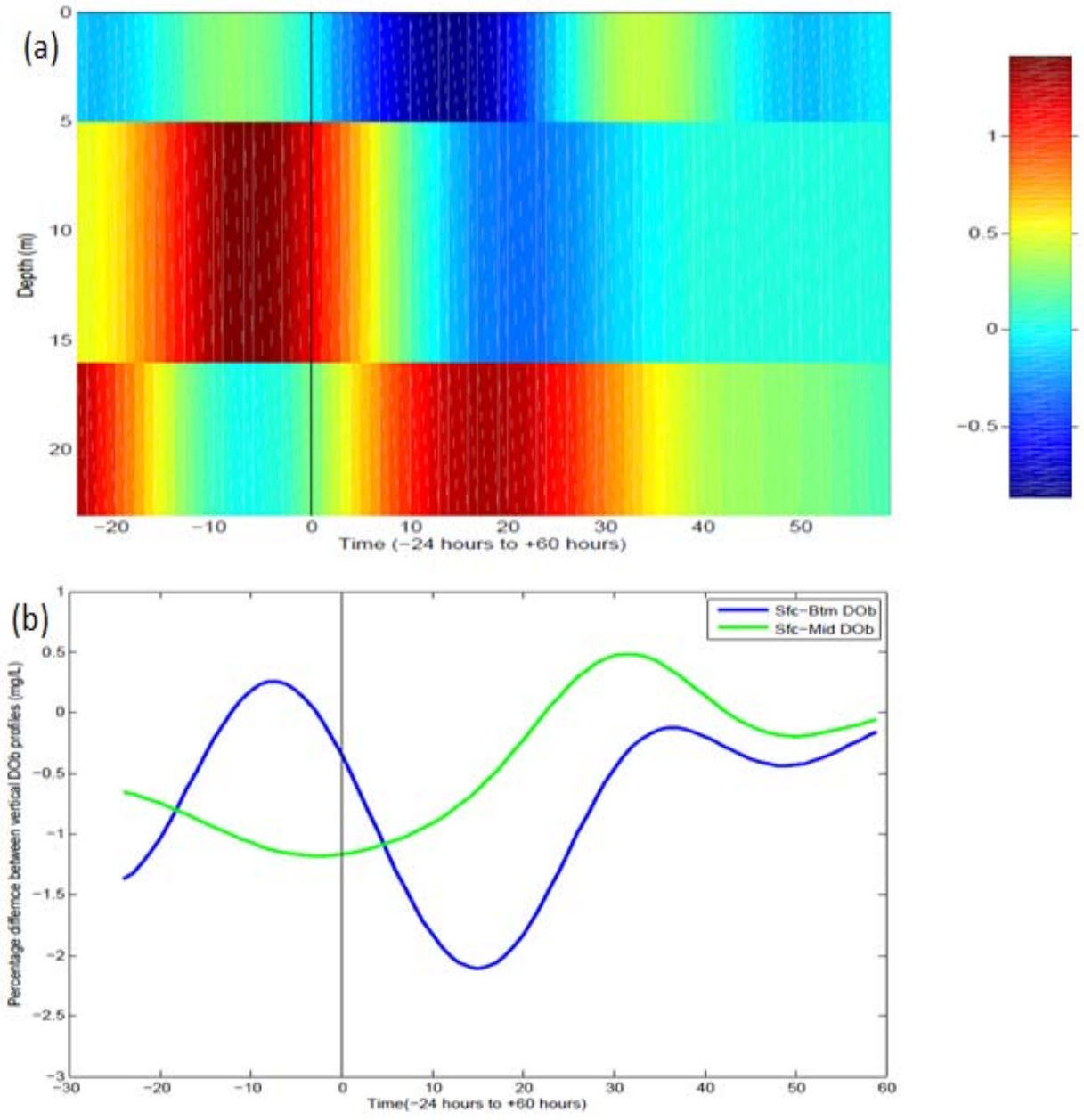

Figure 3.16 (a) Average hourly changes in DO (dDO/dt) percentages for 24 hours prior to 60 after mixing events for three column depths, .3 m , 7.5 m, and 15.5 m. (b) Average percentage change difference between surface and bottom (blue line) and surface and mid-level (green line) for each dDO/dt observation period.

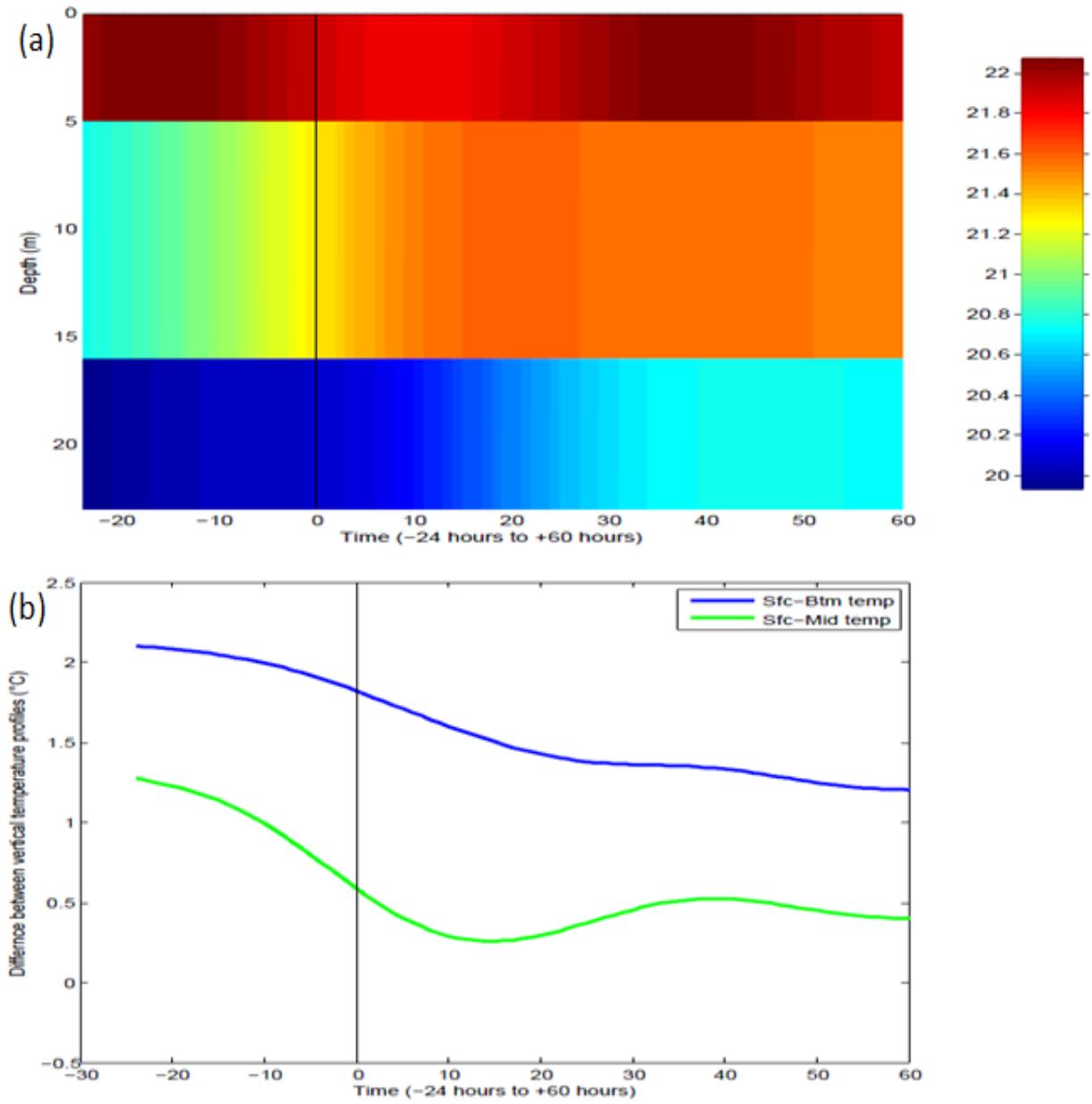

Figure 3.17 Same as figure 3.15 but for temperature (°C).

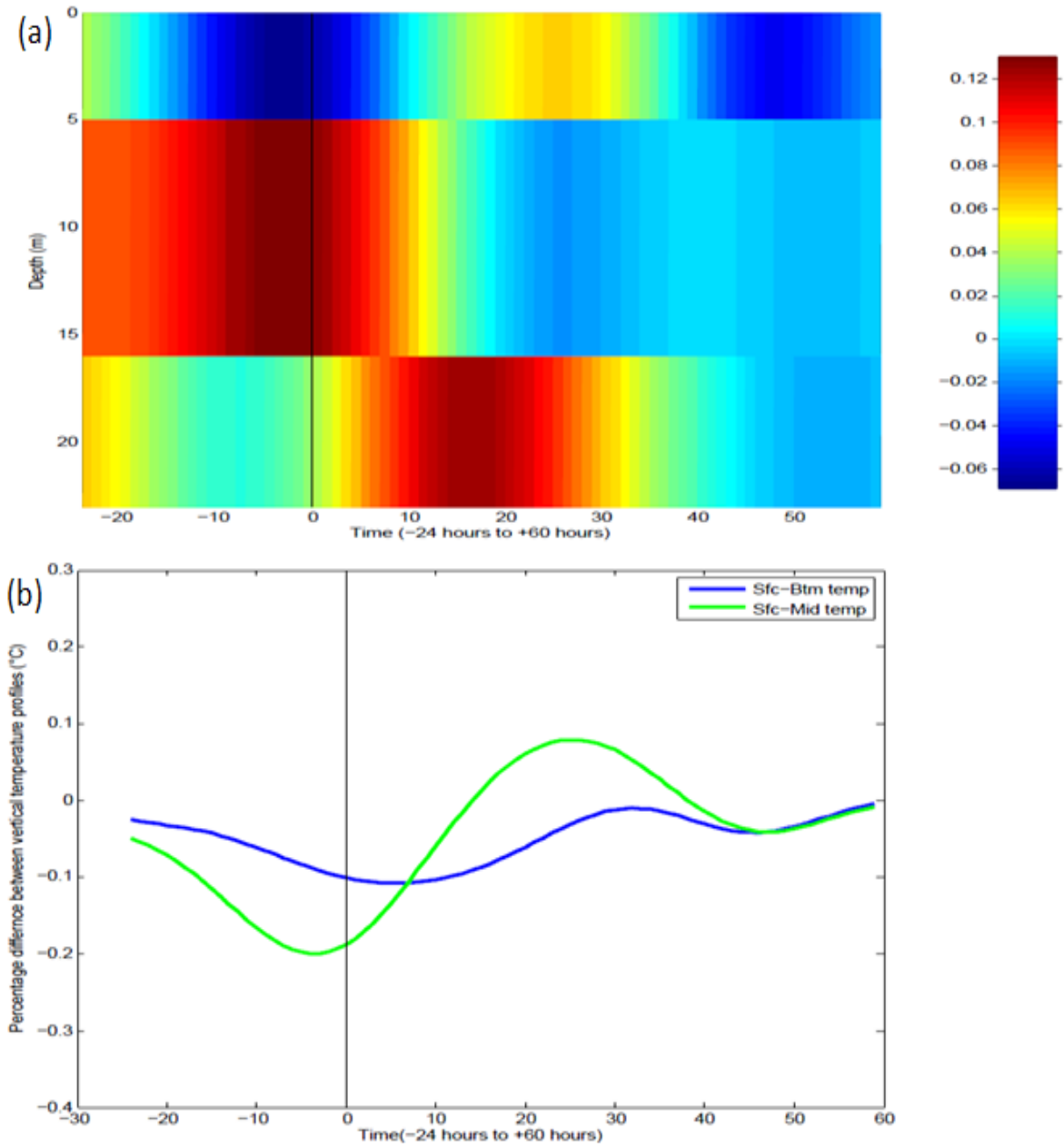

Figure 3.18 Same as figure 3.16 but for temperature (°C) (dT/dt).

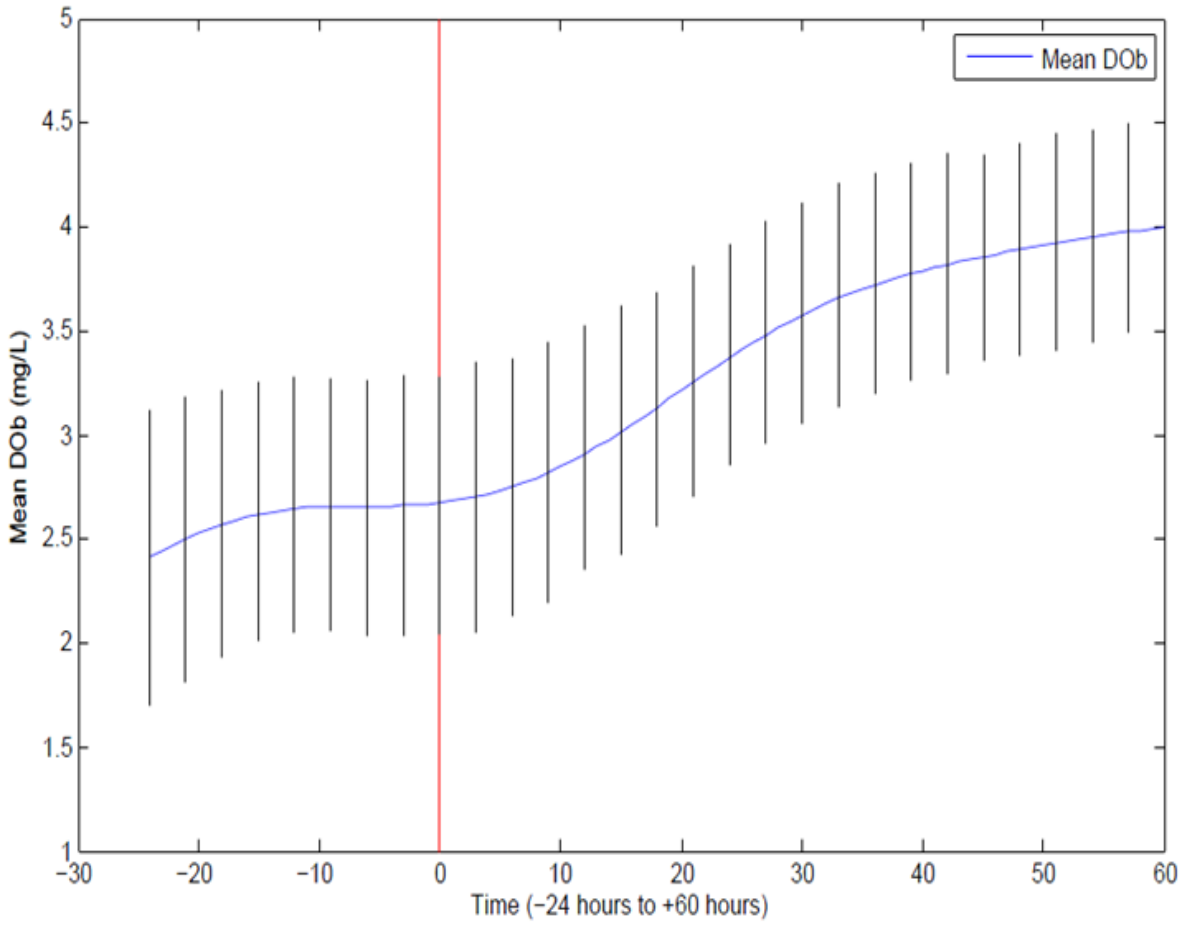

Figure 3.19 90% confidence intervals for mean DOb (mg L^{-1}) values, 24 hours prior to 60 hour after mixing events. Confidence intervals are provided every 3 time steps indicated by the black vertical lines. Red lines represent the start time of mixing events in relation to the DOb profile.

Chapter IV: Synoptic climatology associated with mixing events

This chapter investigates the synoptic pressure and wind patterns that favor mixing within wLIS. Mixing event days, calculated using 30°-110° with speeds >= 4 m s^{-1} , are categorized into synoptic groups to determine relevant synoptic patterns for mixing and the evolution of these synoptic patterns from daily lag -4 to day of event using mSLP and 500-hPa geopotential heights.

4.1. Climatology of mixing events

Mixing event frequencies (Fig. 4.1a), average LGA surface winds associated with mixing events (Fig. 4.1b), and average mixing event duration (Fig. 4.1c) are metrics used to describe the seasonal mixing event characteristics from the summer (JJAS) seasons of 1950 to 2009. Black dotted lines in figures 4.1a-c represent recent trends from 1990-2009. While mixing event frequencies are increasing slightly, average surface winds and event duration are decreasing slightly.

Figure 4.2 shows the percentage of each synoptic high and low pressure category for all warm season (JJAS) mixing events that occurred from 1950-2009. High pressure systems are the most abundant systems, accounting for 39.0% of the events. Hybrid patterns (36.3%) are the second most common, followed by low pressure systems (23.1%) and miscellaneous events

(1.6%). This suggests that high pressure systems have a significant influence on mixing event frequencies, since over 75.3% of all events involve a high pressure system (hybrid or high pressure).

Monthly breakdown for all synoptic groups for June (Fig. 4.3a) July (Fig. 4.3b) August (Fig 4.3c) and September (Fig 4.3 d) are provided to determine if there is a preference for certain synoptic patterns for select months. For the early summer months (June and July), a high percentage of low pressure systems contribute to the total number of mixing events either as low pressure or hybrid events. In comparison, during the months of August (Fig. 4.3c) and September (Fig. 4.3d), when mixing is most important, the frequency of high pressure patterns increase from near 30% in June-July to over 40% in August-September, while the frequency of low pressure patterns decreases from over 25% in June-July to around 20% or below for August-September. Overall, there is an almost 10% decreases in the number of low pressure events and an over 15% increase in the number of high pressure events between June and September.

To determine decadal trends for each synoptic group, total percentages and seasonal average number of mixing events for each decade are plotted with 90% confidence intervals in figures 4.4 to 4.6. Percentages are used in addition to average frequency for each decade as a way of noting the relative importance of each pressure pattern.

Figure 4.4a represents the percentage breakdown of Regional Low (RL) and Coastal Low(CL) events for each decade (1950-2000). With the exception of the 1950's and 1980's the total percentages for each decade are below 25%. In addition, no statistically significant trend to the 90% confidence interval is present for this decadal time series (Fig. 4.4b). These results indicate that both a relatively small percentage and number of total mixing events are associated with low pressure events.

The Extended High (EH) and Pre-High (PH) patterns show a more significant trend seen in both the percentage (Fig. 4.5a) and average number (Fig. 4.5b) of high pressure events. A significant increase in both the percentage and seasonal average of high pressure systems from the 1950's to the 1990's occurred which is significant at the 90% confidence level. During the 1950's about 1.6 events per season (25.4% of the total decadal events) were associated with high pressure systems. Conversely, in the 1990's these frequency and percentage numbers increased to ~ 3.7 and ~47.1%, respectively.

Figure 4.6 shows the percentage and seasonal average number of events for each decade for Northern High-west (NHw), Northern High-central (NHc), and Northern High-east (NHe) patterns. The percentage of hybrid events for each decade has been declining on average, from 42.8% in the 1950's to 30.4% during the 1990's (Fig. 4.6a). However, the average number of hybrid events for each season for the decades 1950-2000 remains nearly constant, except for the 1990's (Fig. 4.6b). These results demonstrate that the percent of mixing events attributed to hybrid patterns has been decreasing on average.

4.2. Evolution of surface and upper level synoptic conditions for mixing patterns

In order to determine the evolution of the synoptic weather patterns that favor mixing, seasonal (June-September) mean and anomaly mSLP and 500-hPa heights are presented for periods -4 to 0 days before the start of identified mixing days. Anomalies are obtained by subtracting daily variable mean from the total mean for the 1981 to 2009 period using the daily-averaged NCEP/NCAR reanalysis datasets. This synoptic evolution analysis is provided for low

and high pressure mixing events including RL, CL, PH, and EH patterns. Because hybrid patterns are a combination of high and low pressure patterns they are not included.

4.2.1. Spatial synoptic features during all mixing events

Figure 4.7 shows mSLP and 500-hPa height averages and anomalies for all mixing event days during time of event. 500-hPa zonal flow is observed across the U.S., with a short-wave ridge over southeastern Canada associated with +40 m positive height anomaly. A weak trough over the southeast U.S. and a trough to the east of North America are also observed (Fig. 4.7a). At the surface there is a region of high pressure (~1020 hPa) over northern New England associated with an extensive mSLP anomaly field of +4 hPa. A weak area of low pressure (anomalies ~ -2hPa) exist off the southeastern U.S. coast creating a dipole pattern between the surface high pressure and surface low pressure anomalies (Fig. 4.7b).

4.2.2. Evolution of Low pressure patterns

The evolution of low pressure patterns, including RL and CL patterns, is presented in figures 4.8 -4.12. On day -4 fairly zonal flow at the 500-hPa level is observed with three areas of anomalously low heights (U.S. west coast, off southeast coast, and over Hudson Bay) (Fig. 4.8a). These features also emerge at the surface, with the strongest mSLP anomaly over the mountainous western U.S. (>= -2hPa) (Fig. 4.8b). On Day -3 the areas of anomalously low heights and mSLP over the western U.S., southeast Canada, and off the southeast U.S. coast track east , southeast, and northeast, respectively (Fig. 4.9a-b). The 500-hPa pattern continues to be zonal on day -2, except over southeast Canada where a trough deepens associated a -30m negative height anomalies (Fig. 4.10a). Negative surface pressure anomalies (~ -2hPa) over the central U.S. and off the southeast U.S. coast continue to move eastward and northeastward,

respectively. In addition, an area of positive mSLP anomalies ~3 hPa is over the Hudson Bay region (Fig. 4.10b). On day -1 the 500-hPa heights are more amplified with increasing heights over the western states, decreasing heights downstream associated with a short-wave trough over the central U.S., and a trough off the North American coast that deepens. A relatively weak upper-level ridge is also noted over the Hudson Bay region (Fig. 4.11a). The surface anomaly patterns over the surrounding northeast United States intensify from day -2 with a merger of the mid-latitude and coastal negative mSLP anomalies south of the Great Lakes, associated with negative mSLP anomalies of -3hPa (Fig. 4.11b) . On day 0 (day of mixing) a 500-hPa trough sets up over the eastern U.S. and a ridge over the western states. There are -40m negative height anomalies to the south of the Great lakes at 500hPa (Fig. 4.12a). Meanwhile, surface low pressure anomalies cover the eastern third of the country intensifying from day -1, associated with negative anomalies of >= -4hPa (Fig. 4.12b).

4.2.3. Evolution of high pressure patterns

The evolution of high pressure patterns, including PH and EH patterns are presented in figures 4.13-4.17. On day -4 the 500-hPa flow is nearly zonal except over northeastern Canada where a large trough sets up associated with -40m negative height anomalies (Fig. 4.13a). A large area of positive mSLP anomalies (~2hpa) is observed over western Canada with negative mSLP anomalies over northeastern Canada (Fig 4.13b). On day -3 the flow remains relatively zonal across the domain, except over northeast Canada where the -40m negative height anomaly trough persists (Fig. 4.14a). At the surface, positive and negative mSLP anomalies over northwestern and northeastern Canada strengthen, and track southeast and east, respectively. In addition, a Bermuda high extends into the eastern U.S., with +1hPa positive mSLP height anomalies over the northeast U.S. (Fig. 4.14b). The 500-hPa flow becomes amplified on day -2,

with a weak ridge building into the North American interior, deepening the downstream trough over eastern Canada (Fig. 4.15a). Low pressure anomalies move off the North American northeast coast as positive height anomalies of almost +4hPa track to the south of the Hudson Bay. The mean high pressure off the east U.S. coast extends north and west merging with the positive mSLP anomaly over the Hudson Bay and Great Lakes region (Fig.4.15b). This indicates that the extension of this subtropical high may be important in the intensification and track of this positive mSLP anomaly. By day -1 the 500-hPa flow continues to amplify as a ridge continues to build over the north-central United States, and a trough digs into northeastern U.S. (Fig. 4.16a). The area of positive mSLP anomalies >=4hPa continues to intensify extending over the Hudson Bay and Great Lakes regions (Fig. 4.16b). On day 0 (day of mixing), there is a broad 500-hPa ridge over the north and eastern third of the United States. This ridge results in a ~1022 hPa area of high pressure just to the east of the Great Lakes (Fig. 4.17a). There is a +40m positive height anomaly over Quebec and a +4 hPa positive mSLP anomaly over the northeast U.S. and Canadian Maritimes (Fig. 4.17b).

4.2.4. Hybrid patterns

The evolution of the hybrid pattern is very similar to the low pressure patterns so it is not shown. Instead, the mean and anomaly 500-hPa geopotential height and mSLP fields are presented only for the day of hybrid mixing events. At 500-hPa there is a weak trough over the southeastern U.S. associated with -40m negative height anomalies. To the north there is a weak ridge over the Hudson Bay and Great Lakes regions associated with +40m positive height anomalies over the Canadian Maritimes (Fig. 4.18a). A large area of mean high pressure (~1020hPa) sets up over the northeast U.S. and Canadian Maritimes with >= 4 hPa mSLP anomalies. The other important synoptic cell for hybrid events is low pressure. These systems are

typically associated with -2 hPa negative pressure anomaly that extends over the Atlantic states (Fig. 4.18b).

4.3. Connections to DOb

Two extreme seasons are used to establish a clear connection between the seasonal DOb concentrations and mixing event frequencies. Both the 1985 and 1988 seasons were associated with an anomalous number of seasonal mixing events and seasonally averaged DOb. These seasons will be compared to relate timing and frequency of mixing events to the seasonal evolution of DOb. Figure 4.19 shows the anomalously high frequency of mixing events, totaling 9, in concurrence with the anomalously high average seasonal DOb concentration of over 6 mg L^{-1} for the 1985 season. In comparison, for the 1988 season, there were no calculated mixing events and seasonally averaged DOb dropped to below 4 mg L^{-1} on average.

4.3.1. Active year (1985)

Figure 4.20a shows the seasonal DOb profile (black lines) time series in addition to the periods within the season in which mixing events occurred (vertical blue lines) for the 1985 season. Over the course of this season nine events were calculated, with many of them occurring from late July through September. This can also be reflected in the wind rose plot in Figure 4.21a, where wind percentages are evenly distributed throughout the season, especially out of the northeast quadrant. This resulted in DOb levels remaining above hypoxic levels (> 3.5 mg L^{-1}) throughout the season. Typically DOb levels continuously plunge toward hypoxic values until late August or early September when the water column overturns. However, In mid July DOb levels reached their lowest at almost 4 mg L^{-1}, after which several mixing events occurred

between then and the end of the season. This helped raise the concentration levels to almost 6 mg L^{-1}, close to a 2 mg L^{-1} increase by early August. It is hypothesized that because there were several mixing events during the period in which DOb levels normally decrease rapidly, DOb concentrations recover and remained above hypoxic levels, for the rest of the season.

4.3.2. Inactive year (1988)

In 1988 DOb levels dipped below 1 mg L^{-1} in early August and took until almost the middle of September for DOb levels to rise above 3.5 mg L^{-1}. There were no observed mixing events over the course of the 1988 season (Fig. 4.20b). Figure 4.21b supports these findings, where a majority of the seasonal winds were out of the southwest to northwest directions which can be linked to increased stratification. As a result, DOb levels continued to drop throughout the summer season, especially in early August, after which the minimum value was observed. It is hypothesized that enhanced thermal stratification from the lack of water column ventilation from mixing events led to this elongated period of hypoxia.

Figures

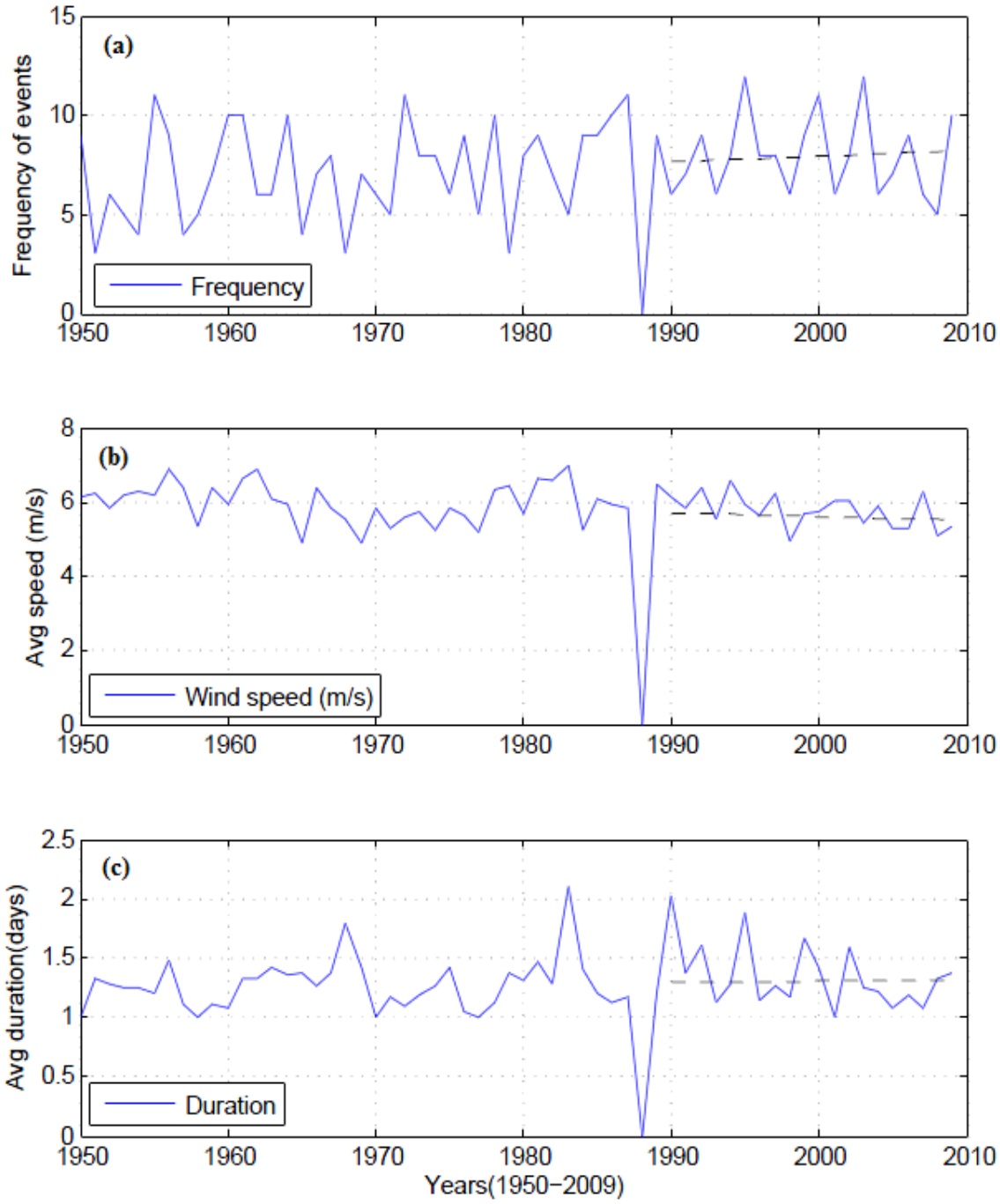

Figure 4.1 (a) Time series of mixing event frequencies, (b) average wind speed (m s^{-1}) for seasonal mixing events, and (c) average duration (days) for seasonal mixing events. Black dashed lines represent least squares regression lines for periods 1990-2009.

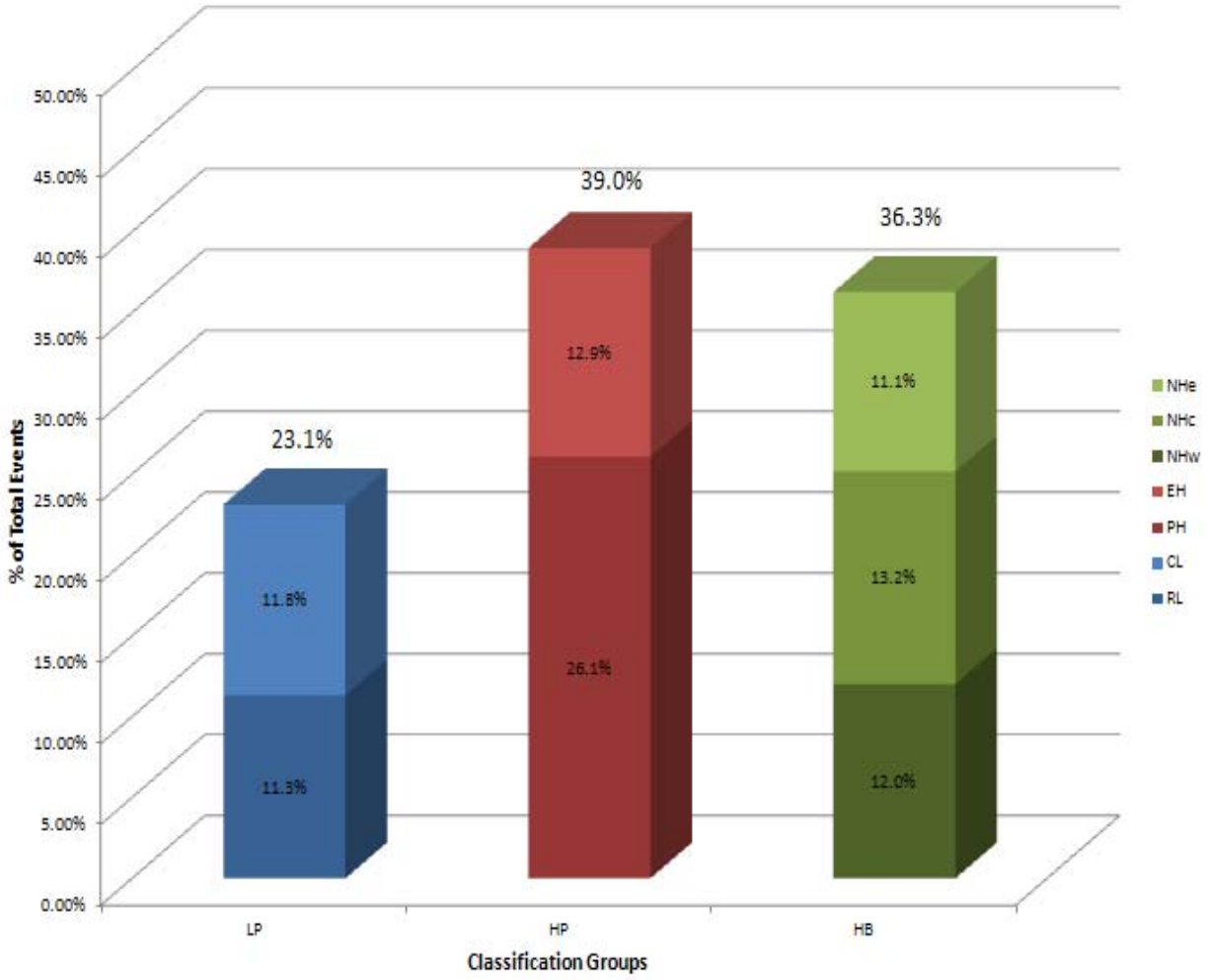

Figure 4.2 Percentage breakdown for all synoptic patterns with the low pressure (LP), high pressure(HP) and Hybrid(HB) synoptic groups for all years 1950 through 2009.

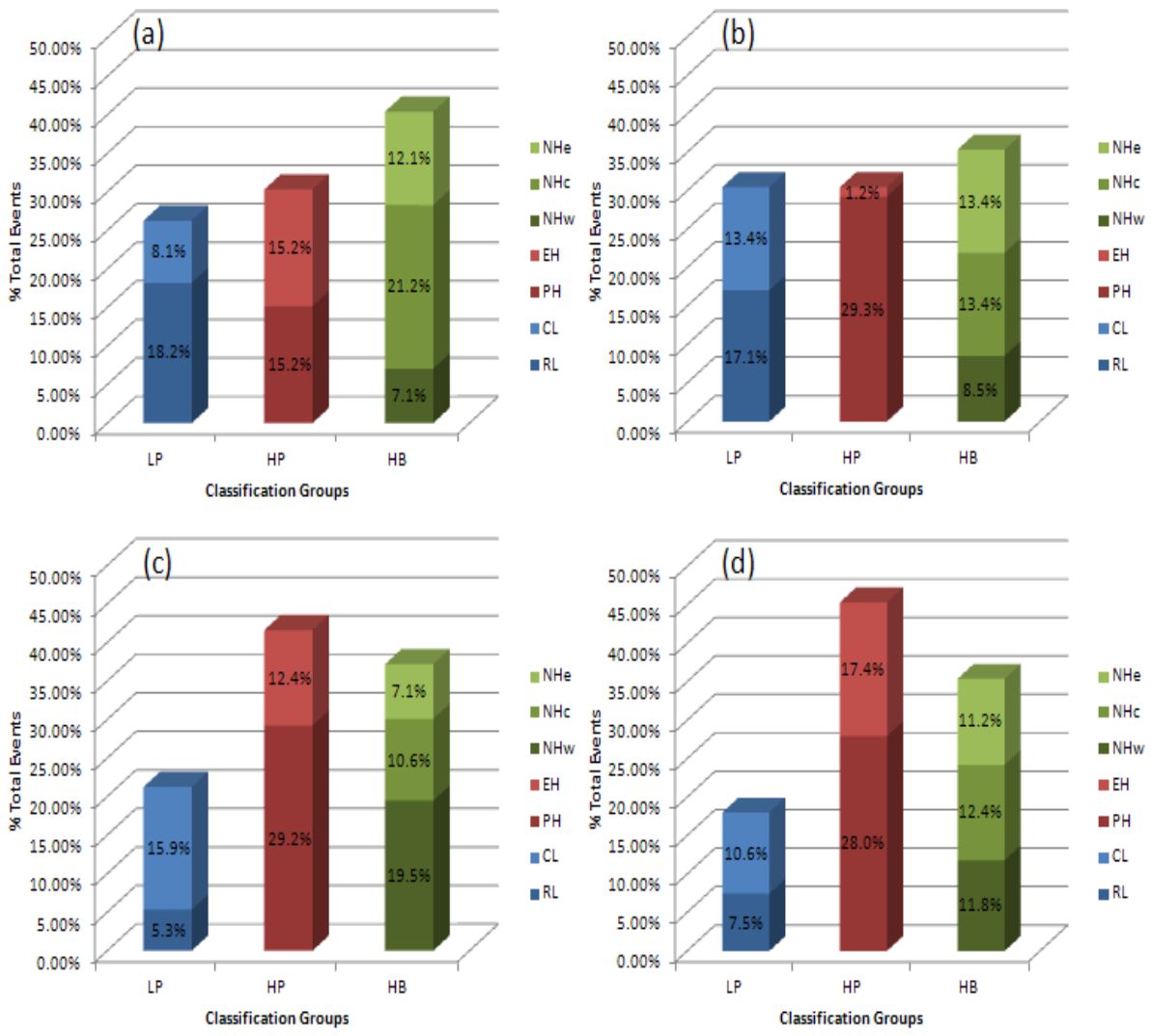

Figure 4.3 Percentage Breakdown for all synoptic patterns within the low pressure(LP), high pressure(HP) and Hybrid(HB) synoptic groups for months including (a) June, (b) July, (c) August, and (d) September.

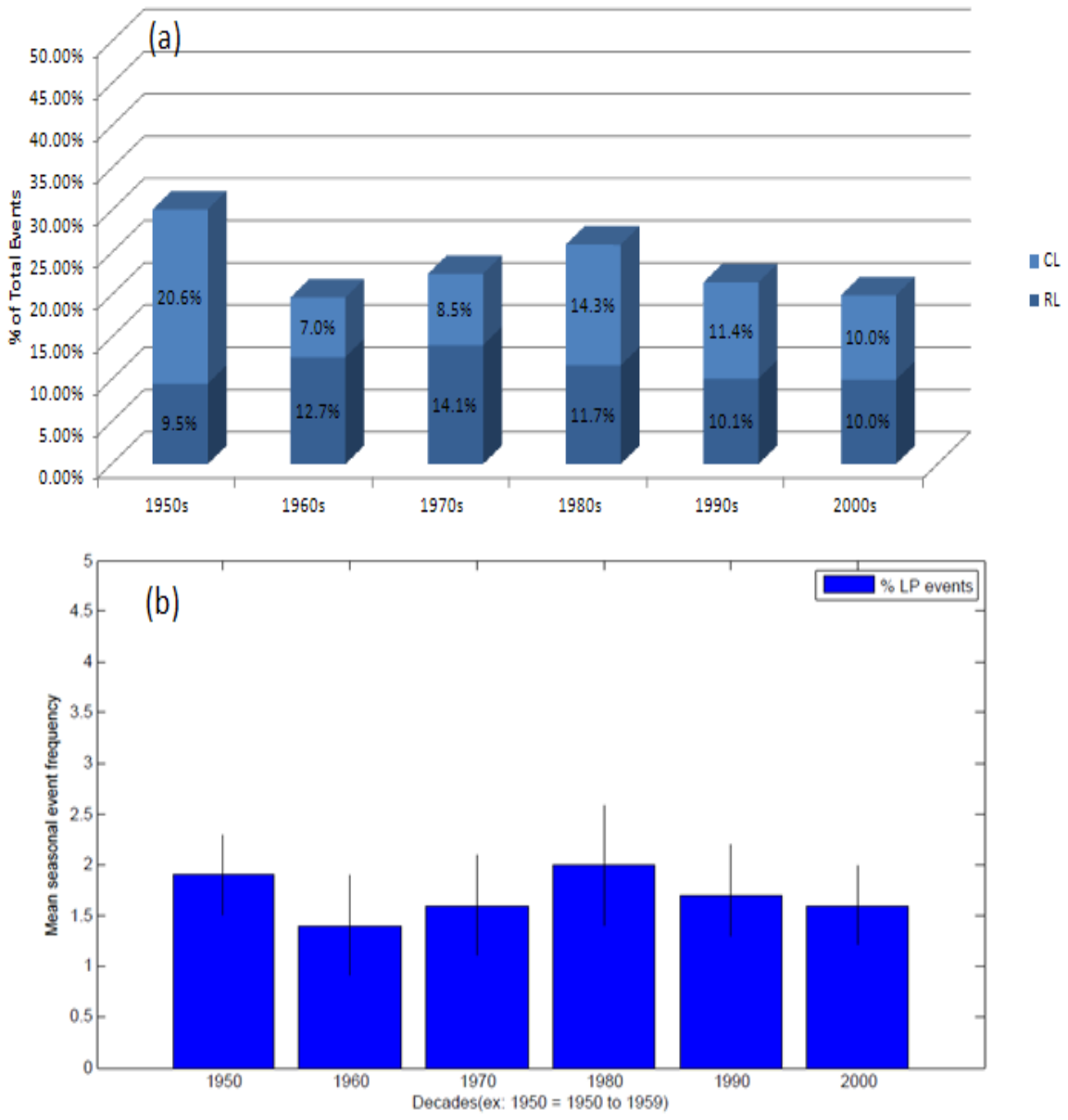

Figure 4.4 (a) Decadal breakdown (1950-2000) of percentages for Low pressure events. (b) Decadal breakdown of total events with 90% confidence intervals (black lines)

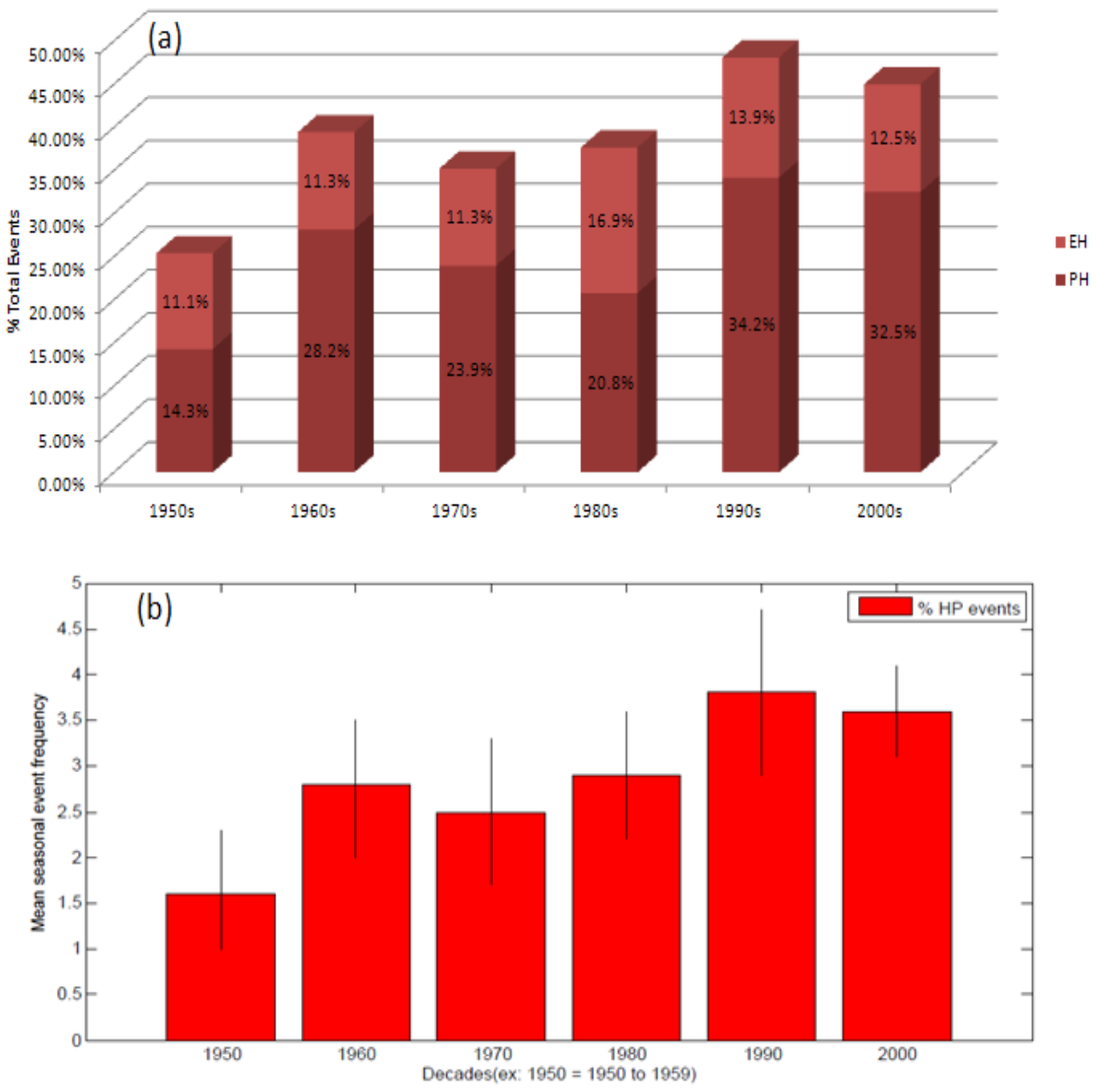

Figure 4.5 Same as figure 4.4 but for high pressure events.

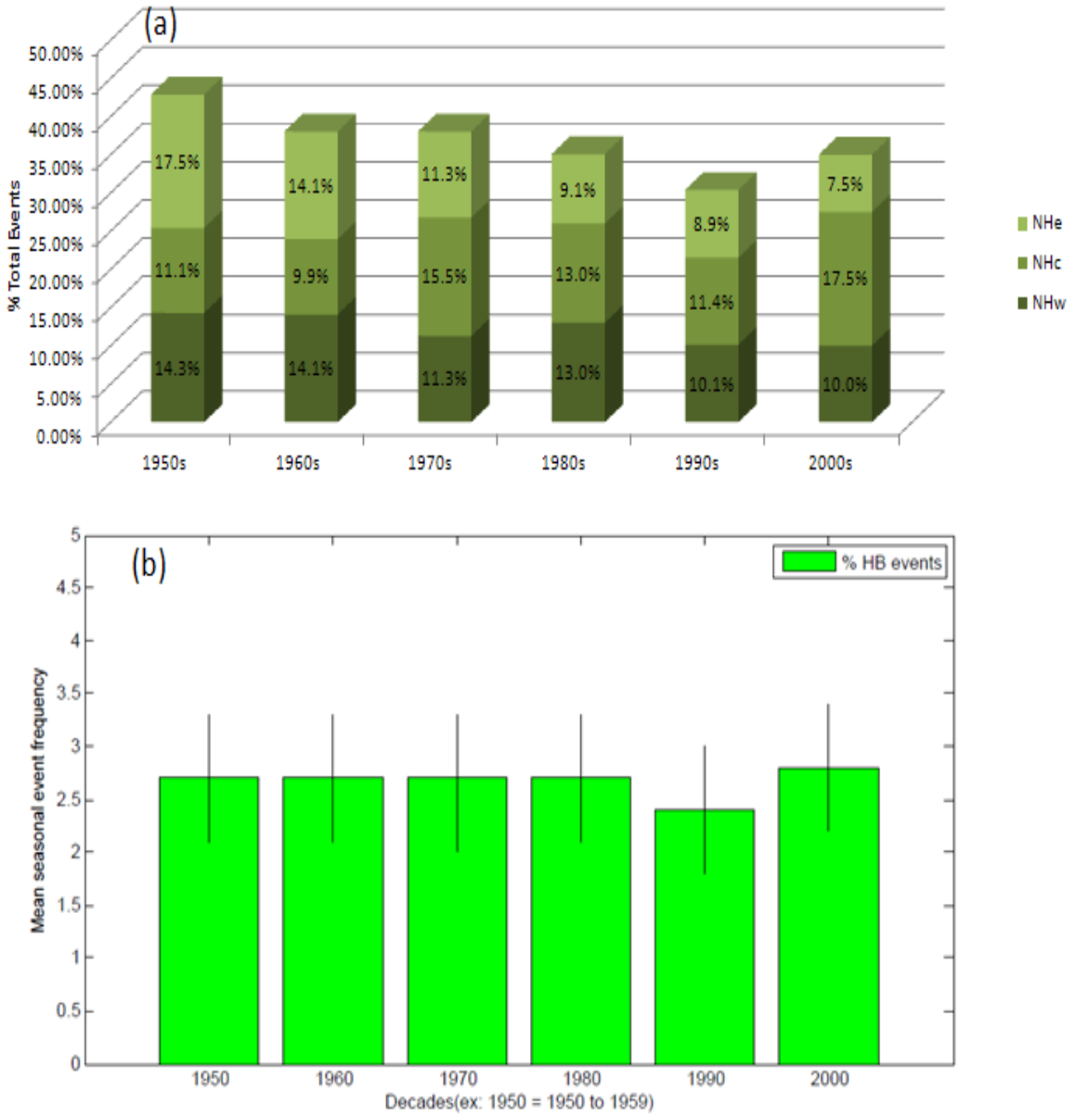

Figure 4.6 Same as figure 4.4 but for hybrid events.

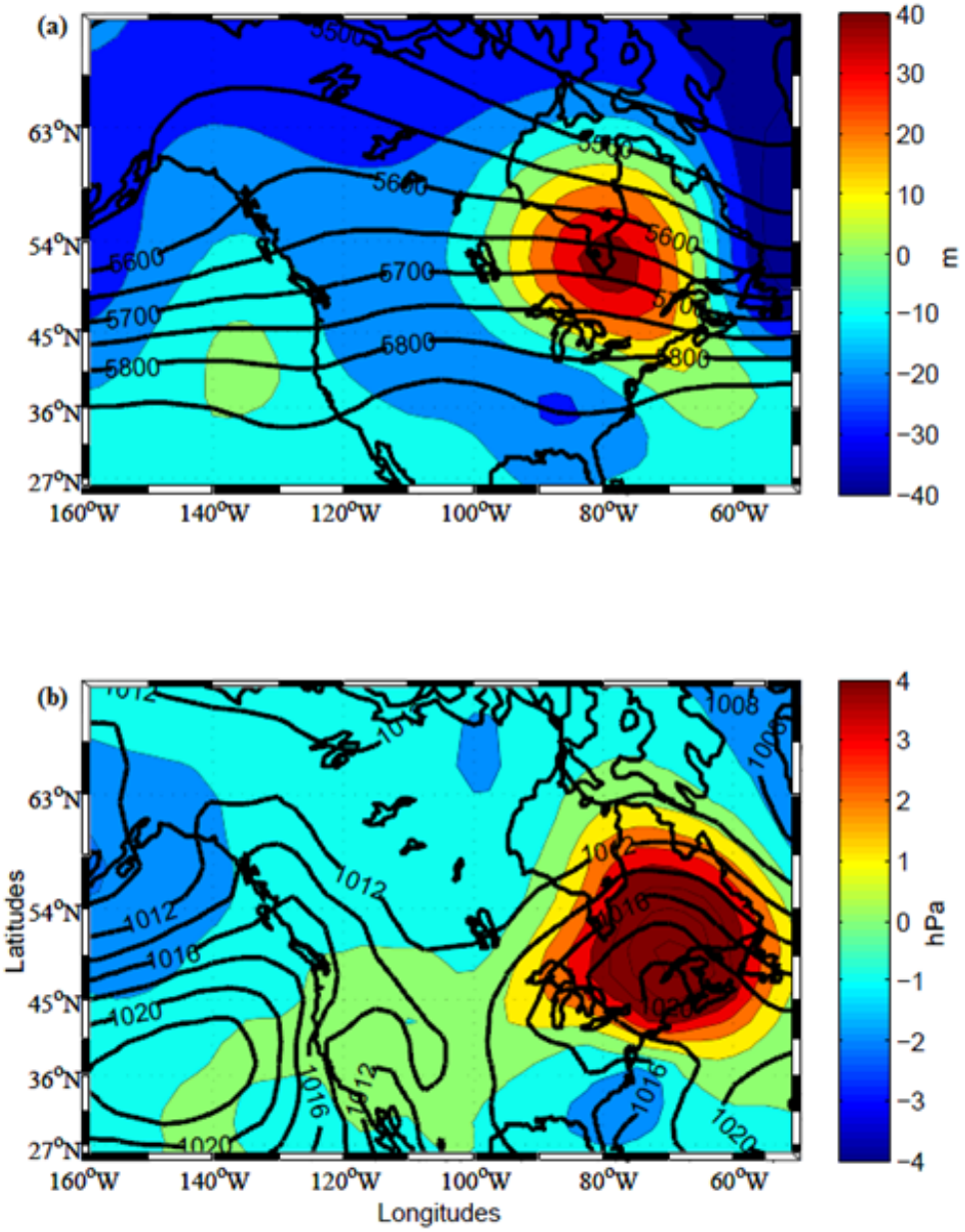

Figure 4.7 (a) Mean (contoured) and anomaly (color filled contour) NCEP/NCAR mSLP(hPa) and (b) 500-hPa heights (m) data for all mixing events 1950 to 2009. Anomalies based on 1981-2009 daily averages.

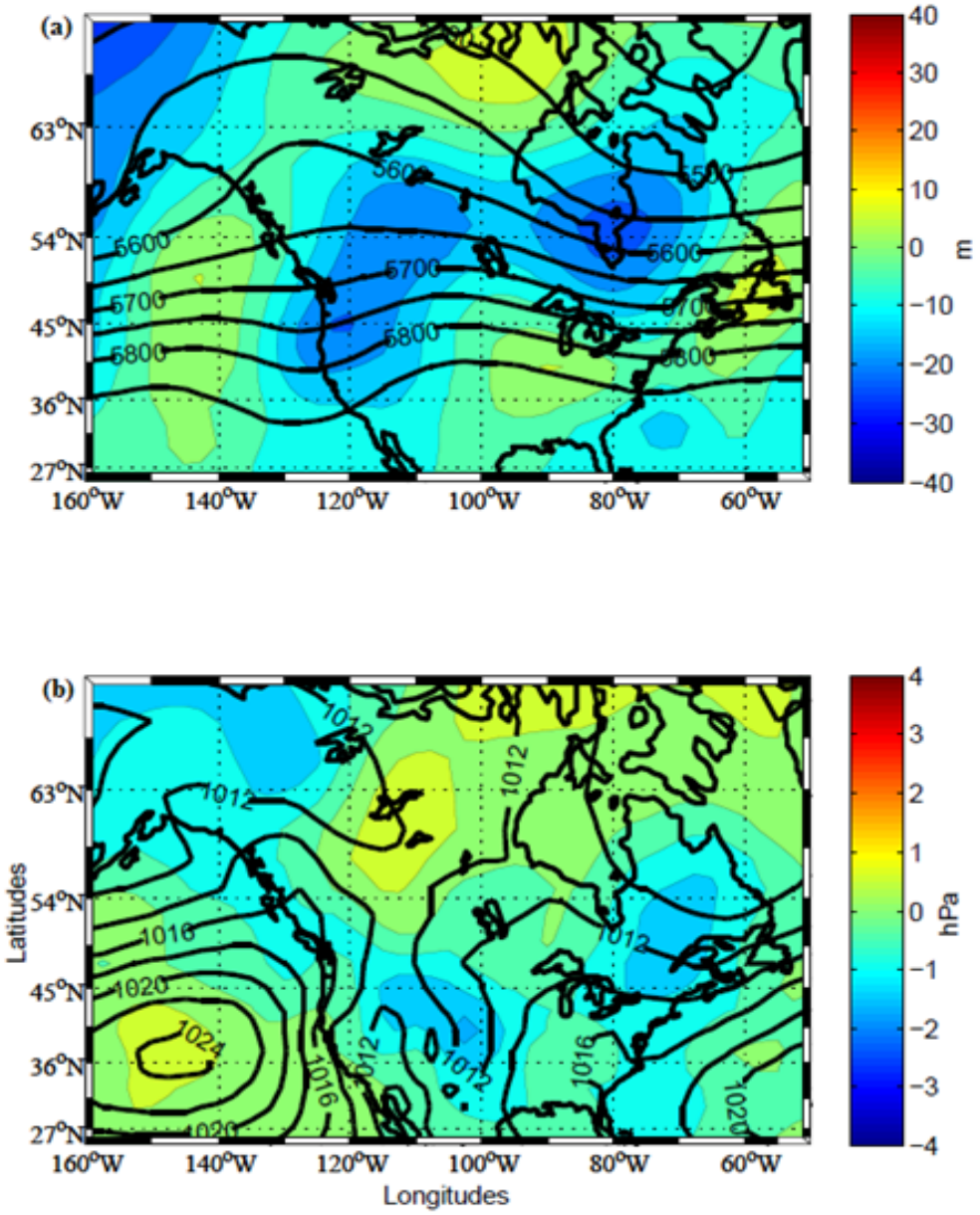

Figure 4.8 (a) Mean (contoured) and anomaly (color filled contour) NCEP/NCAR mSLP (hPa) and (b) 500-hPa heights (m) for daily lag -4 from day of all low pressure group mixing events 1950 to 2009. Anomalies based on 1981-2009 daily averages.

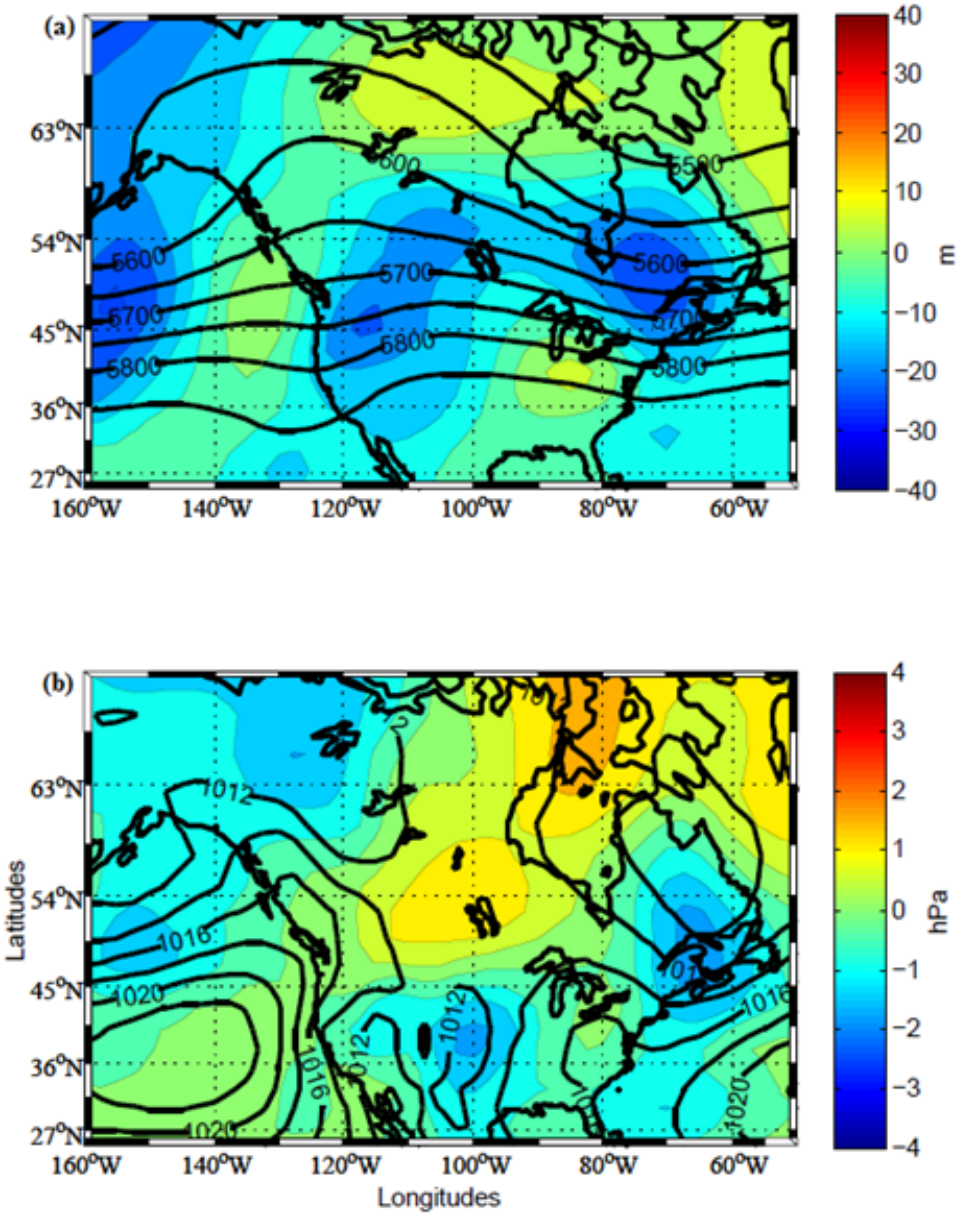

Figure 4.9 (a) Mean (contoured) and anomaly (color filled contour) NCEP/NCAR mSLP (hPa) and (b) 500-hPa heights (m) for daily lag -3 from day of all low pressure group mixing events 1950 to 2009. Anomalies based on 1981-2009 daily averages.

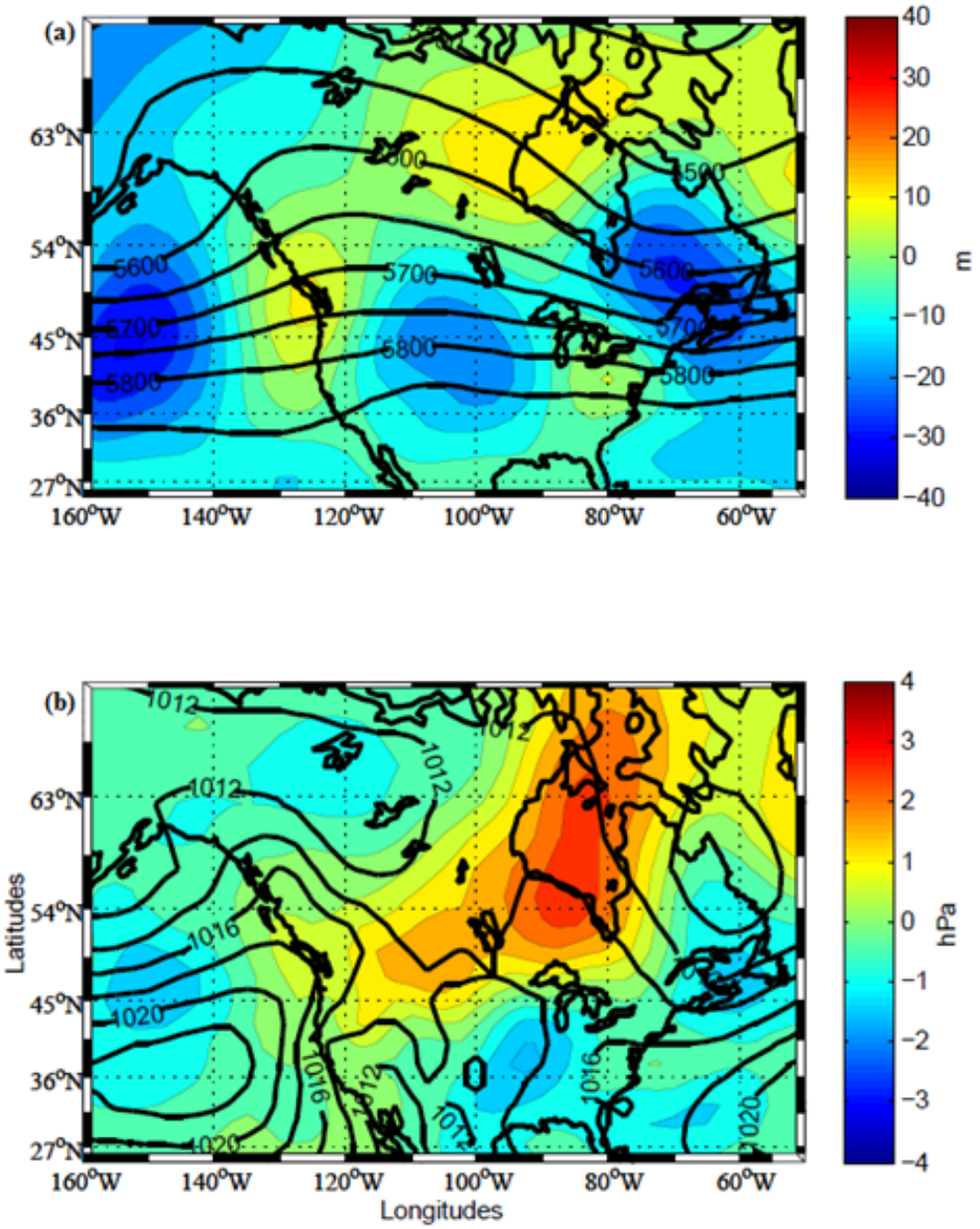

Figure 4.10 (a) Mean (contoured) and anomaly (color filled contour) NCEP/NCAR mSLP (hPa) and (b) 500-hPa heights (m) for daily lag -2 from day of all low pressure group mixing events 1950 to 2009. Anomalies based on 1981-2009 daily averages.

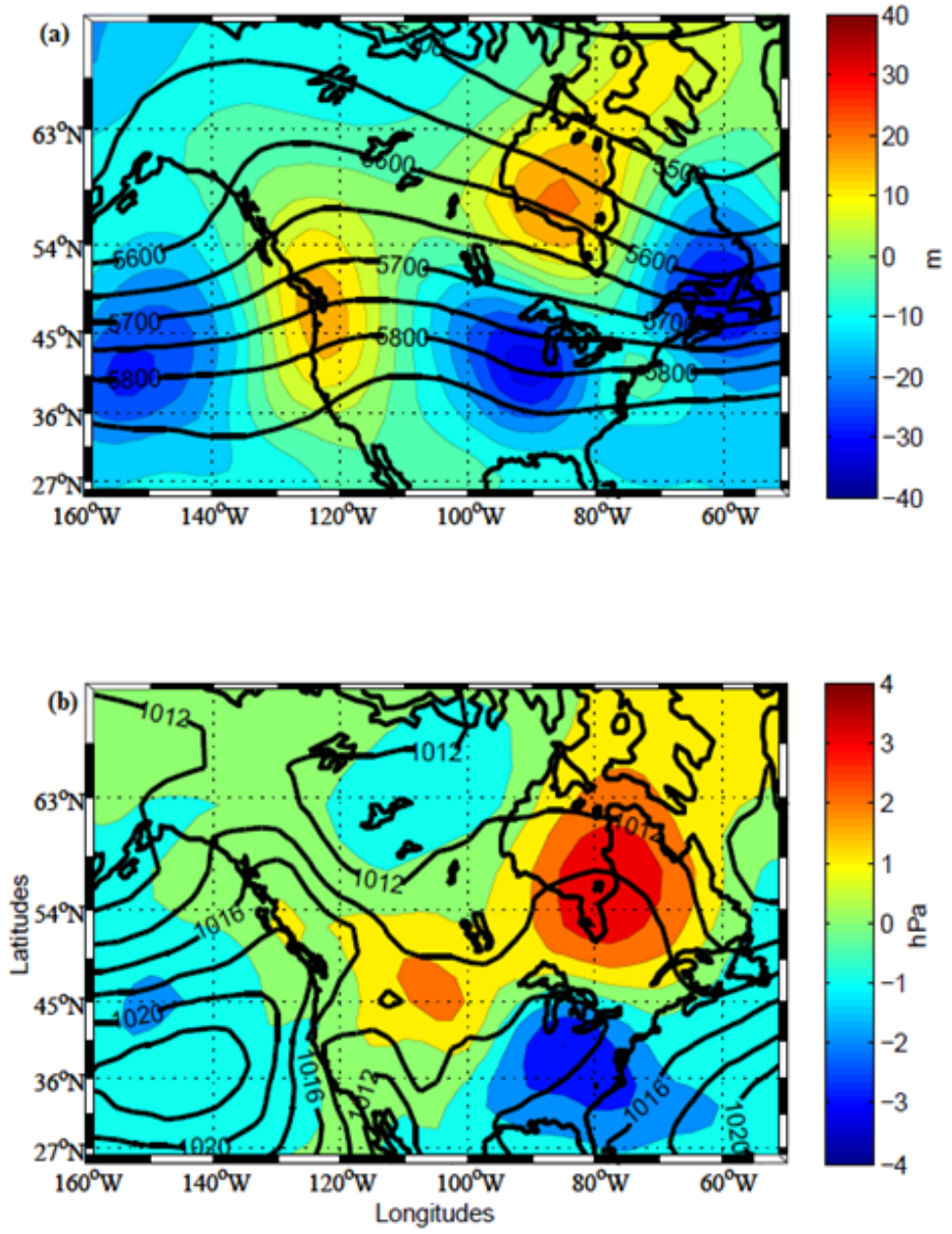

Figure 4.11 (a) Mean (contoured) and anomaly (color filled contour) NCEP/NCAR mSLP (hPa) and (b) 500-hPa heights (m) for daily lag -1 from day of low pressure group mixing events 1950 to 2009. Anomalies based on 1981-2009 daily averages.

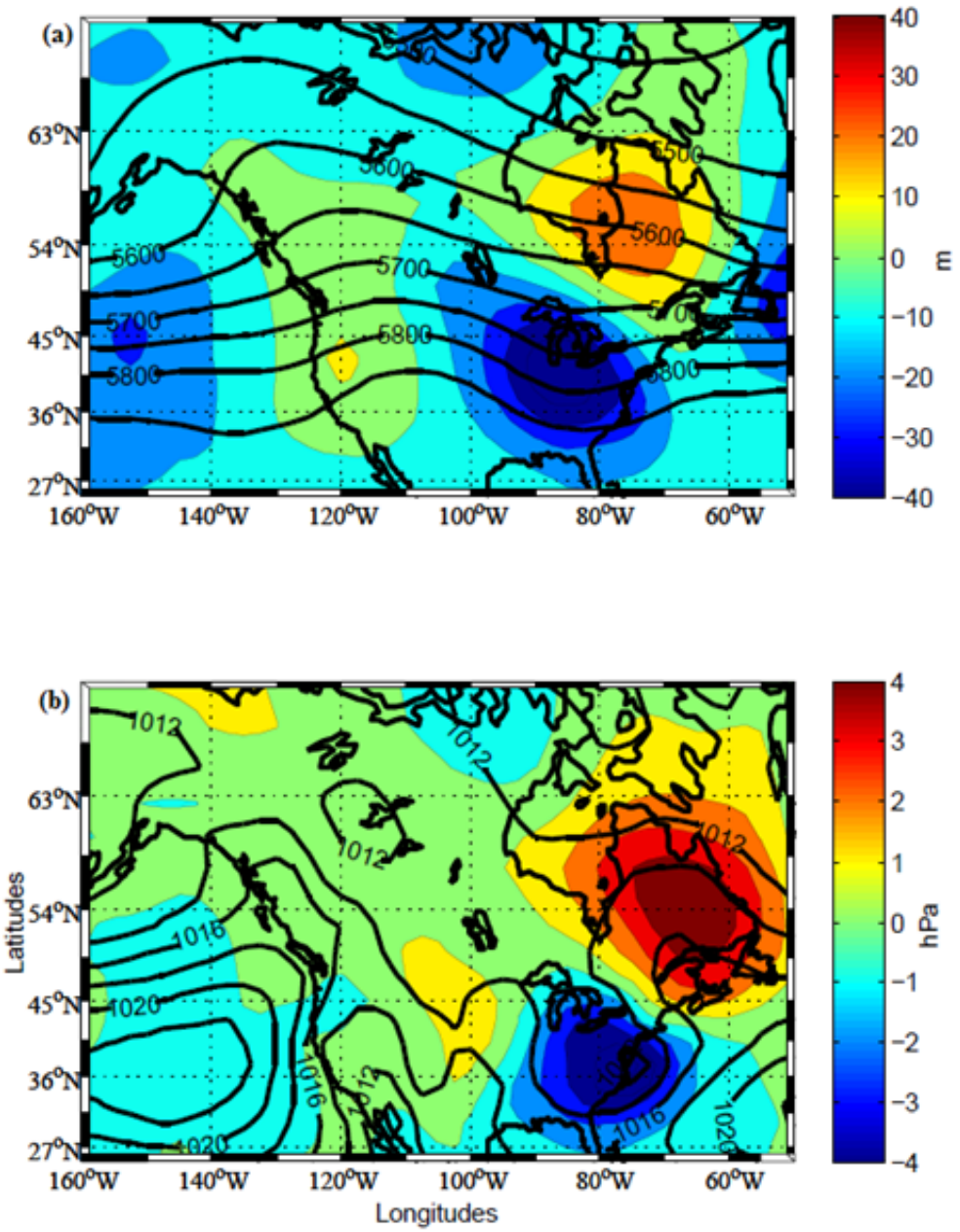

Figure 4.12 (a) Mean (contoured) and anomaly (color filled contour) NCEP/NCAR mSLP (hPa) and (b) 500-hPa heights (m) for day of all low pressure group mixing events 1950 to 2009. Anomalies based on 1981-2009 daily averages.

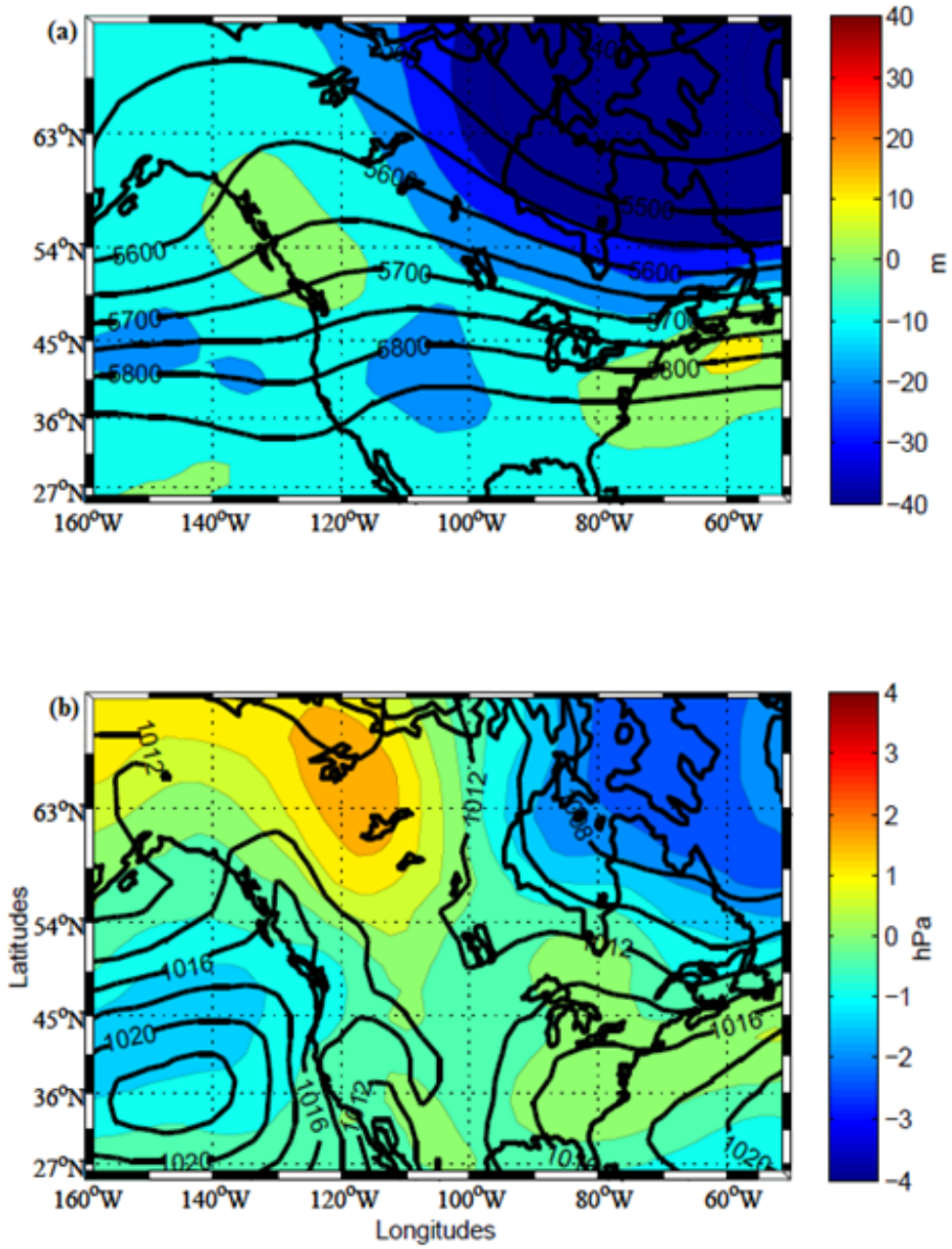

Figure 4.13 Same as figure 4.8 but for all high pressure group mixing events.

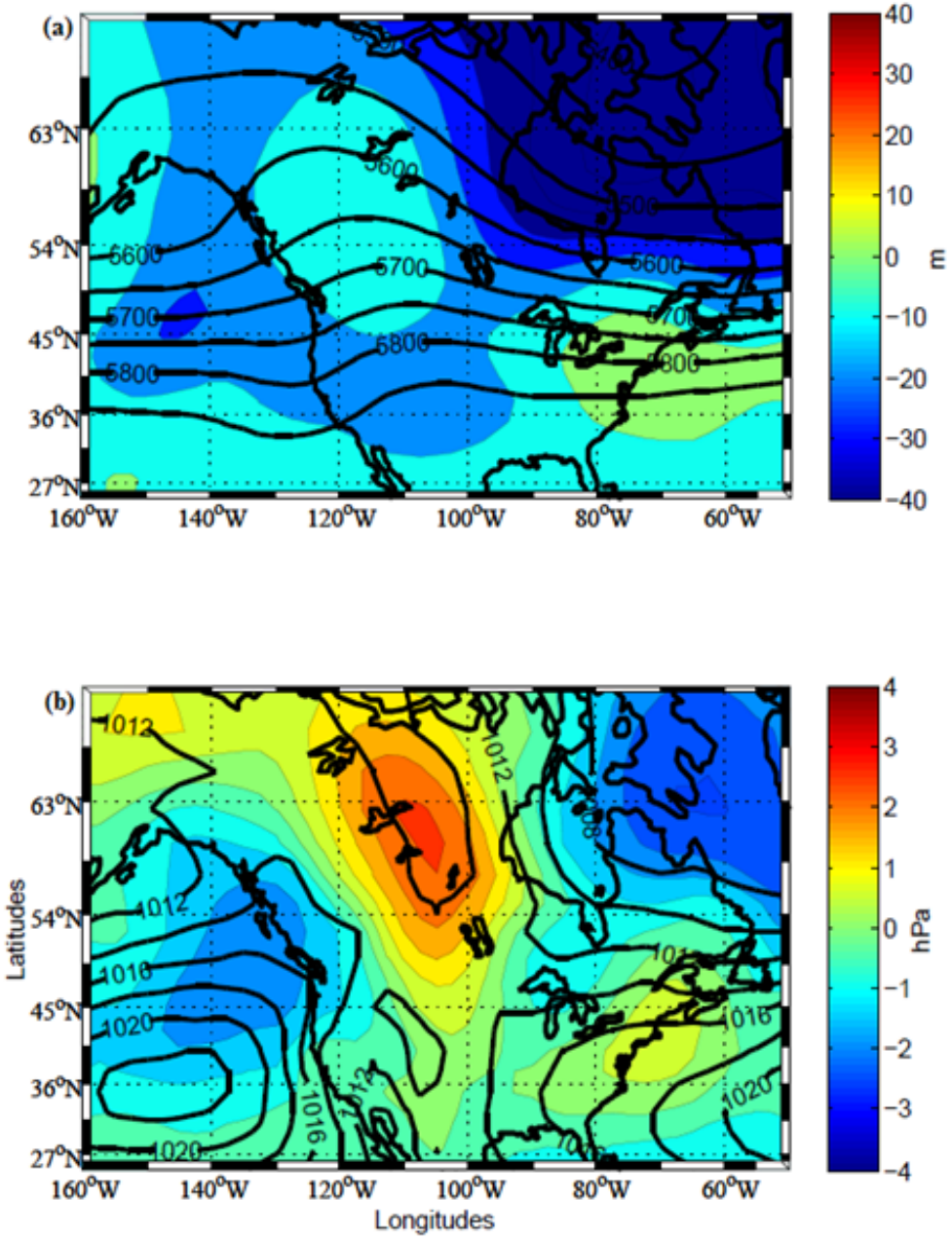

Figure 4.14 Same as figure 4.9 but for all high pressure group mixing events.

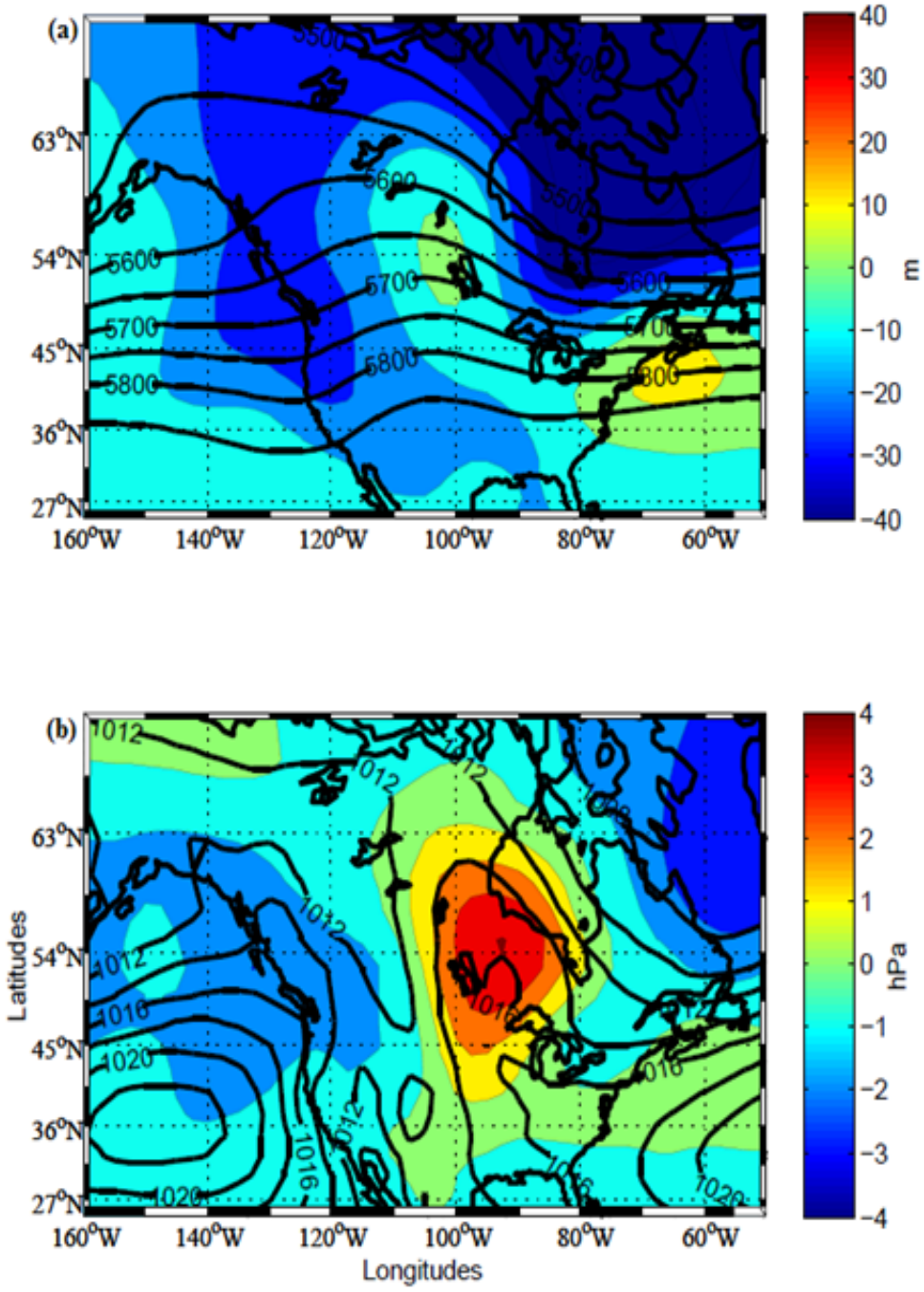

Figure 4.15 Same as figure 4.10 but for all high pressure group mixing events.

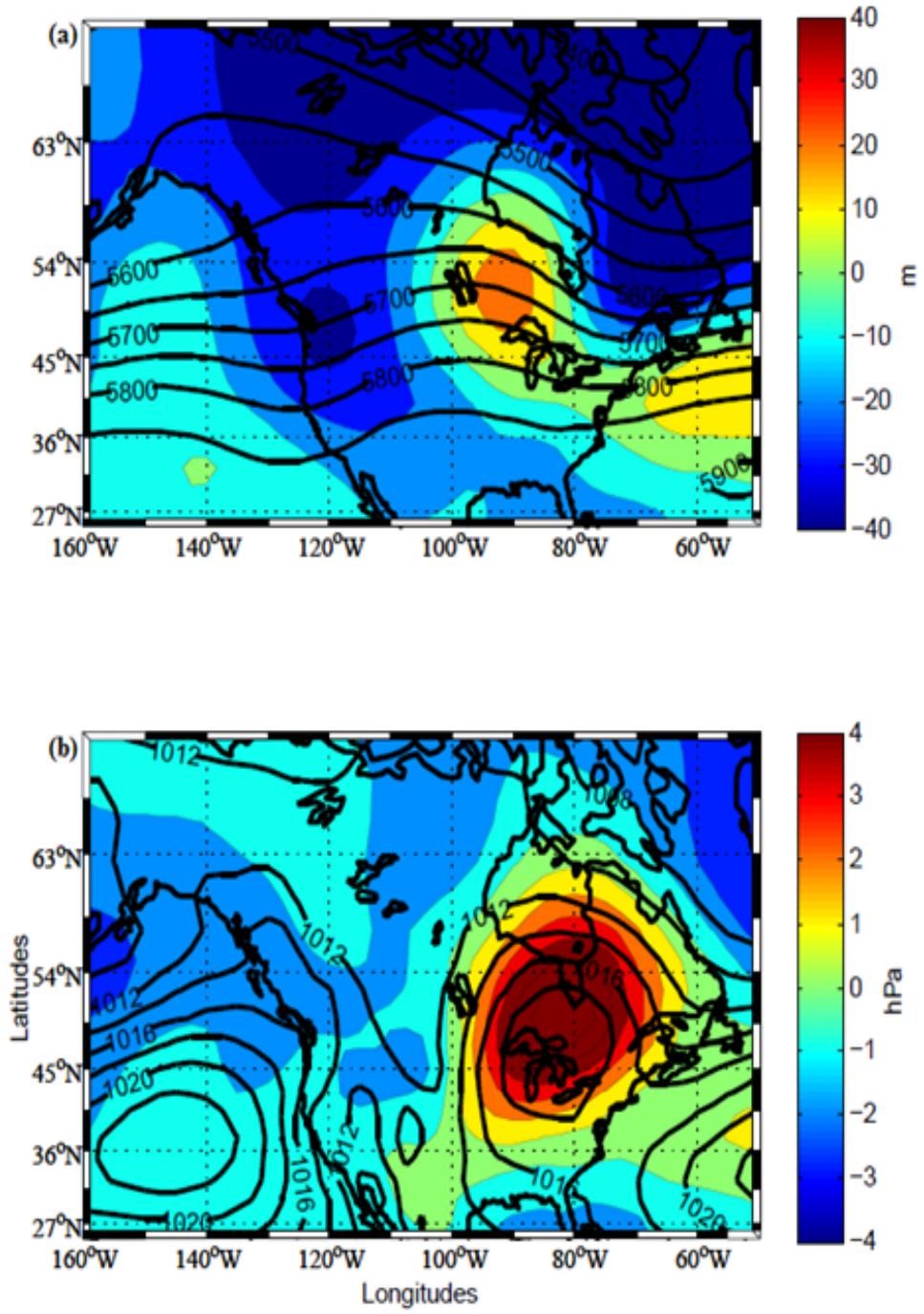

Figure 4.16 Same as figure 4.11 but for all high pressure group mixing events.

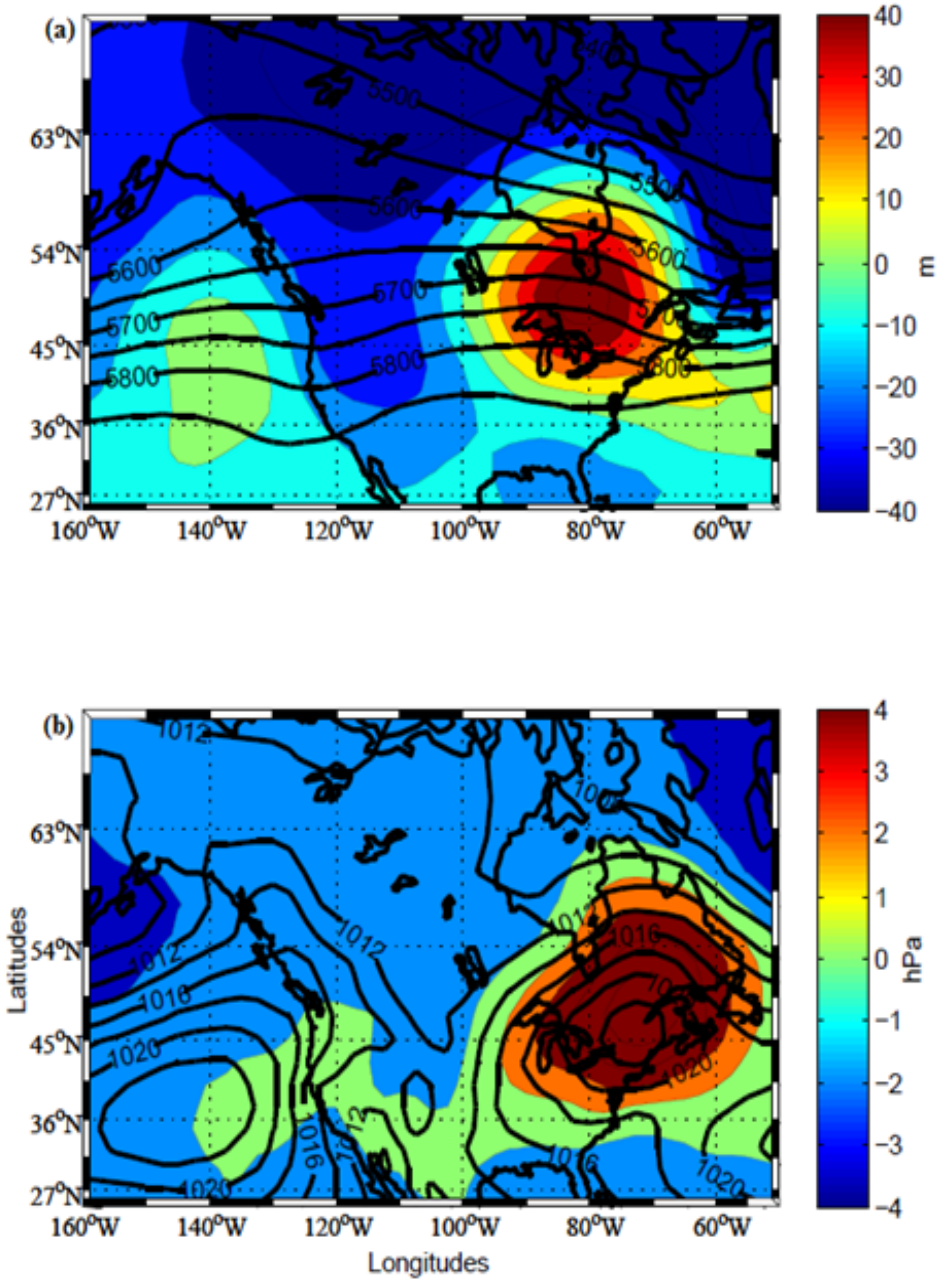

Figure 4.17 Same as figure 4.12 but for all high pressure group mixing events.

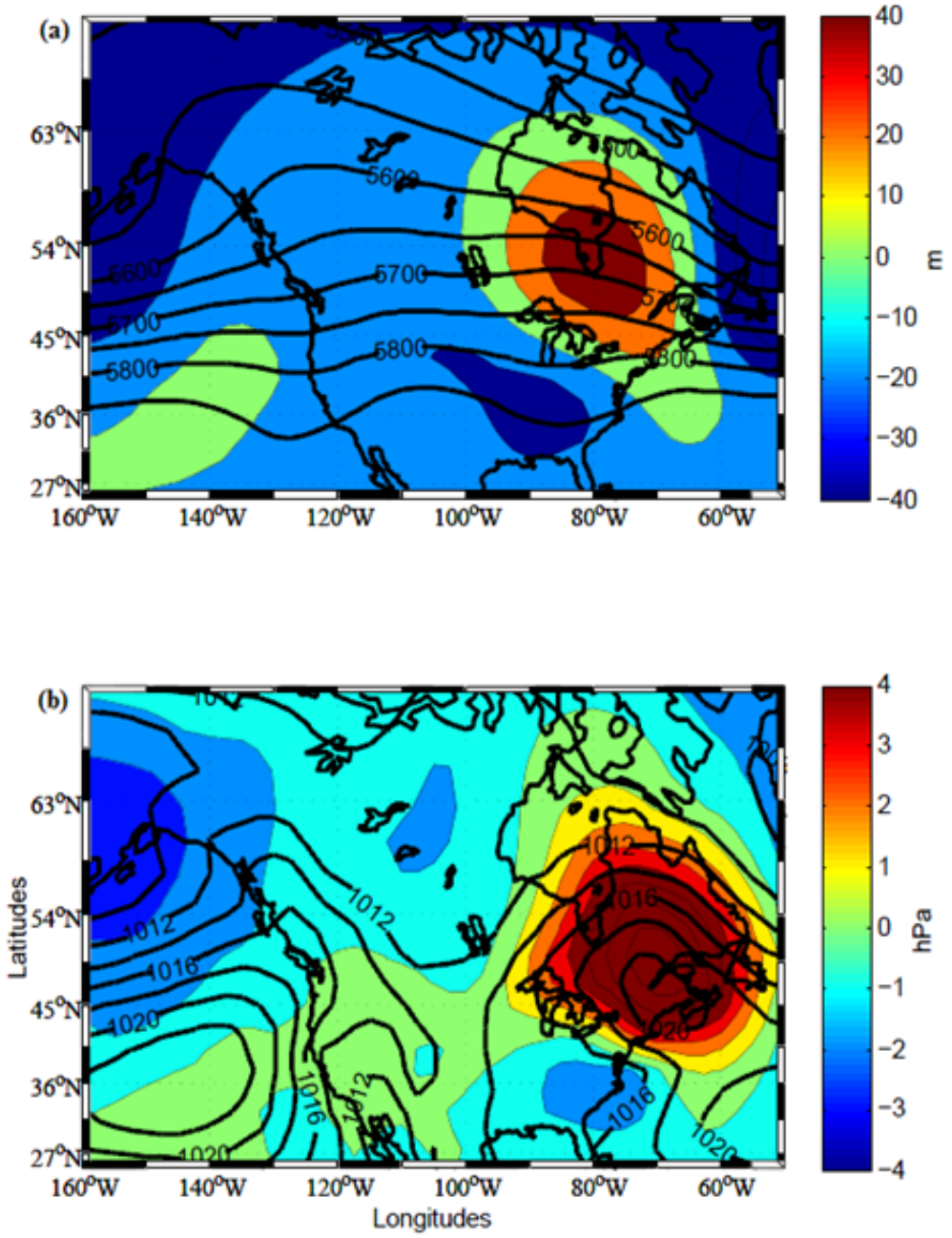

Figure 4.18 Mean (contoured) and anomaly (color filled contour) NCEP/NCAR (a) mSLP (hPa) and (b) 500-hPa heights (m) for day of all hybrid group mixing events 1950 to 2009. Anomalies based on 1971-2000 daily averages.

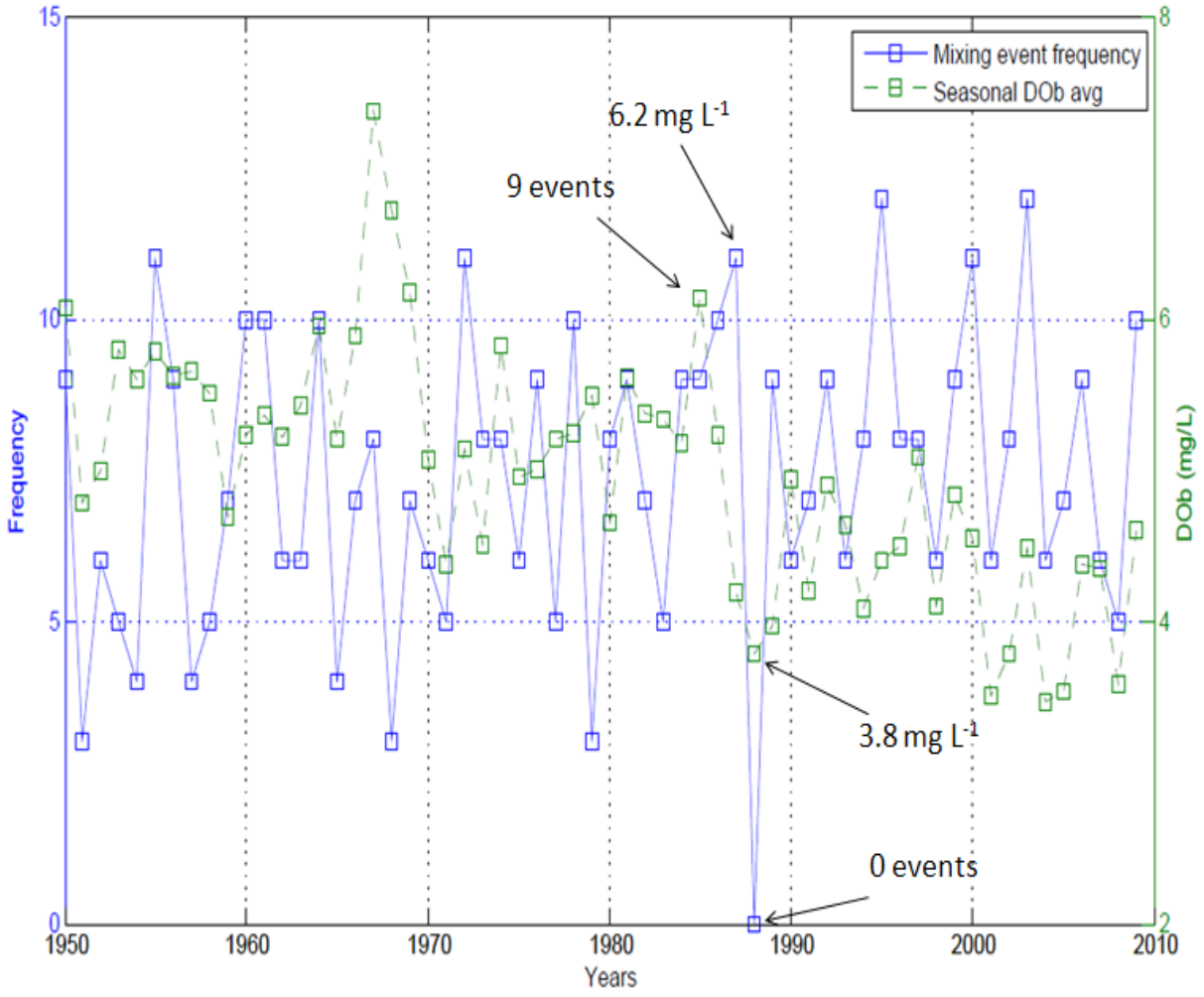

Figure 4.19 Time series of mixing event frequencies (blue line) and seasonal DOb averages (green dashed line) extending from 1950-2009. Black arrows indicate the active and inactive mixing periods for years 1985 and 1988 respectively.

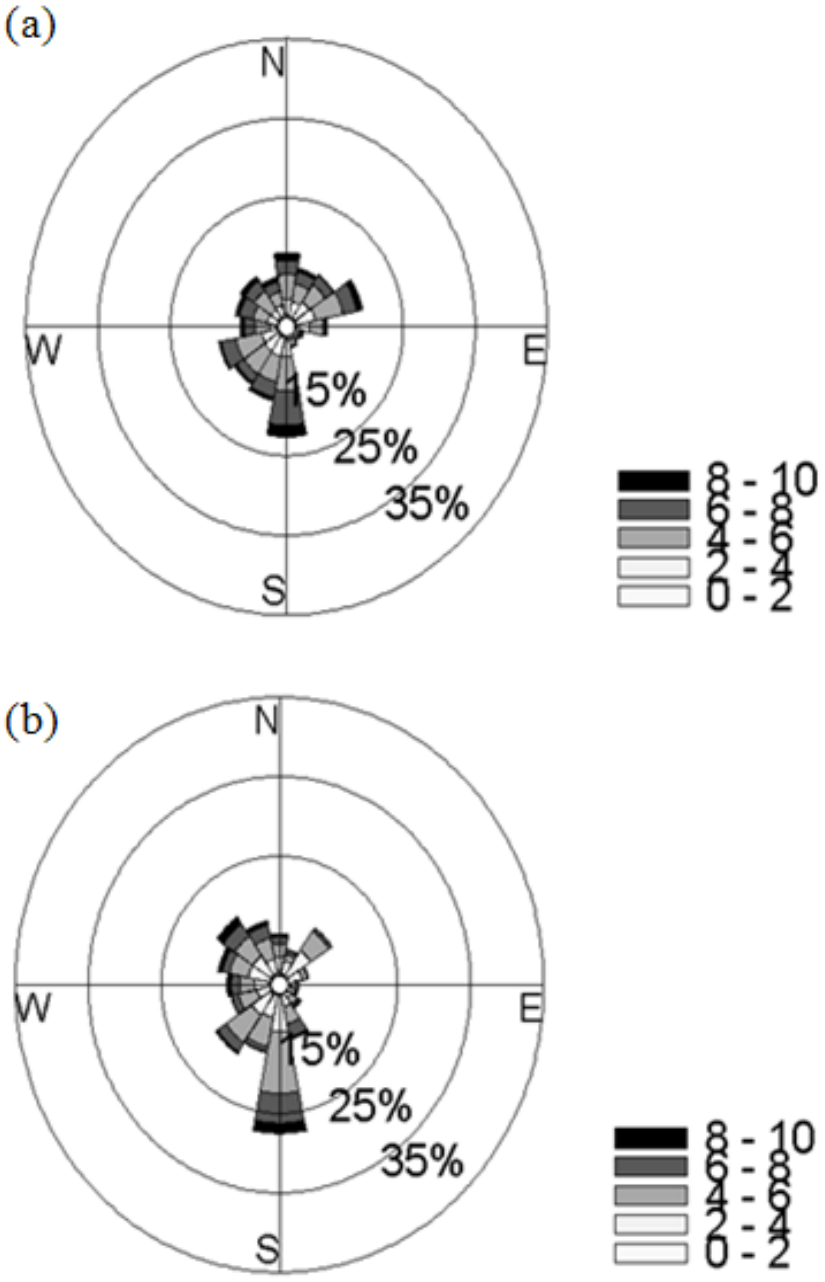

Figure 4.20 (a) Wind rose percentages for eighteen 20° wind bins using 5 wind speed criteria incremented every 2 m s^{-1} for the months of June-Sept of 1985 and (b) 1988 using LGA wind data.

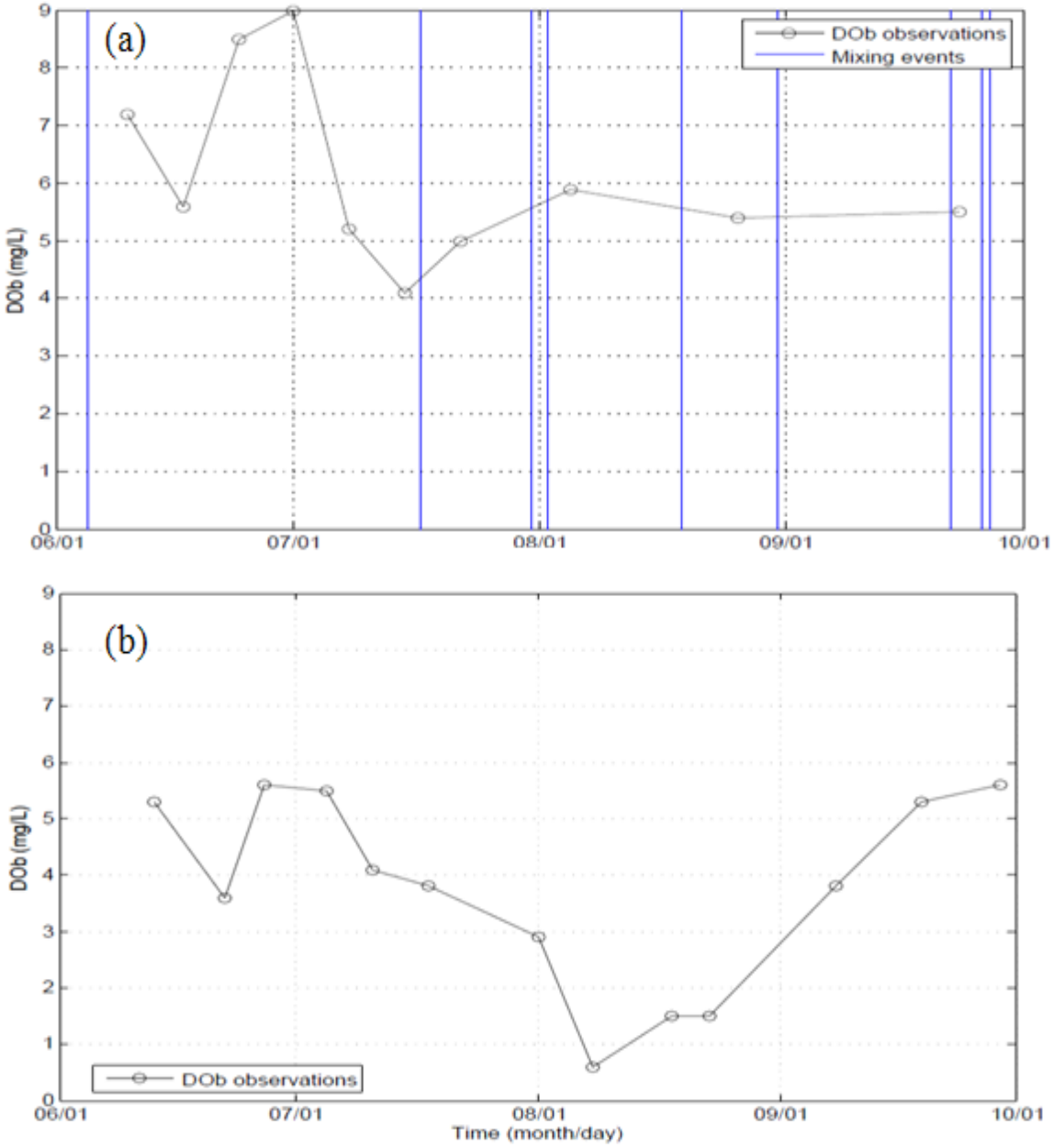

Figure 4.21 DOb time series (June-September) using NYC DEP mooring data for the (a) 1985 and (b) 1988 seasons with blue vertical lines representing mixing events.

Chapter VII: Discussion and conclusions

Hypoxia has been a chronic problem over the western Long Island Sound (wLIS) region for several decades, with more frequent hypoxic episodes experienced since the mid-1980s. These hypoxic events continue despite New York City having upgraded sewage treatment plants, and introduced nitrogen control. Due to the lack of research investigating the temporal and spatial components of the wind field that are conducive to mixing, this study aimed to better understand the seasonal synoptic setup (high and low pressure systems) responsible for wind induced de-stratification over western Long Island Sound and its corresponding influence on hypoxia events during summer on various temporal scales. Using long term and short term analysis of meteorological winds and marine DOb and temperature over wLIS, this study has identified wind directions and speeds that are preferable for mixing, using correlation and comparison analyses. Using these wind criteria, mixing event days were calculated for each season (1950-2009). To highlight meaningful synoptic patterns that resulted in mixing wind regimes, a synoptic climatology was presented taking into consideration all mixing event days. In addition, evolutionary patterns for high and low pressure for daily lag -4 days to day of the event were performed using mSLP and 500-hPa heights. Lastly, mixing event metrics (frequency, spacing, duration, speed) and hypoxia data (duration days, seasonally averaged DOb) were compared to determine if wind-induced mixing metrics can help explain multi-decadal trends in the hypoxia data.

The following important results were found from this study:

1. The connection between wind and DOb is present on a variety of temporal scales from weekly to decadal.

2. Wind criteria preferable for mixing include winds 30°-110° with speeds >= 4 m s^{-1} for a minimum of 50% of the daily observations.

3. The water column response to mixing event wind criteria resulted in a 1.5 mg L^{-1} increase in DOb on average for each event.

4. There exist seven main synoptic patterns associated with wind regimes that influence mixing (Regional Low (RL), Coastal Low (CL), Pre-High (PH), Extended high (EH), Northern High west (NHw), Northern High central (NHc), and Northern High east (NHe)) that were categorized into three main groups (High Pressure (HP), Low Pressure LP, and Hybrid (HB) patterns).

5. The most important synoptic system relevant to mixing are high pressure systems. Trends show an increase in the number of high pressure events that is significant to the 90% confidence interval. High pressure systems are typically located to the northwest of LIS. The systems typically form over western Canada and track southeast over the Hudson Bay and Great Lakes regions.

6. Mixing event frequencies are partly able to explain the inter-annual variability within the seasonal DOb and hypoxia duration time series, but are not able to explain the decreasing trend that has been occurring over the last several decades (discussed in section 5.2.3).

These conclusions will be discussed further in the following sections.

5.1. Directional wind response to DOb

It was originally hypothesized a vertical water column response, due to persistent northeast seasonal winds, would have a direct effect on DOb and bottom temperature due to de-stratification of the water column. La Guardia airport (LGA) wind observations from 1948-2009 and National Buoy Data Center (NBDC) Execution Rock (EXRX) buoy wind data as well as the Long Island Sound Integrated Coastal Observing System (LISICOS) EXRX buoy monitoring station and New York City Department of Environmental Protection (NYC DEP) dissolved oxygen and temperature data were used to evaluate this response over wLIS. DOb fluctuates on a variety of temporal scales. The summer months, specifically August, are at highest risk for hypoxia due to maximized thermal stratification and accelerated benthic oxygen consumption. It was found that during these summer months hypoxia has become a more frequent occurrence, with 21 seasons from 1980-2009 associated with occurrences of DOb values less than or equal to 2mg L^{-1}; In comparison to only 3 from 1948-1979 (Fig. 1.2). This is similar to the analyses of Wilson et al. (2008), who found rate decreases of -0.031 mg L^{-1} yr^{-1} for the 1946-1985 period increasing to -0.061 mg L^{-1} yr^{-1} for the 1986-2006 period for the months of July and August. It was fond that oxygen dynamics are very sensitive to the direction of wind forcing. Maximum correlations of over 0.4 were found for increasing DOb for winds out of the northeast (30°-80°) over wLIS using buoy derived wind and DOb data for the years 2006, 2008, and 2009 (Fig 4.8). However, for a southeast to southwest wind directions (210° - 260°), the correlation changes sign, with a maximum negative correlations exceeding -0.4 out of the southwest. These southwest winds are also associated with a high frequency of decreasing DOb observations (not shown). Consistent with O'Donnell et al. (2008), it was found on shorter time scales; estuaries have oscillations of DOb on time scales of 3 to 7 days related to vertical mixing. Summer season

statistics using Connecticut Department of Environmental Protection (CT DEP) hypoxia duration day data imply that seasons associated with a high percentage of winds from directions 40° -60° and speeds greater than or equal to 4 m s^{-1} result in a reduced frequency of hypoxic duration days with correlations of -0.7. This is in comparison to winds out of the south in which correlations of approximately 0.4 are observed. On the decadal scale, the seasonal wind percentages using mixing event wind bins of 30°-110° for winds greater than or equal to 4 m s^{-1} and seasonal DOb averages for multiple decadal segments were investigated. Modest correlation values (highlighted in red) are present for the 1950-1969 and 1990-2009 periods (Table 3.1). Hit rate percentages, defined as the total number of events for each wind bin that resulted in a increase in DOb, were determined for eighteen wind bins for speeds equal to or greater than 4m s^{-1}. Surprisingly, wind bins centered 60° to 110° for winds greater than or equal to 4m s^{-1} had resulted in over 85% of the events associated with increasing slopes of DOb. In contrast, 0% of all events calculated for the center of wind bins 180°-280° resulted in increasing DOb slopes using >= 4 m s^{-1} threshold.

Based on high correlation values on various temporal scales between DOb and winds out of the east-northeast directions described above, it was determined that mixing event days would be defined by days in which winds are between 30°-110° that are greater than or equal to 4 m s^{-1} for 50% of the total daily observations. Important to note that a mixing event day does not necessarily mean that mixing and increases in DOb occurred for that day. Instead it means conditions are favorable for mixing on this day. It was determined that wind events from a east - northeast direction have greatest overall increases in sub-pycnocline oxygen, which is consistent with studies conducted by O'Donnell (2006), O'Donnell (2008), Wilson et al. (2008), and Whitney and Codiga (2011). However, many of these studies imply up estuary (westerly) winds,

or along-channel winds are the general directions that induce water column de-stratification over wLIS, which is consistent with longitudinal density straining discussed by O'Donnell (2008). This would include northeast winds due to the axial orientation of wLIS; more specifically wind between 15°-75° (centered on 45°) discussed in O'Donnell (2006). For this study however, the directional criteria covers a broader 80° range centered more out of the east (30°-110° centered at 70°). This would imply that up-estuary component of the winds (30°-70°) consistent with straining are important, but cross-channel winds (70°-110°) also impact mixing. This suggests that lateral advection (Scully 2010a) is also an important contributor to vertical water column mixing. To interpret this directional response, it is useful to consider the orientation of the thalweg shown in Figure 5.1 which was developed from gridded bathymetry used in numerical simulations by Crowley (2005) and Hao (2008). The thalweg heading varies between 45° to 55° over the wLIS study area suggesting that winds from the east (70°-110°), have a lateral advective component to vertical water column ventilation introduced by Sully (2010a). An example of this mixing process can be seen in figures 5.2 and 5.3 in which a 3-dimensional primitive equation ROMS model simulation conducted by Wilson (manuscript 2011) is used to highlight this mixing mechanism. The Model grid and forcing is discussed by Crowley (2005), Wilson and Swanson (2005), and Hao (2008). A focus is placed on the description of the transient water column structure in a single lateral section in the western sound centered on -73.51^{o} . To the west of this section the basin becomes narrower and the thalweg orientation becomes more northerly. This model was run from 29 August 1999 to 30 August 1999 to visualize mixing associated with lateral advection. For this study, a hybrid storm system associated with high pressure to the west of LIS and a coastal low system to the south of LIS produced a north-northeasterly component of the wind field from the 29 August to 30 of August (Fig. 5.2). During a lateral advection mixing

event, winds induced downwelling on north side of the sound and upwelling on the south side. This allows the near bed residual flow to transport lower near bed oxygenated waters up the southern shoal to the south side of the sound. This allows an increased flux of oxygen into the sound due to a increased sea-surface atmosphere oxygen gradient (Scully et al. 2005). The most distinctive feature is the evolution (Fig. 5.3a-d) of the downward tilting of the isopycnals on the south side of the transect and the advection of deep water from the channel up into the southern shallows where it is mixed vertically (Fig. 5.3d). This provides support that lateral advection is potentially an important mechanism in controlling mixing over wLIS.

Time-depth cross-sections for DOb and temperature were created in chapter 3 to visualize the transient water column response from the surface to the bottom water interface. DOb and temperature observations for all mixing events for the 2006, 2008 and 2009 season were averaged for each hourly observation; -24 hours before the passage of an event to +60 hours after the passage of an event. In general, surface DO decreased followed by an accelerated increase in bottom DO. Later in the period, surface DO values increased again as the air-sea oxygen gradient strengthened and exchange between the air-sea interface took place. This water column change in DO is also documented in Wilson et al. (2008) who emphasized the nature of mixing within the water column associated with passage of an extratropical cyclone. They determined that northeasterly winds associated with the cold front passage produced very brief periods of strong mixing and de-stratification. These brief mixing events were followed by re-stratification associated with gravitational adjustment and southwesterly winds during which time vertical mixing within the water column was extremely weak. O'Donnell et al. (2008) also found a similar characteristic of the 15m depth LISICOS buoy records over the EXRX and wLIS station

in which the presence of several intervals of rapid decline in surface DO were followed by periods of ventilation or increasing oxygen concentration.

5.2. Relevant synoptic patterns and climatology and its significant to extended DOb trends

5.2.1. Climatology of synoptic patterns

It was previously suggested in the original hypothesis that extratropical cyclones are the dominate synoptic system influencing mixing. Thus, if the number cyclones passing further north of wLIS has decreased, as implied by some recent climate studies (Zishka and Smith 1979, Agee 1990, McCabe et al. 2000, Mesquita 2007, Leibensperger 2008), this may imply that wLIS would have fewer mixing events. However, our results found that high pressure system were much more relevant than previously expected, accounting for 75.3% of the total events, either as high pressure events or hybrid (combined low-high) events. This contradicts the Austin and Lentz (1999) study that only inspected cold fronts, and neglected high pressure, associated with late summer DOb variability on the time scales of days to weeks over the inner shelf off North Carolina. Wilson and Swanson (2005) also speculated that extratropical cyclones are the predominant synoptic systems responsible for the surface heat flux and wind stress producing northeasterly winds associated with wLIS mixing. In this study cold fronts were primarily found as precursors to PH and EH synoptic patterns. In addition, the only statistically significant trend to the 90% confidence level can be attributed to high pressure events in which a drastic increase occurred from the 1950's to the 1990's, with a 23% increase in the percentage of high pressure events during this period. Regardless, the long term trend for mixing event frequencies from 1950 to 2009 is weak with a rate increase limited to .027 events yr^{-1}. It does not appear however,

that mixing events are the 'smoking gun' to help explain the recent declining trends of seasonal DOb. This is consistent with Lee and Lwiza (2009) who found only 10% of the total seasonal variability of DOb can be explained by wind speed (independent of direction). However, the authors found that if you combine the factors of: mean spring total chlorophyll, mean summer wind speed, maximum spring discharge into Long Island Sound, and mean spring total nitrogen than 92% of the total seasonal variability can be explained.

5.2.2. Synoptic evolution of mixing event patterns

To determine the synoptic processes responsible for alternating the synoptic features that cause mixing, the synoptic evolution of seasonal (June-September) average and anomaly fields including; mSLP and 500-hPa heights were investigated for high pressure groups, low pressure groups, and hybrid groups. The general synoptic pattern for all mixing patterns includes a fairly zonal 500-hPa flow; with a shortwave ridge over southeastern Canada, and a weak trough over the southeastern United States. A strong area of high pressure (>=1020 hPa) sets up over northern New England at the surface with a weak low pressure off the southeastern U.S. coast.

The synoptic evolution patterns for high and low pressure events were found for all mixing event days using 500-hPa geopotential heights and mSLP mean and anomaly maps. For low pressure systems, cyclones frequently formed just lee of the Rocky Mountains over the western United States. These systems would typically track east just south of the Great Lakes before passing over the northeast United States. In addition, the 500-hPa flow pattern becomes progressively more amplified from day lag -3 to day lag 0, with a trough over the eastern third of the U.S. These results are consistent with Mesquita et al. (2007) who found one of the more important cyclone tracks starts in the eastern part of Canada in the lee of the Rocky Mountains

and extend east-southeast toward the Atlantic Ocean. The other important low pressure system is the CL. These systems would typically develop off the southeast coast or in the tropics associated with a weak trough over the northeast U.S.

The only area of relevant high pressure development was within the mountainous terrain of western Canada. This is in general agreement with those conducted by Ziska and Smith (1979), however, the maximum high pressure genesis densities are located farther north for this study, over interior Canada instead of southwestern Canada as documented in Ziska and Smith (1979). Consistent with Harman (1987), after development these systems typically move to the southeast and strengthen quickly. The 500-hPa flow amplifies by day lag -1 as a ridge begins to build into the north central U.S. and south central Canada. In many cases these high pressure systems approach from just north of the Great Lakes and follow the passage of a cold front associated with a low pressure system that tracked over north-northeastern Canada. These cyclones are similar to the ones described in Leibensperger et al. (2008) who found maximum cyclone densities over east-central Canada.

The evolution of the hybrid pattern is very similar to the low pressure patterns so it is not shown. Instead, the mean and anomaly 500-hPa geopotential height and mSLP fields are presented only for the day of hybrid mixing events. At 500-hPa there is a weak trough over the southeastern U.S. and a weak ridge to the north, over Hudson Bay. A large area of high pressure (>= 1020 hPa) covers almost all of eastern Canada. Weak low pressure (~ 2 hPa) exists over the southeastern states.

An interesting comparison can be made between Zishka and Smith (1979) and Harman (1987) who both found the number of cyclones and anticyclones were decreasing from 1950-

1977 for the summer months. In addition, Leibensperger et al. (2008) found a similar trend for cyclone frequencies from 1980-2006. Strong negative trend for cyclones of -0.14 cyclones yr^{-1} to -0.49 cyclones yr^{-1}, depending on the analysis technique, were found with decreasing rates for anticyclones of -0.51 anticyclones yr^{-1}. In contrast, this study shows the number of anticyclones (cyclones) inducing mixing have increased (remained steady). This would indicate that the preferred tracks for mixing have increased, even though the total frequencies of high and low pressure systems have decreased on average.

5.2.3. Climate related trends

Originally it was hypothesized that there would be a strong relationship between the seasonal evolution of hypoxia and summertime extratropical cyclone frequencies. In addition, it was theorized that inter-annual variations in summertime hypoxia were controlled primarily by meteorological forcing associated with synoptic period weather systems which controlled variations in density stratification and vertical mixing. Therefore, years with severe hypoxia would be associated with periods of prolonged stratification, while those without significant hypoxia would be characterized by frequent wind-induced mixing. This section will discuss the extent of this relationship, and determine if it is able to explain the longer decadal trends in DOb.

Mixing event frequencies using directional thresholds of 30°-100° and wind speeds >= 4 m s^{-1} for 75% (Fig. 5.4a), 50% (Fig. 5.4b), and 25% (Fig 5.4c) of daily observation are presented to determine if the resent trend of a increase in mixing event frequencies is independent of duration criteria. Black dashed lines indicate the least squares regression trend from 1980-2009 (Fig. 5.4a-c). For all daily observation percentages, some degree of an increasing trend is present. Correlations between the 50% criteria and 25% (0.66 with p-value <0.05) as well as

75% (0.73 with p-value <0.05) show good agreement verifying that the inter-annual variations in mixing events remain consist regardless of the duration criteria.

Mixing events and LISICOS EXRX buoy DOb data are plotted for two seasons (2008 and 2009) for the month of September to show the potential importance of late season event spacing (Fig.5.5 and Fig. 5.6). 2008 was associated with 83 CT DEP hypoxia duration days (highest for 19 year period) with hypoxia conditions ending on 20 September. 2009 was only associated with 54 CT DEP hypoxia duration days with hypoxia conditions ending on 3 September. DOb values in the beginning of September of 2008 were between 3 and 4 mg L^{-1} before concentrations dropped over a period extending from ~5 September to ~15 September in which DOb values were below 2 mg L^{-1} (Fig. 5.5). DOb values did not begin to significantly rise until half-way through the month when four mixing events occurred within ten days of each other. These events helped maintain the DOb values above dangerous levels for the remainder of the season but occurred very late in the season. September of 2009 started with DOb levels ~ 3.5 mg L^{-1}. These values increased considerably over the following weeks when two mixing events, occurring within days of each other, help sustain a mixed environment (Fig. 5.6). In the middle of the period two more events occurred, again within days of each other keeping DOb values above 5 mg L^{-1}. This assisted in sustaining DOb values from dropping to hypoxic levels for the remainder of the season.

The key difference between these two months is the time in which the DOb events occurred. Both September of 2008 and September 2009 contained 4 mixing events; however the evolution of DOb was different for these months due to the time of month they occurred. DOb rose slightly in the beginning of September 2008, but the absence of mixing events at the start of the month allowed DOb values to plummet. Because the 4 mixing events that occurred during

this month did not transpire until later in the season, DOb condition remained at hypoxic levels until 20 September. For September of 2009 the 4 mixing events occurred in the beginning of the month to keep DOb values from dropping and subsequently becoming hypoxic. Due to the favorable timing of these events, hypoxic conditions ended on 3 September.

NYC DEP Seasonal DOb and mixing event frequencies are presented in figure 5.7, that are broken up into three multi-decadal segments (1950-1969, 1970-1989, 1990-2009). Correlations in table 5.1 were used to determine the relationship between mixing events and seasonally averaged DOb for these three time periods. Correlations were insignificant for the first two time periods of 1950-1969 and 1970-1989 at 0.13 (p-value 0.60) and 0.22 (p-value 0.35) respectively (Table 5.1). The lower correlations from 1950-1989 are hypothesized to be partially due to poor instrumentation, placement of the buoy, and data collecting techniques until 1986 when improvements to the azide Winkler method for measuring DOb were implemented. For the 1990-2009 period, correlations increased to 0.41 with a p-value of 0.07 (correlations increase to 0.52 if only 1991-2009 period is considered with p-value = 0 .04) (Table 5.1). It was found that the inter-annual variability of seasonal DOb can be partly explained by the mixing event frequencies over the last two decades. However, the longer term trends in mixing event frequencies is not able to explain the last 20-30 year drop in average DOb. This is represented by the linear regression lines in figure 5.7 for both DOb and mixing events for 1990-2009. The seasonal DOb (dotted line) trend shows a steady decrease while the mixing event frequencies (dashed line) remain steady with a slight increasing trend. Because mixing event frequencies are a bulk number for the entire season, other mixing event metrics are used for the months of July and August (critical hypoxia months as seen in figure 1.2) to determine if inter-seasonal trends in; frequency (Fig. 5.8a), mixing event spacing days (Fig. 5.8b), and event duration days (Fig.

5.8c) help explain the recent seasonal DOb trend. The mixing event frequencies for July and August over the last 24 years (1986-2009 period used because post 1986 confidence in the accuracy of the data increased) exhibits a decreasing trend similar to that of the seasonal DOb pattern(Fig. 5.8a). This would indicate that a decrease in the number of mixing events during the most crucial hypoxic months may help explain why DOb has become more sever in recent decades. However, upon further inspection the correlation between these two time series from 1990-2009 is -0.34, which is opposite from what one would expect. This result indicates that the connection between July-August mixing events and seasonal DOb is null. Spacing days and duration days in figures 5.8b-c are also used as proxies to determine the average number of days between mixing events and the average duration (in days) of mixing events for the months of July and August. In theory, the fewer (greater) number of spacing (duration) days between (for) mixing events should result in a better chance of maintaining DOb above hypoxic levels. However, both the trend in spacing between mixing event days and average duration of mixing event days has remained mostly constant over the last two decades. It was concluded that mixing event frequencies, or any other mixing metric, could help explain the recent trends in dropping DOb levels. However, this comparison did highlight that inter-annual variability in seasonally averaged DOb can be partly explained by the frequency of mixing events.

A multi-decadal relationship between DOb/hypoxia data and mixing event data was investigated to determine if wind and mixing events can help explain some of the DOb variability over the last several decades. CT DEP duration day data (1991-2009), NYC DEP seasonally averaged DOb (mg L^{-1}), and mixing events were utilized to establish this connection. In figure 5.9a mixing event frequencies and hypoxia duration days are compared. A significant relationship is present between these time series with correlation values of -0.71 and p-values

0.01. The inter-annual peaks and valleys associated in the hypoxia duration day time series can be explained to a significant level by mixing event frequencies. These results indicate that synoptic events may help raise DOb to above hypoxic levels and shorten the number of hypoxia duration days, indicated by the -0.71 correlation. To determine if hypoxia duration days exhibit a similar trend to that of seasonally averaged DOb, figure 5.9b compares hypoxia duration day and seasonally averaged DOb time series from 1991-2009. Correlations were modest (-0.51 with p-value of 0.03) with hypoxia duration days displaying a lot of inter-annual variability. Hypoxia duration days display a slight increasing trend which is consistent with seasonally averaged DOb exhibiting a declining trend because as lower DOb is experienced over season, it is expected hypoxic conditions would persist for a longer period.

Overall, the results of this study demonstrate that wind is an important factor in controlling the evolution of DOb on several temporal scales, ranging from daily/weekly to decadal. There are several synoptic systems, in the form of 'mixing events' that are associated with wind regimes that are conducive to wind-induced mixing. It was shown that using mixing event wind criteria increased DOb 1.5 mg L^{-1} on average for each mixing event. High pressure systems are the most important pattern related to mixing events and demonstrates an increasing trend in the frequency of events over the last 50-60 years. Although a lack of a connection could be made between mixing event frequencies and the recent decline in average seasonal DOb, a significant relationship still exists in being able to help explain the vigorous inter-annual variations in DOb and hypoxia duration. This inter-annual relationship is present in comparing mixing event frequencies for both NYC DEP seasonally averaged DOb (0.51 correlation for 1991-2009 period) and CT DEP hypoxia duration days (-0.71 correlation for 1991-2009 period). This finding is significant for the fact if a forecast can be made regarding the frequency of

mixing events for a given season then this can be used as an indicator for hypoxia severity and duration.

Future work will investigate why high pressure systems related to mixing event have been increasing. To do this, anticyclones will be counted and tracked for several summer seasons to determine if the frequency of anticyclones are increasing or that anticyclone tracks are in better locations to enhance the chances of wind-induced mixing. In addition, stratifying winds, out of the south-southwest will be further investigated to determine if there is a relationship to the evolution of seasonal DOb patterns. It would also be interesting to apply this study to other partially mixed estuaries, such as Chesapeake Bay, to provide insight as to if this synoptic wind relationship is applicable over other estuarine environments that experience hypoxia. Lastly, an effort should be made to maintain, if not increase, the LISICOS monitoring buoy network. This data was crucial in developing a detailed relationship between wind and DOb. It would be extremely helpful if more of these instrumented buoys were implemented to cover a larger region over wLIS and other parts of Long Island Sound to better be able to understand the temporal, as well as spatial, evolution of DOb over areas that traditionally experience hypoxia.

Tables

Seasonal DOb (mg L^{-1})	Mixing event frequency	Section 1 (1950 – 1969)		Section 2 (1970-1989)		Section 3 (1990-2009)	
		Corr	P-value	Corr	P-value	Corr	P-value
June-Sept	June-Sept	0.13	0.60	0.22	0.35	0.41*	0.07

Table 5.1 Comparison of June-September mixing event frequencies and Seasonally averaged DOb using NYC DEP E10 DOb data from (1950-2009). Time series is broken up into three segments; (1) 1950-1969, (2) 1970-1989, (3) 1990-2009. * (if correlation for period 1991-2009 is used instead of 1990-2009 correlation increases to .52)

Figures

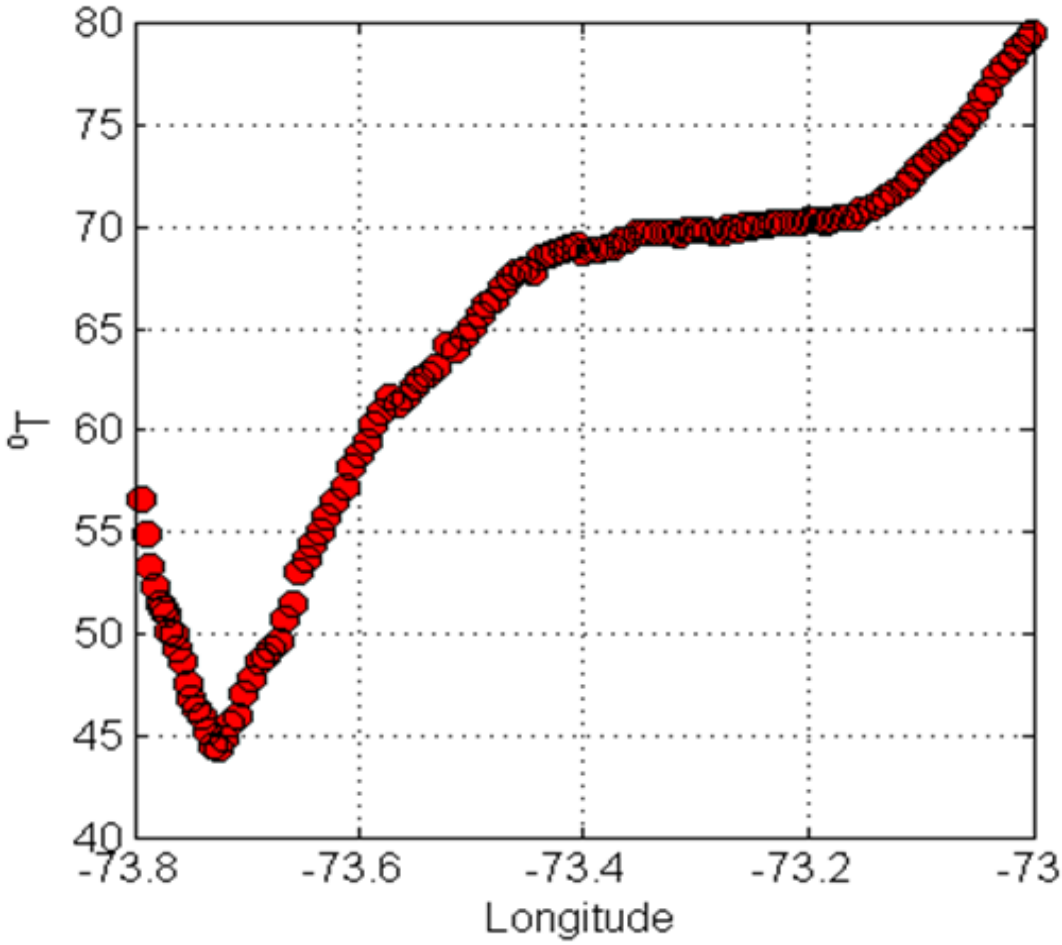

Figure 5.1 Orientation of the thalweg as a function of longitude in west-central Long Island Sound. Y-axis is labeled from degrees true.

\

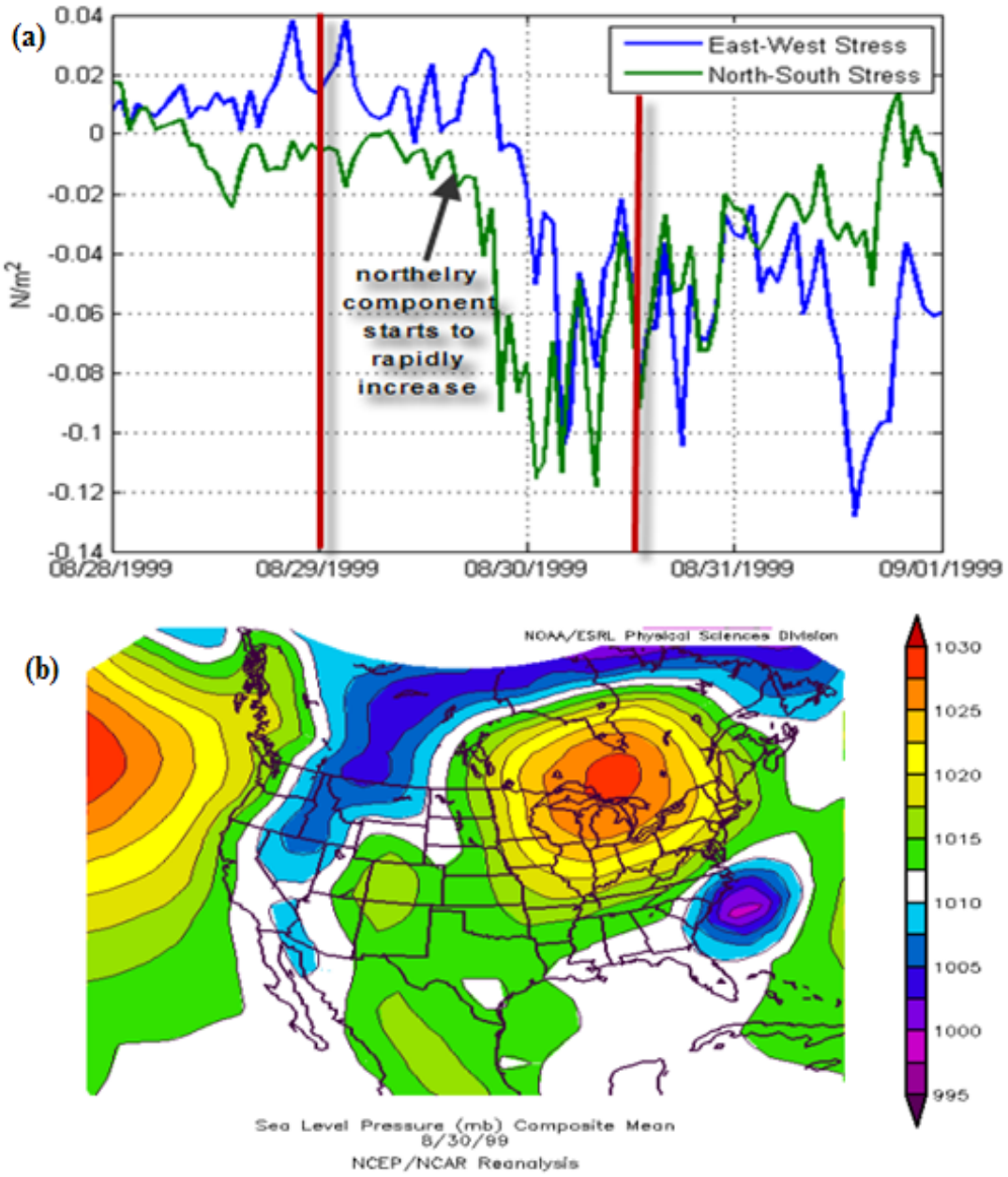

Figure 5.2 (a) X (east-west) and Y(north-south) components of wind stress (N m^{-2}) from 28 August to 1 September 1999 using LGA wind data. Red lines indicate time of event. (b) Daily averaged MSLP for 30 August 1999 using NCEP-NCARR composite.

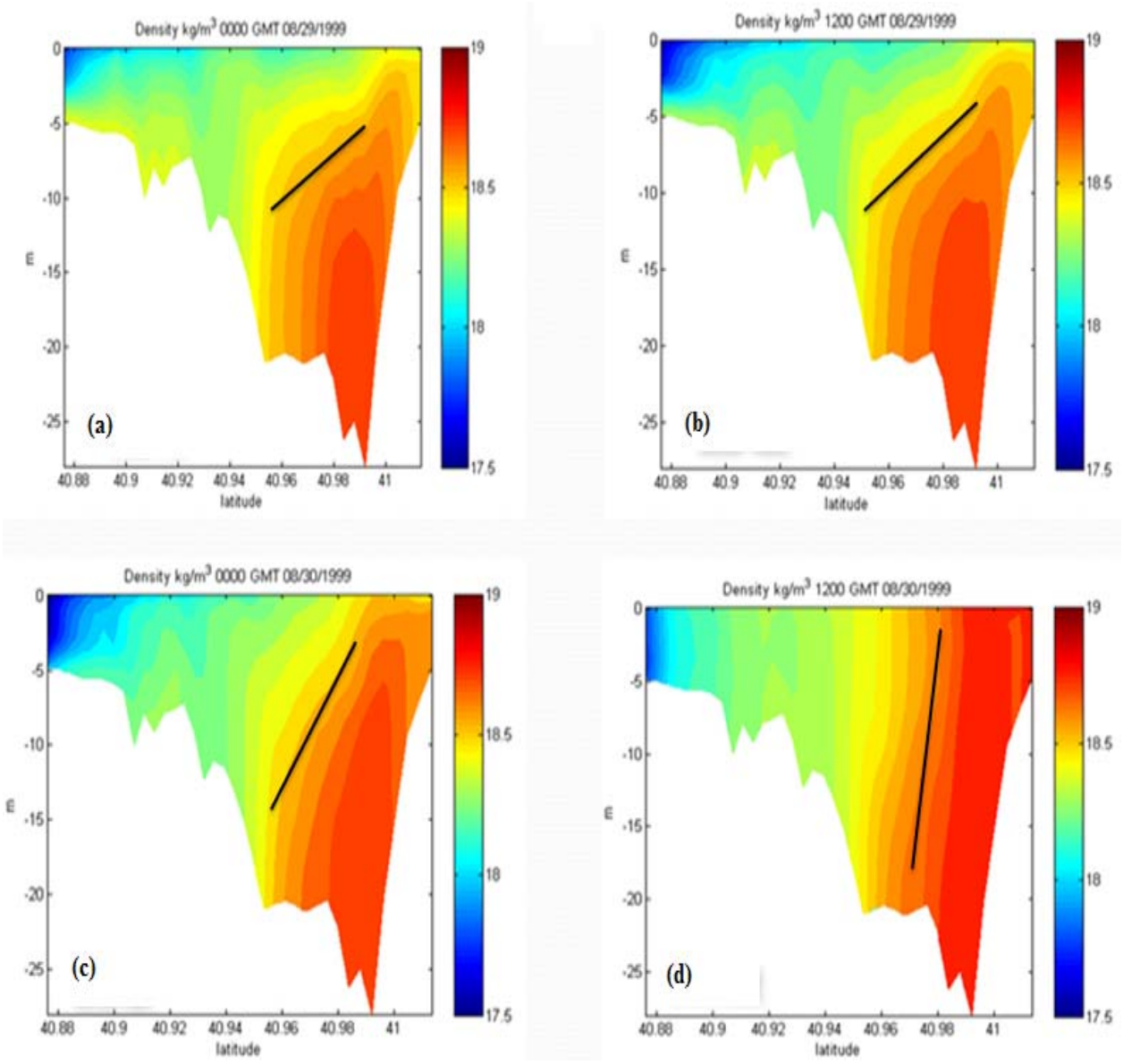

Figure 5.3 ROMS figures for (a) 29 August 00 UTC , (b) 29 August 12 UTC, (c) 30 August 0 UTC, and (d) 30 August 12 UTC of vertical cross-section density (kg m^{-3}) profile during a lateral advection mixing event. Black solid line indicates approximate orientation of pycnocline. Important to note the evolution of the slope of the pycnocline.

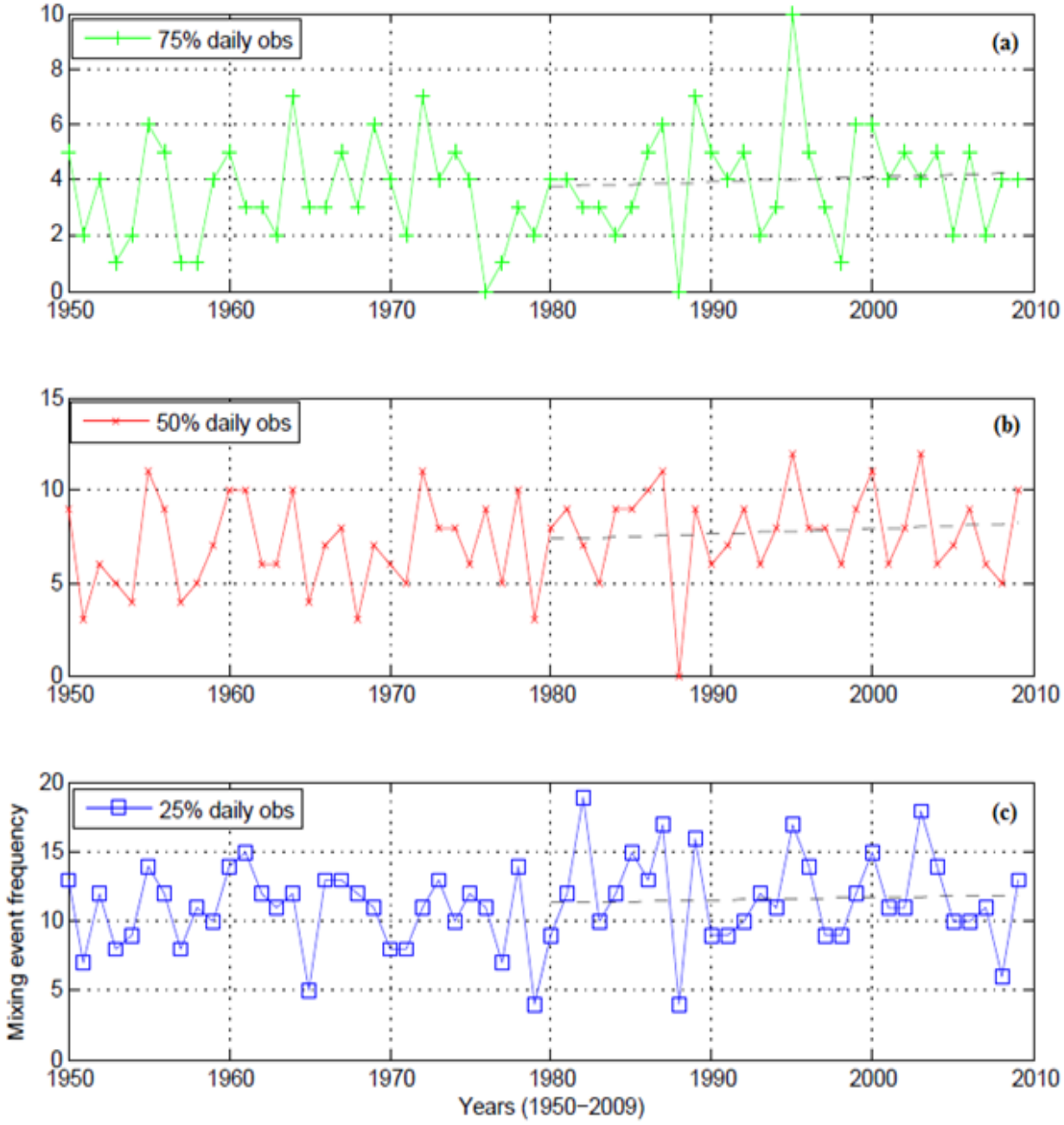

Figure 5.4 Mixing event frequencies for 1950-2009 using (a) 75%, (b) 50%, and (c) 25% of daily observations that have to meet wind criteria. Black dashed least square regression lines represent trend from 1980-2009.

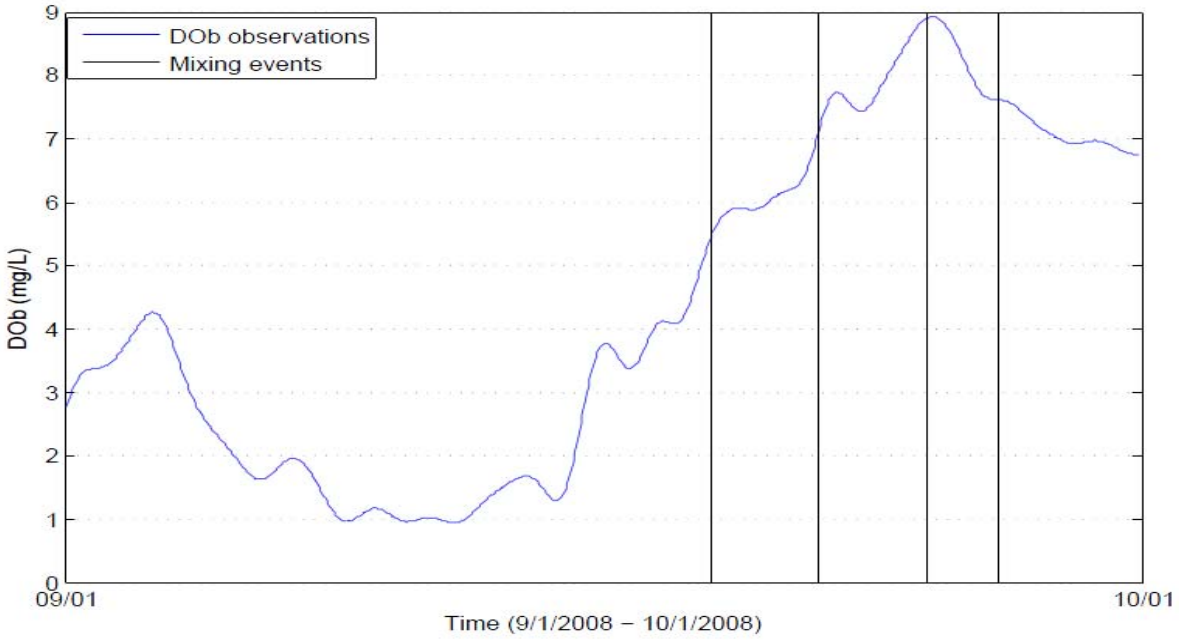

Figure 5.5 Monthly evolution of LISICOS EXRX buoy DOb data for the month of September (9/1 - 10/1) of 2008. Also includes timing of mixing events indicated by black vertical lines.

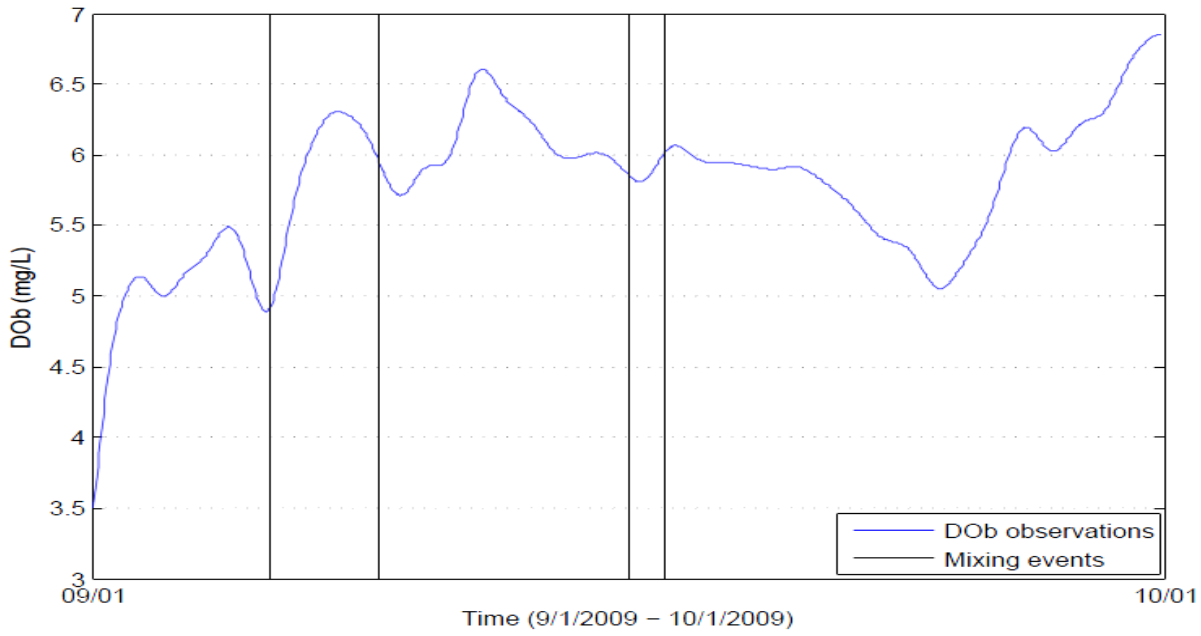

Figure 5.6 Same as Figure 5.5 but for September of 2009.

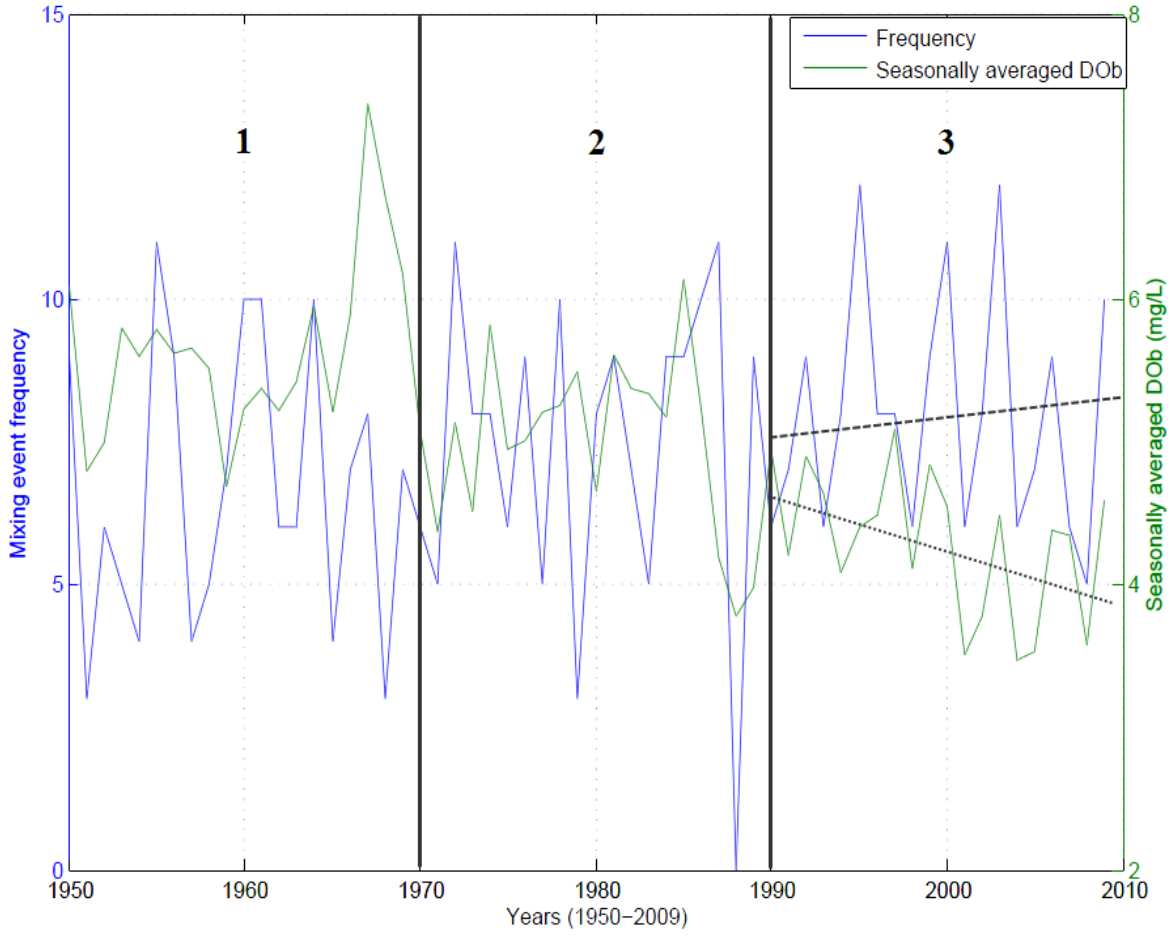

Figure 5.7 Comparison of June-September mixing event frequencies and Seasonally averaged DOb using NYC DEP DOb data from (1950-2009). Time series is broken up into three segments; (1) 1950-1969, (2) 1970-1989, (3) 1990-2009. Black dashed (dotted) line is linear regression line for mixing event frequencies (seasonally averaged DOb) from 1990-2009.

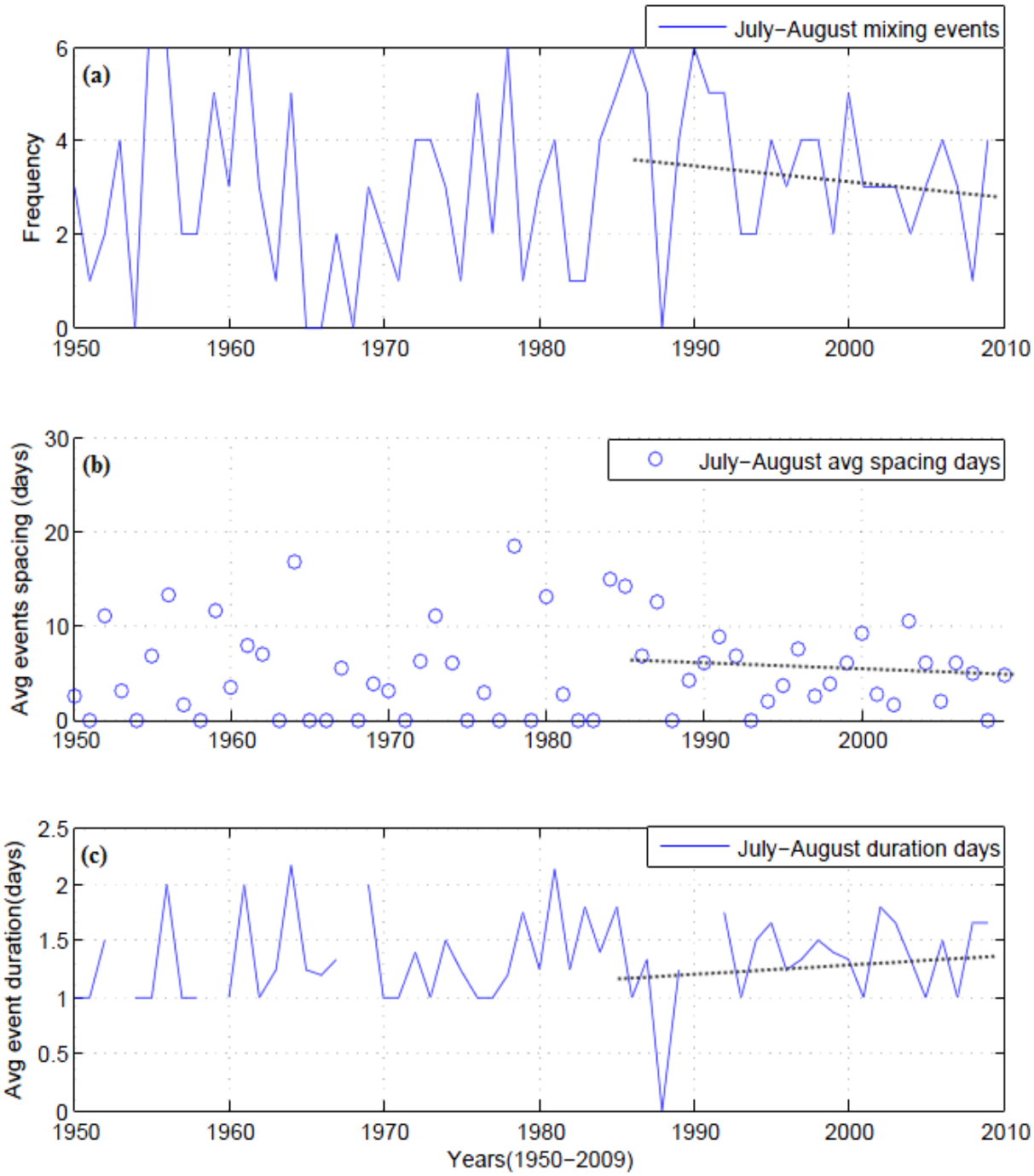

Figure 5.8 July and August time series (1950-2009) of (a) mixing event frequencies (b) scatter plot of average spacing days between events, and (c) average seasonal event durations. Black dotted lines represent linear regression lines for each time series.

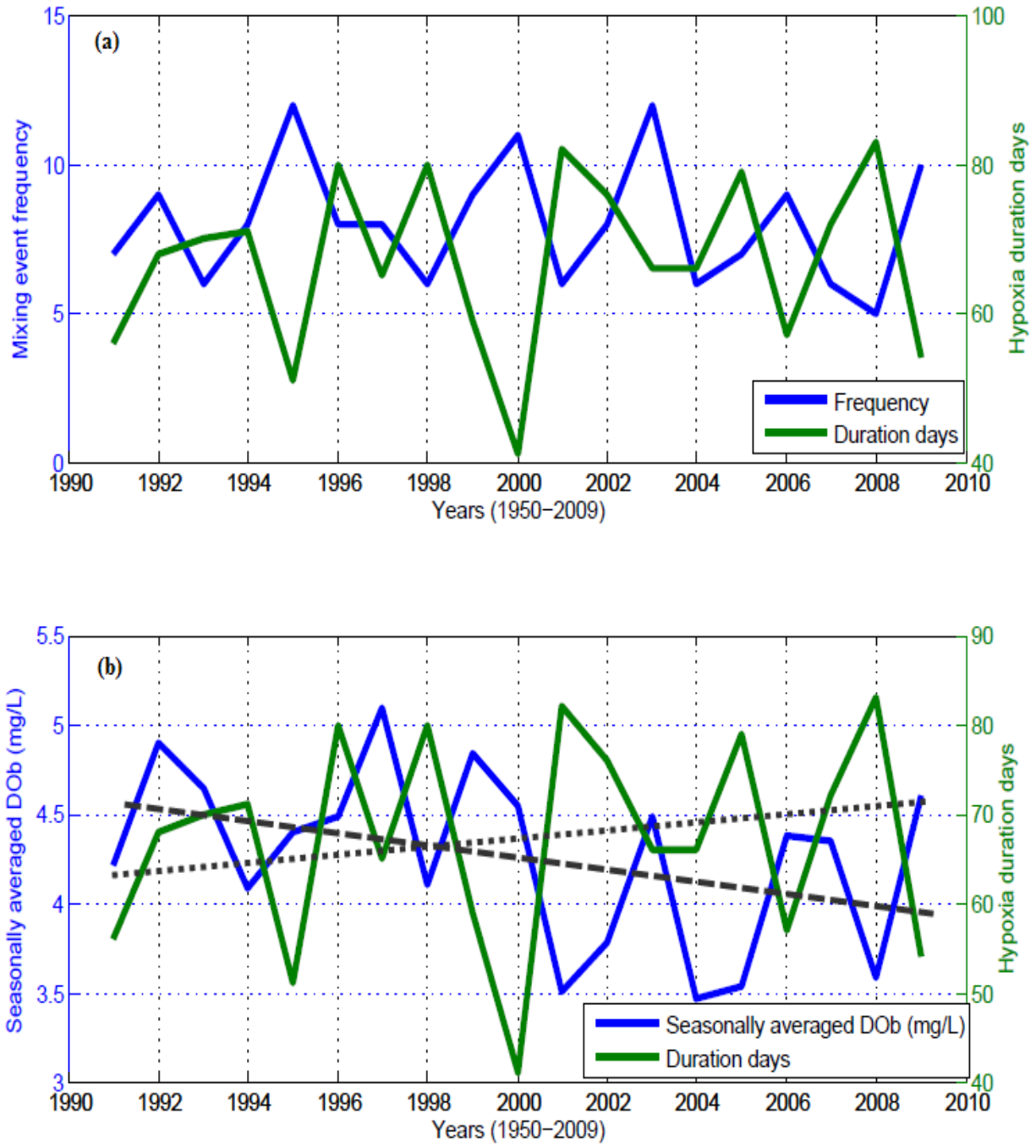

Figure 5.9 (a) Comparison between CT DEP hypoxia duration days (1991-2009) and seasonally averaged DOb. (b) Comparison between hypoxia duration days and mixing event frequencies. Black lines represent least squares regression for hypoxia duration days (dotted) and seasonally averaged DOb (dashed) for 1991-2009 period.

Literature Cited

Agee, E., 1991: Trends in cyclone and anticyclone frequency and comparison with periods of warming and cooling over the northern hemisphere. *Mon. Wea. Rev.*, **4**, 263-267.

American Public Health Association 1985: Standard methods for the examination of water and wastewater, report, 16th ed., Washington, D. C.

Anderson, T. H., and G. T. Taylor 2001: Nutrient pulses, plankton blooms, and seasonal hypoxia in western Long Island Sound, Estuaries, 24(2),228– 243, doi:10.2307/1352947.

Austin, J.A. and S.J. Lentz, 1999: The relationship between synoptic weather systems and meteorological forcing on the North Carolina inner shelf. *J. Geophysical Res.*, **104**, 159-185.

Barnett, T.P. and R. Preisendorfer, 1987: Origins and Levels of Monthly and Seasonal Forecast Skill for United States Surface Air Temperatures Determined by Canonical Correlation Analysis. *Mon. Wea. Rev.*, **115**, 1825-1850.

Chan, C. A., S. J. Colucci, and T. DeGaetano, 2003: Predicting East Coast Winter Storm Frequencies from Midtropospheric Geopotetial Height Patterns. *Wea. Forecasting*, **18**, 1177-1191.

Chen, S., and L. P. Sanford, 2009: Axial wind effects on stratification and longitudinal salt transport in an idealized, partially mixed estuary. *J. Phys. Oceanogr.*, **39**, 1905-1920.

Codiga, D.L., 2008: A moving window trigger algorithm to identify and characterize hypoxic events using time series observations, with application to Narragansett Bay GSO Technical Report 2008-01, Graduate School of Oceanography, University of Rhode Island, Narragansett, RI, 110 pp.

Codiga, D.L., H.E. Stoffel, C.F. Deacutis, S. Kiernan, C. Oviatt, 2008: Narraganset Bay Hypoxic Event Characteristics Based on Fixed-Site Monitoring Network Time Series: Inter-Annual Variability, Geographic Distribution, Intermittency, and Spatial Synchronicity. *Estuaries and Coasts,***32**, 621-641.

Connecticut Department of Environmental Protection, 2010: Long Island Sound Hypoxia Season Review 2010, Hartford, CT, 4 pp.

Crowley, H. 2005: The seasonal evolution of thermohaline circulation in Long Island Sound, Ph.D. thesis, 142 pp., Mar. Sci. Res. Cent., Stony Brook Univ., Stony Brook, N. Y.

Fairall, C.W., Bradley, E.F., Rogers, D.P., Edson, J.B, Young, G.S., 1996: Bulk parameterization of air-sea fluxes for Tropical Ocean-Global Atmosphere Coupled-Ocean Atmosphere Response Experiment. *J. Geophys. Res.,* **101(C2)**, 3747-3764.

Falkowki, P. G., T. S. Hopkins, and J. J. Walsh. ,1980: An analysis of factors affecting oxygen depletion in the New York Bight.J. *Mar. Res.* 38:479-506.

Gay, P. S., J. O'Donnell, and C. A. Edwards, 2004: Exchange between Long Island Sound and adjacent waters, J. Geophys. Res., 109, C06017, doi:10.1029/2004JC002319.

Geyer, R. W., 1997: Influence of wind on dynamics and flushing of shallow estuaries. *Estuarine,Costal and Shelf Science*, **44**, 713-722.

Goodrich D. M., W. C. Boicourt, P. Hamilton, and D. W. Pritchard, 1987: Wind-Induced Destratification in Chesapeake Bay. *J. Phys. Oceanogr.*, **17**, 2232-2240.

Hannachi, A., I.T. Jolliffee and D.B. Stephenson, 2007: Empirical orthogonal functions and related techniques in atmospheric science: A review. *Int. J. climatol.* **27**: 1119-1152.

Hao, Y., 2008: Tidal and residual circulation in Long Island Sound. PhD Dissertation, Marine Sciences Research Center, Stony Brook University, Stony Brook, NY, 70 pp.

Harman, R. J., 1987: Mean monthly North American anticyclone frequencies, 1950-79. *Mon. Wea. Rev.*, **115**, 2840-2848.

Hirsch, E. M., A. T. DeGaetano, and S. J. Colucci, 2001: An east coast winter storm Climatology. *J. Climate*, **14**, 882-899.

Hurrell, W. J., 1996: Influence of variations in extratropical wintertime teleconnections on northern hemisphere temperatures. *Geophys. Res. Lett.*, **23**, 665-668.

HydroQual, 1995. Floatables Pilot Program, Final Report – Evaluation of No-Structural Methods to Control Combined and Storm Sewer Floatable Materials. Prepared by HydroQual, Inc. for the City of New York Department of Environmental Protection, Bureau of Environmental Engineering, January 1995.

Kalnay, E., Coauthors, 1996: The NCEP/NCAR 40-Year Reanalysis Project. *Bull. Amer. Meteor. Soc.*, **77**, 437-471.

Kaputa, N. P., and C. B. Olsen, 2000: Long Island Sound Ambient Water Quality Monitoring Program: Summer Hypoxia Monitoring Survey '91–'98 data review, report, Conn. Dep. Of Environ. Prot., Hartford, Conn.

Leibensperger, M. E., L. J. Mickley and D. J. Jacob, 2008: Sensitivity of US air quality to mid-latitude cyclone frequency and implications of 1980-2006 climate change, *Atmos. Chem. Phys.*, **8**, 7075-7086.

Large, W.G., S. Pond, 1981: Open ocean momentum flux measurement in moderate to strong winds. *J. Phys. Oceanogr.*, **11**, 336-342.

Lee, Y.J., K. Lwiza, 2007: Characteristics of bottom dissolved oxygen in Long island Sound, New York. *J. Geophy. Res.,* **110**, C09022.

_____, 2009: Mechanisms Controlling Variability Over Long Island Sound. Ph.D. dissertation, School of Marine and Atmospheric Sciences, Stony Brook University, 149 pp. [Available from SoMAS, Stony Brook Univ./ SUNY, Stony Brook, NY 11794-5000].

Li, M., L. J. Zhong, W. C. Boicourt, S. L. Zhang, and D. L. Zhang, 2007: Hurricane-induced destratification and restratification in a partially-mixed estuary. *J. Mar. Res.*, **65,** 169–192.

Lowery, T. A., 1998: Modeling estuarine eutrophication in the contest of hypoxia, nitrogen loadings, stratification and nutrient ratios. *Journal of Environmental Management.*, **52**, 289-305.

Lupo, R. A., P. J. Smith, 1998: The interactions between a midlatitude blocking anticyclone and synoptic-scale cyclones that occurred during the summer season. *Mon. Wea. Rev.*, **126**, 502-515.

McCabe, J. G., M. P. Clark, and M. C. Serreze, 2001: Trends in Northern Hemisphere Surface Cyclone Frequency and intensity. *J. Climate*, **14**, 2763-2768.

McCardell, G., J. O'Donnell 2006:Vertical mixing rates and hypoxia in western Long Island Sound, paper presented at the 8th Biennial Long Island Sound Research Conference, Conn. Sea Grant Program, New London, Conn.

Mesquita, S. D. M., N. G. Kvamsto, A. Sorteberg, and D. E. Atkinson, 2008: Climatological properties of summertime extratropical storm tracks in the Northern Hemisphere. *Tells,* DOI: 10.1111/j.1600-0870.

Monismith, S. G., 1986: An experimental study of the upwelling response of stratified reservoirs to surface shear stress. *J. Fluid Mech.*, **171**, 407–439.

Notaro, M., W.C. Wang and W. Gong, 2006: Model and observational analysis of the northeast U.S. regional climate and its relationship to the PNA and NAO patterns during early winter. *Mon. Wea. Rev.*, **134**, 3479-3505.

O'Donnell, J., W. F. Bohlen, and H. G. Dam, 2006: Wind stress and the ventilation of the hypoxic zone of western Long Island Sound, paper presented at the 8th Biennial Long Island Sound Research Conference, Conn. Sea Grant Program, New London, Conn.

_____, and coauthors, 2008: Intermittent ventilation in the hypoxic zone of western Long Island Sound during the summer of 2004. *J. Geophysical Res.*, **113**

Paciorek, J. C., J. S. Risbey, V. Ventura and R. D. Rosen, 2002: Multiple indices of northern hemisphere cyclone activity, winters 1949-99. *J. Climate*, **15**, 1573-1589.

Parker, S. C., and J. E. O'Reilly, 1991: Oxygen depletion in Long Island Sound: A historical perspective. *Estuaries*, **14**, 248-264.

Reynolds-Fleming, and J.V., R. A. Luettich, 2004: Wind-driven lateral variability in a partially mixed estuary. *Estuarine, Coastal and Shell Sciences,* **60**, 395-407.

Rogers, C. J., 1990: Patterns of Low-Frequency Monthly Sea Level Pressure Variability (1899-1986) and Associated Wave Cyclone Frequencies. *J. Climate*, **3**, 1364-1379.

Rohli, V. R., and M. M. Russo, 2004: Tropospheric Ozone in Louisiana and Synoptic Circulation. *J. Appl. Meteor.,* **43**, 1438-1451.

Scully, M.E., C. Friendrichs, and J. Brubaker, 2005: Control of estuarine stratification and mixing by wind induced straining of the estuarine density field. *Estuaries*, **28**, 321-326.

(a)_____, W. R. Geyer, and J. A. Lerczak, 2010: The influence of lateral advection on the residual estuarine circulation: A numerical modeling study of the Hudson River estuary. *J. Phys. Oceanogr.*, **39**, 107-124.

(b)_____, 2010: The Importance of Climate Variability to Wind-Driven Modulation of Hypoxia in Chesapeake Bay. *J. Phys. Oceanogr.*, **40**, 1435–1440.

Sinclair, R. M., 1997: Objective identification of Cyclones and Their circulation Intensity, and Climatology. *Wea. Forecasting*, **12**, 595-612.

Vieira, M. E. C. 2000: The long-term residual circulation in Long Island Sound, *Estuaries*, **23**, 199–207, doi:10.2307/1352827.

Walsh, J. J., and coauthors, 1978: Wind events and food chain dynamics within the New York Bight. *et al. Limnol. Oceanogr.* **23**, 659.

Welsh, B. L. 1995: Hypoxia in Long Island Sound: One researcher's perspective, paper presented at Long Island Sound Research Conference: Is the Sound Getting Better or Worse?, New York Sea Grant Inst., Stony Brook, N. Y.

_____, R.I. Welsh and M.L. DiGiacomo-Cohen. 1994: Quantifying hypoxia and anoxia in Long Island Sound. Changes in Fluxes in Estuaries. Implications from Science to Management. K.R. Dyer and R.J. Orh (Eds.) Olsen & Olsen, Fredensborg, Denmark. 131-137.

_____, and F. C. Eller, 1991: Mechanisms controlling summertime oxygen depletion in western Long Island Sound, Estuaries, 14(3), 265– 278, doi:10.2307/1351661.

Whitney, Michael M., Daniel L. Codiga, 2011: Response of a Large Stratified Estuary to Wind Events: Observations, Simulations, and Theory for Long Island Sound. *J. Phys. Oceanogr.*, **41**, 1308–1327.

Wilson, R. E., 2011: Evidence for directional wind response in controlling inter-annual variations in duration and areal extent of summertime hypoxia in western Long Island Sound, (manuscript).

_____, R.L. Swanson and H.A. Crowley, 2008: perspectives on long-term variations in hypoxic conditions in western Long Island Sound, *J. Geophysical Res.*, **113**, C12011

_____, and R.L. Swanson, 2005: A perspective on bottom water temperature anomalies in Long Island Sound during the 1999 lobster mortality event. *Journal of Shellfish Research*, **24**, 825-830.

_____, 1976: Gravitational circulation in Long Island Sound. Estuarine and Coastal Marine Science 4:443-453.

Xu, K.-M.,2006: Using the bootstrap method for a statistical significance test of differences between summary histograms. *Mon.Wea. Rev.,* **134,** 1442–1453.

Yarnal, B., 1993: Synoptic Climatology in Environmental Analysis: A Primer. Bellhaven Press, London, 41 pp.

Zhang, K., B. C. Douglas, and S. P. Leatherman, 2000: Twentieth- Century Strom Activity along the U.S. East Coast. *J. Climate*, **13**, 1748-1761.

Zishka, M. K., and P. J. Smith, 1980: The Climatology of Cyclones and Anticyclones over North America and Surrounding Ocean Environs for January and July, 1950-77. *Mon. Wea. Rev.*, **108**, 387-400.